# SENSITIVITY OF ATMOSPHERIC POLLUTANTS TO CHANGES IN MODELED NATURAL AND ANTHROPOGENIC EMISSIONS

by

Erica Scotty

A Master's Thesis

submitted in partial fulfillment of the degree requirements for the

degree of

Master of Science

Department of Atmospheric and Oceanic Sciences

at the

UNIVERSITY OF WISCONSIN-MADISON

2014

# Abstract

Ozone and fine particulate matter are the two most significant air pollutants, of widespread concern to human health across the U.S., and actively regulated by the U.S. EPA. Anthropogenic emissions affect both of these pollutants, but natural processes can also contribute to violations of health-based standards set by the United States Environmental Protection Agency (EPA). Many counties across the U.S. are out of attainment of the EPA's National Ambient Air Quality Standards (NAAQS) for ozone and particulate matter smaller that is 2.5 μm ($PM_{2.5}$). This work improves the understanding of natural and anthropogenic contributions to ground-level air quality. We investigate changes in pollution levels by altering emissions, using the U.S. EPA's Community Multi-scale Air Quality Model (CMAQ).

The first part of this study investigates the effects of adding an emission source from lightning. We use convective precipitation and cloud top height as a proxy for lightning flash activity. Lightning emits varying levels of $NO_x$ across the U.S., and is an important contributor to upper tropospheric $NO_2$. Although lightning's contribution to surface $NO_2$ is relatively small, the importance of this source is acute, when comparing to satellite data. Lightning emissions result in about a 10% increase in surface ozone across the southern U.S.

The second part of this study evaluates source-receptor relationships for ozone across the Great Lakes Region. Previous studies have observed increased ozone levels above the Great Lakes due to certain meteorological conditions and emissions sources near the lakes. Wind patterns can advect these elevated pollution levels on shore, causing counties around the lake to violate the NAAQS for ozone and particulate matter. This study is the first to

investigate the contribution of emissions in near-lake counties in Wisconsin, Illinois, Indiana, and Michigan to high pollution levels in coastal cities.

# Acknowledgments

First off I would like to thank my advisor Professor Tracey Holloway for all her help and guidance. This work would not have been possible without her support and leadership. It has been a privilege to work with her, and I am ever grateful for the abundance of knowledge I have learned from her.

I am also ever grateful for the members of the Holloway Research Group, both past and present. I would like to thank Dr. Monica Harkey, Alexandra Karambelas, Ryan Kladar, Dr. Erica Bickford, Jacob Oberman, Keith Maki, Arber Rrushaj, Zach Jensen, Phillip Duran and many more. Without their assistance and guidance this work would not have been as successful, and I am thankful for all of their help and teamwork.

I would like to thank my thesis readers: Dr. Grant Petty and Dr. Tristan L'Ecuyer. I also want to acknowledge the sources of funding that made this research possible: the NASA Air Quality Applied Sciences Team and the National Center for Freight and Infrastructure Research and Education.

Lastly, I would like to dedicate this thesis to my family. I am ever grateful for their constant encouragement and support. Without their multifaceted help, this endeavor would never have been possible.

# Table of Contents

# Chapter 1: Introduction and Motivation

## Research overview

Ozone and fine particulate matter are the two most significant air pollutants of concern to human health across the U.S. Since the United States Environmental Protection Agency (EPA) enacted the Clean Air Act in 1970, fine particle concentrations have reduced 37% and ozone has reduced by 25% [*U.S. EPA,* 2014]. These reductions are vital, as the World Health Organization now estimates that about seven million people die, world-wide, each year from both indoor and outdoor air pollution exposure [*WHO*, 2014]. Aside from air pollutants causing premature mortality, pollutants can cause a multitude of health issues, including asthma [*Sunyer et al.,* 2002; *Weinmayr et al,* 2010], chronic bronchitis, non-fatal heart attacks, and other respiratory and cardiovascular complications [*U.S. EPA*, 2011]. Emission controls and policies set by the EPA help to mitigate these negative health issues, but there are still areas that experience high levels of pollution. These health effects are large motivating factors to fully understand air quality.

Ambient air pollution is influenced by several factors: emissions, chemical processes, and meteorology. There are many emission sources across the globe, which include emissions from motor vehicles, power plants, industrial plants, forest fires, lightning, vegetation, and many more. Emissions can come from anthropogenic sources like power plants, as well as natural sources like vegetation. Quantifying all the emissions from each of these sources is a complex process, but necessary for fully understanding ambient air pollution and potential reduction strategies. To add to the complexity, meteorology also affects pollution levels and chemical processes. For example, when skies are clear, winds are slow, temperatures are high, and the sun is near its zenith, formation of ozone readily occurs [*Lin et al.,* 2001]. Another example is that particulate matter concentrations are typically lowest in the springtime [*Spak et al.,* 2009]. There are many more relationships between chemical processes and meteorology, as well as weather impacts on emissions sources.

In order to quantify chemical release into the atmosphere the EPA and other air quality management and research organizations calculated emissions inventories. Inventories from various sources then need to be combined to understand the complete level of emissions in an area for each atmospheric pollutant. These inventories only provide information on what is being directly emitted into the air, and not what might be chemically formed in the atmosphere due to these emissions. This is where air quality model comes in as a tool. Air quality models bring together chemical processes, emissions, and meteorology, in order to output air pollution concentrations across a specified domain.

This work utilizes an advances air quality model to understand the sensitivity of ambient pollution to changes in natural and anthropogenic emissions. As mentioned, there are complexities involved when developing an emissions inventory, and most inventories omit emissions sources that are not viewed as essential for a particular analysis need. As air quality modeling and knowledge of atmospheric processes advance, often new inventories are developed and expanded. The most current inventory utilized by our research group focused on anthopogenic sources, but did not include emissions from lightning and forest fires. This gap was the motivation behind developing an inventory for lightning emissions, which will be discussed in Chapter 3.

Aside from building a comprehensive emissions inventory, understanding what occurs in areas that are air pollution "hot spots" can help to understand how to reduce these elevated pollution levels in hopes to reduce population exposure. There are several areas around the United States that have elevated pollution levels. The most severe of these can be seen by looking at the areas that have violated the National Ambient Air Quality Standards (NAAQS) (Figures 1.1 and 1.2). Because the EPA considers individual counties as the defined area of NAAQS compliance, an assessment of county emissions can help to understand how to best avoid these exceedances. One particular area of interest is along the Great Lakes, which has historically had many counties out of attainment of the air quality standards. Chapter 4 presents and analysis of near-lake county air quality.

## Lightning impacts on $NO_x$

Nitrogen oxides, or $NO_x$ ($NO_x$ = NO + $NO_2$), are directly emitted from both anthropogenic as well as natural sources, and are also formed in the atmosphere. Anthropogenic $NO_x$ accounts for 87% of the total emissions, of which, 60% is from mobile sources [*U.S. EPA*, 2008]. Natural sources of $NO_x$ account for the remaining 13%, of which includes wildfires, lightning, stratospheric injection, and soil emissions [*U.S. EPA*, 1993]. Nitrogen oxides pose a threat to air quality and human health, and are therefore one of the six pollutants regulated by the (NAAQS). $NO_x$ impacts respiratory morbidity and asthma [*U.S. EPA,* 2008] and the standard for $NO_2$ is set at 100 ppb for a 1-hour average and 53 ppb for annual average. These regulations are set to protect human health and the environment, and have the potential to be affected by lightning emissions [*Allen et al.,* 2012; *Kaynak et al.,* 2008]. For this study, we will be focusing on nitrogen oxides, or $NO_x$ ($NO_x$ = NO + $NO_2$), emitted by lightning, as lightning is still a very uncertain, but significant natural source of $NO_x$ in the troposphere [*Bierle et al.,* 2010; *Kaynak et al.,* 2008; *Griffing,* 1977; *Bond et al.,* 2001; *DeCaria et al.,* 2005; *Zhao et al.,* 2009; *Biazar and McNider,* 1995; *Wang et al.,* 2013;

*Ott et al.,* 2007].

Lightning flash frequency is the metric that is typically recorded and used as the basis for $NO_x$ emissions estimates. Most notably, the National Lightning Detection Network (NLDN) is a network of over 100 sensors across the U.S. that has the capability to detect cloud-to-ground (CG) and intracloud (IC) lightning strokes [*Orville et al*., 2002]. Satellite instruments from the Tropical Rainfall Measurement Mission (TRMM) Lightning Imaging Sensor (LIS), the Optical Transient Detector (OTD) have also been used to detect total optical pulses that are translated into individual flashes [*Murray et al.,* 2012*; Beirle et al.,* 2010; *Schumann and Huntrieser,* 2007; *Huntrieser et al.,* 2008; *Nesbitt et al*., 2000]. These methods of measuring flash frequency are only half of the information necessary to translate lightning into emissions values; the amount of $NO_x$ from each strike needs to be measured or estimated.

The total amount of $NO_x$ released per lightning strike, and distributions across the globe are still widely uncertain [*Allen and Pickering,* 2002; *Martini et al.,* 2011; *Schumann and Huntrieser,* 2007; *Price et al*., 1997; *Morris et al*., 2010]. This uncertainty is due to several factors, and is largely based off minimal observational data. The factors that contribute to estimates of the $NO_x$ emissions are: the amount emitted by each strike, difference in emissions from IC vs. CG, and totals over the globe. The contribution of these factors are still widely uncertain, and highly debated.

Improvements have been made in estimating the global budget of lightning $NO_x$, converging from an approximation of 1-20 Tg of N per year to 2-8 Tg of N per year across the globe [*Schumann and Huntrieser*, 2007]. The range of 2-8 Tg of N per year has increasingly become the most utilized estimate and has been employed in the most recent studies [*Allen et al.,* 2012; *Beirle et al.,* 2010; *Tost et al.,* 2007, *Morris et al.,* 2010]. Although these numbers have converged due to additional observational data, this is still a wide range, and account for the entire globe as opposed to a single continent or region. Estimates for the United States range from 0.21 – 5.87 Tg N per year with an average of 1.63 Tg N per year [*Bond et al.,* 2001; *Hudman et al.*, 2007; *Fang et al.,* 2010; *Zhang et al.*, 2003; *Wang et al*., 2013; *Lamsal et al*., 2010; *Pierce et al*., 2007; *Martin et al*., 2006; *Jourdain et al*., 2010]. To further understand the significance of lightning emissions, as a comparison, the global rate of $NO_x$ emissions is 32 Tg N per year [*Zhang et al., 2003*], resulting in lightning emissions accounting for roughly 6-25% of the global $NO_x$ budget. Although this is a large range, these are the best estimates to date.

The next uncertainty lies in the amount of $NO_x$ emitted by each stroke. This has been estimated through use of field experiments and aircraft measurements [*Ott et al*., 2007; *Fehr et al.,* 2004; *DeCaria et al*., 2005]. The range in estimates of this value are quite large, as Zhang et al., [2003] summarized a range of 8 to 5000 moles per flash, which was determined through field experiments and global models. Through the use of model simulations and aircraft measurements, DeCaria et al. [2000] and DeCaria et al. [2005] estimate that each CG strike produces 200-500 moles of NO per flash, while Allen et al. [2012] utilized the high end of this scale, 500 moles per flash, to match with three separate field experiments. The most frequent value utilized per flash is about 500 moles [*Allen et al.,* 2010; *Allen et al.,* 2012; *Ott et al*., 2010; *Murray et al.,* 2012; *Hudman et al*., 2007; *Kaynak et al.,* 2008; *DeCaria et al.,* 2005; *Martini et al.,* 2011].

Another uncertainty is due to the ratio of IC and CG emissions per strike. This is a significant distinction in order to develop the emission totals for each strike, as CG strokes are potentially more energetic than IC, and IC strokes are more frequent [*Huntrieser et al.,* 1998]. Several studies have concluded that CG strokes emit 10 times the amount of $NO_x$ in comparison to IC strokes [*Tost et al*., 2007; *Martin et al.,* 2007; *Schumann and Huntrieser*, 2007], while others have estimated the IC/CG ratio to be 3 [*Allen et al*., 2010; *Jourdain et al*., 2010; *Smith and Mueller,* 2010; *Price and Rind*, 1993]. More recently, field experiments have found that IC strikes are just as energetic as CG strikes, emitting the same amount of $NO_x$ resulting in a 1-to-1 ratio [*Allen et al.,* 2012], and has been utilized in several studies [*Ott et al*., 2003; *Choi et al*., 2005; *Allen et al.,* 2012].

Once these uncertainties are addressed, an emission inventory is then developed, used as input to chemical transport models (CTM). Lightning emissions have not been added to regional air quality models until the last several years even though their effect on air quality has been recognized for the past 20 years [*Allen et al*., 2012]. There are a wide range of models utilized to simulate the effects of lightning emissions including: GEOS-Chem an a global scale [*Martin et al.,* 2007; *Bey et al.,* 2001; *Lamsal et al.,* 2010; *Mitovski et al.,* 2012], and regional scale [*Jourdain et al.,* 2010; *Lee et al.,* 2011; *Lin,* 2012], EPA's Community Multi-scale Air Quality (CMAQ) Model on a regional scale [*Allen et al*., 2012; *Mueller et al.,* 2011; *Mao et al.,* 2010; *Wang et al.,* 2013; *Kaynak et al.,* 2013], the Model of Ozone and Related Chemical Tracers (MOZART) on a global scale [*Zhang et al.,* 2003] and regional scale [*Fang et al.,* 2010], the Model of Atmospheric Transport and Chemistry – Max Planck Institute for Chemistry (MATCH-MPIC) on a global scale[*Lawrence et al*., 2003; *Labrador et al.,* 2005], the Global Modeling Initiative (GMI) on a regional scale [*Allen et al.,* 2010], a cloud-scale chemical transport model (CSCTM) on individual cells [*Ott et al.,* 2007; *Ott et al.,* 2010], the ECHAM5/MESSy atmospheric chemistry model on a global scale [Tost et al., 2010; Tost et al., 2007], and the Goddard Cumulus Ensemble (GCE) model on individual cells [*Pickering et al.,* 1998; *Ott et al.,* 2007; *Thompson et al.,* 1994; *DeCaria et al.,* 2000]. These model simulations are then compared to past field measurement data, most often from flight campaigns [*Allen et al.,* 2010; *Martin et al.*, 2007; *Allen et al.*, 2012], or satellite retrievals from the SCanning Imaging Absorption spectroMeter for Atmospheric CHartographY (SCIAMACHY) [*Martin et al.,* 2006; *Yuan et al.*, 2012], or the Ozone Monitoring Instrument (OMI) [*Yuan et al.,* 2012; *Huijnen et al.,* 2010; *Allen et al.,* 2010].

## Regional strategies to reduce $O_3$ and $PM_{2.5}$

Ozone is not directly emitted, but formed in the troposphere. Ozone is primarily formed when $NO_x$ reacts with volatile organic compounds (VOCs) in the presence of sunlight to form ozone ($O_3$) [*Tong et al.,* 2009]. Ozone is a photochemically formed pollutant, and is therefore highest in the summer time [*Chameides and Walker,* 1973]. The non-linear relationship between VOCs and $NO_x$ with respect to ozone generation can be see in Figure 1.3. This figure shows two extreme scenarios, VOC and $NO_x$ limited regimes. When VOC concentrations are low, any increase in $NO_x$ will not increase ozone concentration, and visa versa for low $NO_x$ concentrations. This means that there needs to be a balance between $NO_x$ and VOCs to largely increase ozone concentrations. Rural areas are typically $NO_x$ limited, whereas urban areas are VOC limited [*Liao et al.,* 2014].

Ozone is known to have adverse health affects, including respiratory problems, premature mortality, cardiovascular, and central nervous system problems [*Dockery et al.,* 1993; *Bell et al.,* 2005; *U.S. EPA*, 2013a]. For these reasons along with environmental impacts, ozone is also regulated under the NAAQS. The current regulation for ground level ozone in the NAAQS is 75 ppb over an 8-hour average.

Particulate matter (PM) is both a naturally emitted and chemically formed substance in the atmosphere. PM can be directly emitted, such as wind-blown dust, or can be formed photochemistry and/or condensed through chemical reactions [*Koo et al*., 2010]. Two of the main precursors that contribute to chemically formed PM are $NO_2$ and $SO_2$ [*U.S. EPA*, 2011]. Particulate matter that is 2.5 μm in diameter, or less, is denoted as $PM_{2.5}$, and will be the focus in this study. This particular size of PM is significant, as it has direct implications in human health and morbidity [*Dutkiewicz et al.,* 2004].

Federal standards require that every county within a state be in compliance with air quality rules. The EPA implements rules for each state to follow, and standards (especially the NAAQS), which must be met. Each state is required to develop an individual state implementation plane (SIP), to ensure that each county is in attainment of the federal rule.

There have been several studies that investigated the impact of state-to-state transport of ozone and ozone precursors [*Tong et al.,* 2008; *Tong et al.,* 2009; *Bergin et al.,* 2005; *Bergin et al.,* 2007]. Bergin et al. [2007] found that 77% of each state's ozone concentrations, in the eastern U.S., was contributed to by emissions from upwind states. On average, in-state emissions account for less than 15% of ozone in 90% of the states [*Tong et al.,* 2009]. As further evidence for these findings, Tong et al. [2008] find for over 80% of states, interstate transport is more significant than in-state emissions and that 77% of each state's surface ozone concentrations are sensitive to precursor emissions from other states. Turning to look at the ozone precursor of $NO_x$, Tong et al. [2009] found in 43 states $NO_x$ emissions from upwind states contributed more to ozone concentrations than the states' own emissions. Tong et al. [2009] also found that in-state $NO_x$ emissions can affect 2 to 40 states downwind by a minimum of 0.1 ppb. Overall, these studies conclude that ozone levels seen in a particular location are over 77% likely to have been formed in a neighboring state.

For particulate pollution transport, Dutkiewicz et al. [2004] calculated trajectories from New York to show that 44-60% of sulfate concentrations were transported from other states. Bergin et al. [2007] had similar findings, but concluded that 77% of each state's $PM_{2.5}$ concentrations, in the eastern U.S., were contributed by emissions from upwind states. Although Bari et al. [2003] did not specifically study state-to-state transport; they concluded that 43% of sulfate and 30% of $PM_{2.5}$ mass in metropolitan New York was attributed to upwind emissions. Husain and Dutkiewicz [1990] concluded that over 60% of the total sulfate concentrations at two sites in New York originated from Midwestern emissions. Overall, past studies conclude that 30% or more of particle pollution is transported from another state. Here we focus on the unique case of stat-to-state transport across Lake Michigan.

### *Lake breeze affects on air quality*

Past studies have investigated the relationship between lake-land breeze circulations and air pollution [*Levy et al.,* 2011; *Lyons and Cole,* 1976; *Hastie et al.,* 1999; etc.]. These lake breeze circulations often develop in the spring and summer due to differences in land and water temperatures [*Lyons and Olsson,* 1973]. Prior to the development of the circulation, a stable layer is often observed over the body of water, allowing for the build up of emissions, and chemical reactions to take place [*Foley et al*., 2011]. The pollutants are then advected from above water to the land through the localized lake-land breeze circulation, raising local pollution levels [*Levy et al.,* 2011]. In fact, lake breeze circulations developed on 40-45 % of days over a 10-summer month study period in Milwaukee and 36% of days in

Chicago [*Lyons,* 1972]. This process has been known to cause exceedances in the EPA air quality standards, which also have corresponding negative health and environmental impacts.

One reason high levels of pollution are associated with lake breeze circulations is through above-lake chemistry [*Lyons and Cole,* 1976]. Ozone formation, generally increases with increasing temperature and decreases with increasing relative humidity [*Camalier et al.,* 2007]. Due to the temperature difference between land and the lakes in summer, the atmosphere is very stable and provides for an “efficient reaction chamber for ozone formation” through photochemistry [*Foley et al.,* 2011]. *Hayden et al*. [2011] observed this, and found a layer of shallow mixing causing limited dispersion, and therefore leading to enhanced oxidation of primary pollutants like sulfur dioxide and organics. Levy et al. [2010] found, through observations and model studies, that ozone concentrations were 5 to 15 ppb higher above the lake than compared to rural and urban sites over the southern Great Lakes [*Levy et al.,* 2010]. Hastie et al. [1999] found that when a lake breeze forms over Lake Ontario, ozone precursors along with other oxidation products have been seen in higher concentrations, which provides for a significant impact on local air quality as levels of ozone rise on the order of 10’s of ppb. VOC and $NO_x$ profiles contribute to the formation of ozone, and were categorized by Foley et al. [2011]. The study states that below 200m above Lake Michigan, ozone formation is VOC limited in the morning, and becomes $NO_x$ limited in the afternoon, and that onshore VOC concentrations peak in the early morning, whereas above the lake, VOC concentrations peak in mid-morning [*Foley et al.,* 2011].

The wind flow pattern associated with lake and sea breezes have an association with raising levels of air pollutants, especially ozone, onshore [*Foley et al.,* 2011*, Wellman et al.,* 1992*, Eshel & Bernstein,* 2006*, Hastie et al.,* 1999*, Lyons & Olsson,* 1973*, Cheng,* 2002, *Hayden et al.,* 2011*, Lin et al.,* 2010*, Lyons,* 1972]. During the spring and summer months, land temperatures often exceed the surface temperature of the water through daytime heating [*Foley et al., 2011*]. This, along with light gradient winds and strong insolation, causes lake and/or sea breeze circulations to develop [*Lyons,* 1972]. When these lake breezes form, they also interact with the large scale synoptic flow, causing complex circulations to develop and advect a build up of ozone, ozone precursors, and emissions from local sources, over the lake [*Levy et al.,* 2010]. Although the circulation is complex, Wellman et al. [1992] found a correlation between specific wind directions around Lake Michigan, with high levels of ozone. If a high-pressure system was located to the east of the lake, and winds were out of the southwest over the southern portion of the lake, increased levels of ozone were detected on the eastern shore [*Wellman et al.,* 1992]. This wind profile allowed for fairly stable conditions, allowing for less mixing to occur, and therefore even higher levels of ozone to be detected. If winds were out of the south, higher levels of ozone were detected on the western shore, and were accompanied by deep vertical mixing [*Wellman et al.,* 1992]. Wellman et al. [1992] also concluded that when winds were out of the southwest, higher levels of ozone were detected on the eastern shore, but vertical mixing was limited, causing even higher levels to be seen onshore.

After the lake breeze circulation ceases, an elevated stable layer often develops, causing a build-up of pollutants in that layer [*Makar et al.,* 2010]. Levy et al. [2010] conclude that after this layer has formed, it is not exposed to fresh emissions and encounters limited removal through dry deposition. This can lead to enhanced ozone formation the following day and therefore allowing for local emissions to have an even larger impact on local air quality [*Levy et al.,* 2010]. This phenomenon has also been seen by Lin et al. [2010], who describe it as an elevated ozone layer, which is "the air layer between the nocturnal boundary layer and the top of the daily mixing layer in an ozone- polluted area", and stated that the ozone that was formed and mixed in the atmosphere during the previous day is preserved in that layer. After sea breeze circulations cease, elevated ozone reservoirs form from surface cooling in the evening and are left to descend to the surface through nocturnal subsidence [*Makar et al*., 2010]. Lin et al. [2010] state that due to the depth of the sea breeze circulations versus lake breeze, large point sources on the coastal region play a large role in increasing ozone. This is due to plumes being advected inland through the sea breeze during the day, and advected inland again in a returning land breeze at night [*Lin et al.,* 2010]. Lin et al. [2010] also conclude that ozone from the reservoir from the previous day "contribute 50% more to daily ozone pollution than the ozone produced on the day of interest." Not only does the reservoir cause elevated pollution levels, but recirculating pollutants do as well. Particulates have been seen at increased levels around Lake Michigan, and Lyons and Olsson [1973] suggest that particulates are in part recirculated in the lake breeze cell causing accumulating levels that wouldn't otherwise be seen, which are continually contributed to by local sources [*Lyons and Olsson,* 1973]. Taiwan is also subject to these frequent circulations, but in the form of larger sea breezes, where shallow terrain driven circulations often develop, allowing for vertical mixing to be limited and therefore an increase in ozone concentrations downwind [*Cheng,* 2002].

Several model studies have investigated lake and sea breeze simulations and corresponding chemical processes in the atmosphere. Lyons et al. [1994] used the Regional Atmospheric Modeling System (RAMS) along with Lagrangian Particle Dispersion Model (LPDM) to simulate a sea breeze and plume advection. They discovered that within the sea breeze front, entire plumes can be vertically displaced aloft, then recirculate within the sea breeze cell, but still leave large concentrations pooled aloft that can affect the next days pollution concentration levels [*Lyons et al.,* 1994]. Harris and Kotamarthi [2005] used the Fifth-Generation NCAR / Penn State Mesoscale Model (MM5) at a 4 km grid, and also simulated particles trapped within the circulation, which then recirculated several times. Makar et al. [2010] investigated lake breeze circulations using A Unified Regional Air-Quality Modeling System (AURAMS). The model simulations showed that the interaction between the synoptic flow and the lake breeze circulation contributed to the transport of ozone and the enhancement of photochemical production of ozone through convergence zones [*Makar et al.,* 2010]. Through this model study, Makar et al. [2010] conclude that Lake Erie and St. Clair showed a photochemical production of ozone up to 3 ppb per hour, leading to the enhancement of ozone on shore of around 30 ppb. These model simulations also showed that the synoptic wind pattern can advect these high levels of ozone and ozone precursors in narrow bands hundreds of kilometers from the lake [*Makar et al.,* 2010]. This study suggests that local emission sources may have a large impact on ozone production in this area especially if they are located near a convergence line associated with the lake breeze circulation [*Makar et al.,* 2010]. Levy et al. [2010] also used the AURAMS model, and were able to properly simulate the circulation and obtained similar ozone concentrations as observations.

Overall, lake breeze circulations and above lake chemistry play a large role in pollution concentrations inland, especially near the coast. Model studies do a fair job in simulating the lake and sea breeze circulations along with corresponding chemical processes. Observational studies also provided a wealth of information, but are generally data limited due to short field campaigns. Although there were a large number of studies dealing with lake breeze circulations and corresponding pollution levels, one aspect not investigated were case studies involving altering emissions to see the impact on ozone and particulate formation over the lake. This sensitivity approach is explored in our study.

## Thesis overview

This research focuses is on air quality impacts of adding lightning $NO_x$ to the existing emissions inventory, and running the new inventory through an air quality model, in order to asses the overall contribution of lightning to $NO_x$ (Chapter 3). We also consider how county reductions in emissions impact air quality over a multi-state region (Chapter 4). For this study, I investigate the changes in $PM_{2.5}$ and ozone when emissions are altered in the Great Lakes Region. Together, the analysis of ozone and PM sensitivity to lightning and county-level emissions highlights the complex response of ambient air quality to natural and anthropogenic emissions.

# Figures

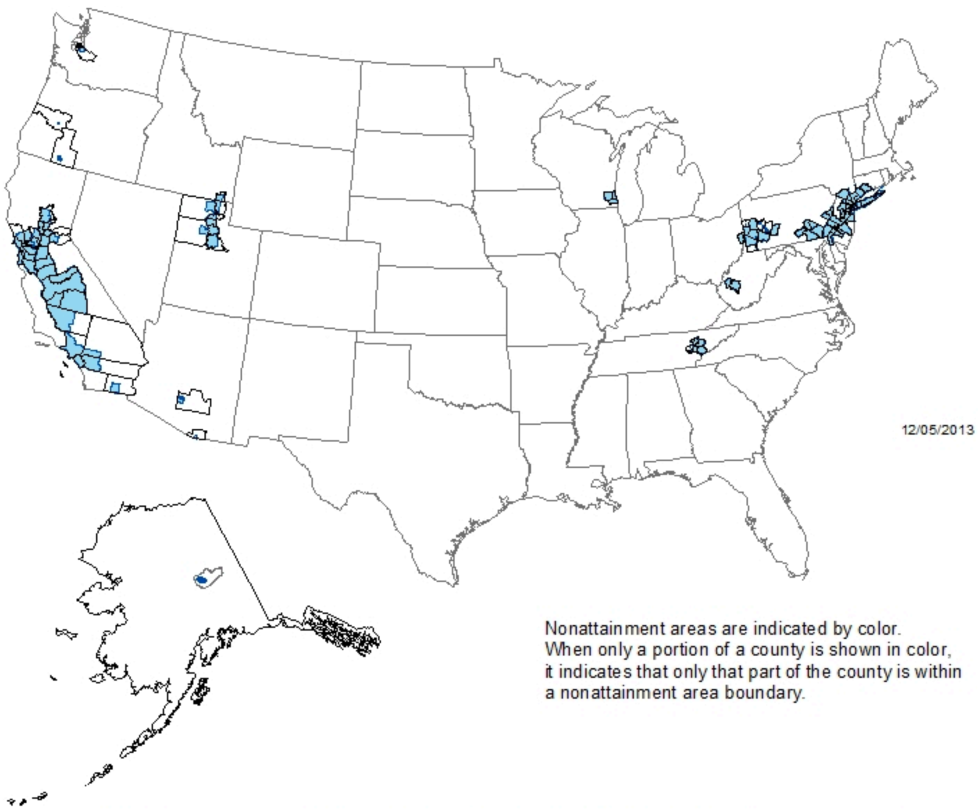


**Figure 1.1: The U.S. EPA PM-2.5 nonattainment area map according to the 2006 standard from U.S. EPA [2013b].**

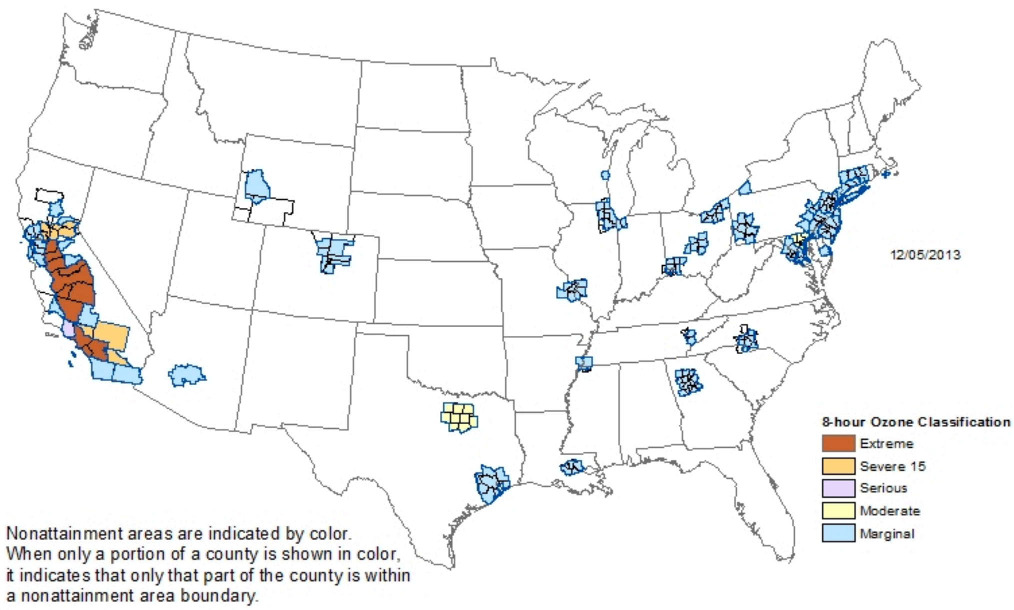


**Figure 1.2: The U.S. EPA 8-hour ozone nonattainment area map according to the 2008 standard from U.S. EPA [2013c].**

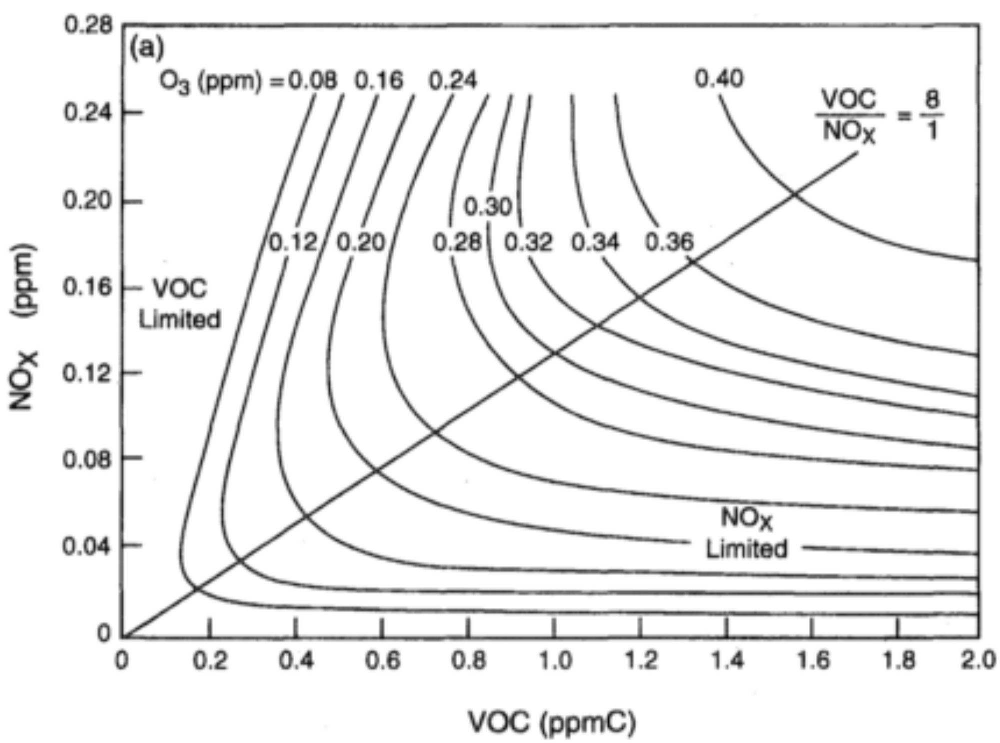


**Figure 1.3: Ozone isopleth map from Finlayson-Pitts and Pitts (1993).**

## References

Allen, D. J., and K. Pickering (2002), Evaluation of lightning flash rate parameterizations for use in a global chemical transport model, *J. Geophys. Res.*, *107*(D23), 4711, doi:10.1029/2002JD002066.

Allen, D., K. Pickering, B. Duncan, and M. Damon (2010), Impact of lightning NO emissions on North American photochemistry as determined using the Global Modeling Initiative (GMI) model, *J. Geophys. Res.*, *115*(D22), D22301, doi:10.1029/2010JD014062.

Allen, D. J., K. E. Pickering, R. W. Pinder, B. H. Henderson, K. W. Appel, and a. Prados (2012), Impact of lightning-NO on eastern United States photochemistry during the summer of 2006 as determined using the CMAQ model, *Atmos. Chem. Phys.*, *12*, 1737–1758, doi:10.5194/acp-12-1737-2012.

Bari, A., V. a. Dutkiewicz, C. D. Judd, L. R. Wilson, D. Luttinger, and L. Husain (2003), Regional sources of particulate sulfate, SO2, PM2.5, HCl, and HNO3, in New York, NY, *Atmos. Environ.*, *37*(20), 2837–2844, doi:10.1016/S1352-2310(03)00200-0.

Beirle, S., H. Huntrieser, and T. Wagner (2010), Direct satellite observation of lightning-produced $NO_x$, *Atmos. Chem. Phys.*, *10*, 10965–10986, doi:10.5194/acp-10-10965-2010.

Bell, Michelle; Dominici, Francesca; Samet, J. (2005), A Meta-Analysis of Time-Series Studies of Ozone and Mortality With Comparison to the National Morbidity, Mortality, and Air Pollution Study, *16*(4), 436–445.

Bergin, M. S., J. J. West, T. J. Keating, and A. G. Russell (2005), Regional Atmospheric Pollution and Transboundary Air Quality Management*, Annual Review of Environment and Resources, 30(1), 1–37, doi:10.1146/annurev.energy.30.050504.144138.

Bergin, M. S., J.-S. Shih, A. J. Krupnick, J. W. Boylan, J. G. Wilkinson, M. T. Odman, and A. G. Russell (2007), Regional air quality: local and interstate impacts of NO(x) and SO2 emissions on ozone and fine particulate matter in the eastern United States., Environmental science & technology, 41(13), 4677–89.

Bey, I., D. J. Jacob, R. M. Yantosca, J. a. Logan, B. D. Field, A. M. Fiore, Q. Li, H. Y. Liu, L. J. Mickley, and M. G. Schultz (2001), Global modeling of tropospheric chemistry with assimilated meteorology: Model description and evaluation, *J. Geophys. Res.*, *106*(D19), 23073, doi:10.1029/2001JD000807.

Biazar, A., and T. Mcnider (1995), Regional estimates of lightning production of nitrogen oxides, *J. Geophys. Res.*, *100*(D11), 22,861–22,874.

Bond, W., R. Xhang, X. Tie, G. Brasseur, G. Huffines, E. Orville, and J. Boccippio (2001), NOx production by lightning over the continental United States, *J. Geophys. Res.*, *106*(D21), 27,701–27,710.

Byun, D., and K. L. Schere (2006), Review of the Governing Equations, Computational Algorithms, and Other Components of the Models-3 Community Multiscale Air Quality (CMAQ) Modeling System, *Appl. Mech. Rev.*, *59*(2), 51, doi:10.1115/1.2128636.

Camalier, L., Cox, W., & Dolwick, P. (2007). The effects of meteorology on ozone in urban areas and their use in assessing ozone trends. *Atmospheric Environment*, *41*(33), 7127–7137. doi:10.1016/j.atmosenv.2007.04.061

Chameides, W., and J. C. G. Walker (1973), A photochemical theory of tropospheric ozone, *J. Geophys. Res.*, *78*(36), 8751–8760, doi:10.1029/JC078i036p08751.

Cheng, W.-L. (2002). Ozone distribution in coastal central Taiwan under sea-breeze conditions. *Atmospheric Environment*, *36*(21), 3445–3459. doi:10.1016/S1352-2310(02)00307-2

Choi, Y., Y. Wang, T. Zeng, R. Martin, T. Kurosu, and K. Chance (2005), Evidence of lightning NOx and convective transport of pollutants in satellite observations over North America, *Geophys. Res. Lett.*, *32*(L02805), 1–5, doi:10.1029/2004GL021436.

Cooper, O. R. et al. (2006), Large upper tropospheric ozone enhancements above midlatitude North America during summer: In situ evidence from the IONS and MOZAIC ozone measurement network, *J. Geophys. Res.*, *111*(D24), D24S05, doi:10.1029/2006JD007306.

Decaria, A. J., K. E. Pickering, G. L. Stenchikov, J. R. Scala, J. L. Stith, J. E. Dye, B. A. Ridley, and P. Laroche (2000), A cloud-scale model study of lightning-generated NOx in an individual thunderstorm during STERAO-A, *J. Geophys. Res.*, *105*, D9, 11,601–11,616.

DeCaria, A. J., K. Pickering, G. Stenshikov, and L. Ott (2005), Lightning-generated NO X and its impact on tropospheric ozone production: A three-dimensional modeling study of a Stratosphere-Troposphere Experiment: Radiation, Aerosols and Ozone (STERAO-A) thunderstorm, *J. Geophys. Res.*, *110*, D14303, doi:10.1029/2004JD005556.

Dockery, D., A. Pope III, X. Xu, J. Spengler, J. Ware, M. Fay, B. Ferris, F. S. (1993), An Association Between Air Pollution and Mortality in Six U.S. Cities, *N. Engl. J. Med.*, *329*(24).

Dutkiewicz, V. a., S. Qureshi, A. R. Khan, V. Ferraro, J. Schwab, K. Demerjian, and L. Husain (2004), Sources of fine particulate sulfate in New York, *Atmos. Environ.*, *38*(20), 3179–3189, doi:10.1016/j.atmosenv.2004.03.029.

Eshel, G., & Bernstein, J. J. (2006). Relationship Between Large-Scale Atmospheric States, Subsidence, Static Stability and Ground-Level Ozone in Illinois, USA. *Water, Air, & Soil Pollution*, *171*(1-4), 111–133. doi:10.1007/s11270-005-9021-x

Fang, Y., a. M. Fiore, L. W. Horowitz, H. Levy, Y. Hu, and a. G. Russell (2010), Sensitivity of the NO y budget over the United States to anthropogenic and lightning NO x in summer, *J. Geophys. Res.*, *115*(D18), D18312, doi:10.1029/2010JD014079.

Fehr, T., H. Holler, and H. Huntrieser (2004), Model study on production and transport of lightning-produced NO x in a EULINOX supercell storm, *J. Geophys. Res.*, *109*(D9102), doi:10.1029/2003JD003935.

Finlayson-Pitts, B.J. & J.N. Pitts Jr. (1993) Atmospheric Chemistry of Tropospheric Ozone Formation: Scientific and Regulatory Implications, Air & Waste, 43:8, 1091-1100, DOI: 10.1080/1073161X.1993.10467187

Foley, T., Betterton, E. a., Robert Jacko, P. E., & Hillery, J. (2011). Lake Michigan air quality: The 1994–2003 LADCO Aircraft Project (LAP). *Atmospheric Environment*, *45*(18), 3192–3202. doi:10.1016/j.atmosenv.2011.02.033

Griffing, G. W. (1977), Ozone and Oxides of Nitrogen Production During Thunderstorms, *J. Geophys. Res.*, *82*(6), 943–950, doi:10.1029/JC082i006p00943.

Hanna, S., and J. Chang (1994), Relations between Meteorology and Ozone in the Lake MIchigan Region, *J. Appl. Meteorol.*, *34*, 670–678.

Harris, L., & Kotamarthi, V. R. (2005). The Characteristics of the Chicago Lake Breeze and Its Effects on Trace Particle Transport: Results from an Episodic Event Simulation. *Journal of Applied Meteorology*, *44*(11), 1637–1654. doi:10.1175/JAM2301.1

Hastie, D. R., Narayan, J., Schiller, C., Niki, H., Shepson, P. B., Sills, D. M. L., Taylor, P. a., et al. (1999). Observational evidence for the impact of the lake breeze circulation on ozone concentrations in Southern Ontario. *Atmospheric Environment*, *33*(2), 323–335. doi:10.1016/S1352-2310(98)00199-X

Hayden, K. L., Sills, D. M. L., Brook, J. R., Li, S.-M., Makar, P. a., Markovic, M. Z., Liu, P., et al. (2011). Aircraft study of the impact of lake-breeze circulations on trace gases and particles during BAQS-Met 2007. *Atmospheric Chemistry and Physics*, *11*(19), 10173–10192. doi:10.5194/acp-11-10173-2011

Hudman, R. C. et al. (2007), Surface and lightning sources of nitrogen oxides over the United States: Magnitudes, chemical evolution, and outflow, *J. Geophys. Res.*, *112*(D12), D12S05, doi:10.1029/2006JD007912.

Huijnen, V. et al. (2010), Comparison of OMI $NO_2$ tropospheric columns with an ensemble of global and European regional air quality models, *Atmos. Chem. Phys.*, *10*(7), 3273–3296, doi:10.5194/acp-10-3273-2010.

Huntrieser, H., H. Schlager, C. Feigl, and H. Holler (1998), Transport and production of NOx in electrified thunderstorms: Survey of previous studies and new observations at midlatitudes, *J. Geophys. Res.*, *103*(D21), 28,247–28,264.

Huntrieser, H., U. Schumann, H. Schlager, H. Höller, A. Giez, H.-D. Betz, D. Brunner, C. Forster, O. Pinto, and R. Calheiros (2008), Lightning activity in Brazilian thunderstorms during TROCCINOX: implications for NOx production, *Atmos. Chem. Phys.*, *8*, 921–953, doi:10.5194/acp-8-921-2008.

Husain, L., and V. A. Dutkiewicz (1990), A LONG - TERM (1975-1988) STUDY OF ATMOSPHERIC SULFATE: REGIONAL CONTRIBUTIONS AND CONCENTRATION TRENDS, *Atmos. Environ.*, *24A*(5), 1175–1187.

Jourdain, L., S. S. Kulawik, H. M. Worden, K. E. Pickering, J. Worden, and a. M. Thompson (2010), Lightning NOx emissions over the USA constrained by TES ozone observations and the GEOS-Chem model, *Atmos. Chem. Phys.*, *10*, 107–119, doi:10.5194/acp-10-107-2010.

Kaynak, B., Y. Hu, R. V. Martin, a. G. Russell, Y. Choi, and Y. Wang (2008), The effect of lightning NOx production on surface ozone in the continental United States, *Atmos. Chem. Phys. Discuss.*, *8*, 5061–5089, doi:10.5194/acpd-8-5061-2008.

Kaynak, B., Y. Hu, and A. G. Russell (2013), Analysis of NO, NO2, and O3 Between Model Simulations and Ground-Based, Aircraft, and Satellite Observations, *Water, Air, Soil Pollut.*, *224*, 1674, doi:10.1007/s11270-013-1674-2.

Koo, B., C.-J. Chien, G. Tonnesen, R. Morris, J. Johnson, T. Sakulyanontvittaya, P. Piyachaturawat, and G. Yarwood (2010), Natural emissions for regional modeling of background ozone and particulate matter and impacts on emissions control strategies, *Atmos. Environ.*, *44*, 2372–2382, doi:10.1016/j.atmosenv.2010.02.041.

Kroon, M., De Haan, J. F., Veefkind, J. P., Froidevaux, L., Wang, R., Kivi, R., & Hakkarainen, J. J. (2011). Validation of operational ozone profiles from the Ozone Monitoring Instrument. *Journal of Geophysical Research*, *116*(D18), 1–25. doi:10.1029/2010JD015100

Labrador, L. J., R. Von Kuhlmann, and M. G. Lawrence (2005), The effects of lightning-produced NOx and its vertical distribution on atmospheric chemistry : sensitivity simulations with MATCH-MPIC, *Atmos. Chem. Phys.*, *5*, 1815–1834.

Lamsal, L. N., R. V. Martin, a. van Donkelaar, E. a. Celarier, E. J. Bucsela, K. F. Boersma, R. Dirksen, C. Luo, and Y. Wang (2010), Indirect validation of tropospheric nitrogen dioxide retrieved from the OMI satellite instrument: Insight into the seasonal variation of nitrogen oxides at northern midlatitudes, *J. Geophys. Res.*, *115*(D5), D05302, doi:10.1029/2009JD013351.

Lawrence, M. G. (2003), The balance of effects of deep convective mixing on tropospheric ozone, *Geophys. Res. Lett.*, *30*(18), 3–6, doi:10.1029/2003GL017644.

Lee, C. J., J. R. Brook, G. J. Evans, R. V. Martin, and C. Mihele (2011), Novel application of satellite and in-situ measurements to map surface-level $NO_2$ in the Great Lakes region, *Atmos. Chem. Phys.*, *11*(22), 11761–11775, doi:10.5194/acp-11-11761-2011.

Lennartson, G. J., and M. D. Schwartz (2002), The lake breeze-ground-level ozone connection in eastern Wisconsin: a climatological perspective, *Int. J. Climatol.*, *22*(11), 1347–1364, doi:10.1002/joc.802.

Levy, I., Makar, P. a., Sills, D., Zhang, J., Hayden, K. L., Mihele, C., Narayan, J., et al. (2010). Unraveling the complex local-scale flows influencing ozone patterns in the southern Great Lakes of North America. *Atmospheric Chemistry and Physics*, *10*(22), 10895–10915. doi:10.5194/acp-10-10895-2010

Liao, K.-J., X. Hou, and D. R. Baker (2014), Impacts of interstate transport of pollutants on high ozone events over the Mid-Atlantic United States, *Atmos. Environ.*, *84*, 100–112, doi:10.1016/j.atmosenv.2013.10.062.

Lin, C. C., D. J. Jacob, and A. M. Fiore (2001), Trends in exceedances of the ozone air quality standard in the continental United States , 1980 – 1998, , *35*(May 1999), 3217–3228.

Lin, C.-H., Wu, Y.-L., & Lai, C.-H. (2010). Ozone reservoir layers in a coastal environment – a case study in southern Taiwan. *Atmospheric Chemistry and Physics*, *10*(9), 4439–4452. doi:10.5194/acp-10-4439-2010

Lin, J.-T. (2012), Satellite constraint for emissions of nitrogen oxides from anthropogenic, lightning and soil sources over East China on a high-resolution grid, *Atmos. Chem. Phys.*, *12*(6), 2881–2898, doi:10.5194/acp-12-2881-2012.

Lu, R., and R. Turco (1994), AIR POLLUTANT TRANSPORT IN A COASTAL ENVIRONMENT. Part 1: Two-DIMENSIONAL SIMULATIONS OF SEA-BREEZE AND MOUNTAIN EFFECTS, *J. Atmos. Sci.*, *51*(15), 2285–2308.

Lyons, W., and H. Cole (1976), Photochemical Oxidant Transport: Mesoscale Lake Breeze and Synoptic-Scale Aspects, *J. Appl. Meteorol.*, *15*, 733–743.

Lyons, W. (1972), The Climatology and Prediction of the Chicago Lake Breeze, *J. Appl. Meteorol.*, *11*, 1259–1270.

Lyons, W., and L. Olsson (1973), Detailed Mesometeorological Studies of Air Pollution Dispersion in the Chicago Lake Breeze, *Mon. Weather Rev.*, *101*(5), 387–403.

Lyons, W. A., Pielke, R. A., Tremback, C. J., Walko, R. L., Moon, D. A., & Keen, C. S. (1995). Modeling Impacts of Mesoscale Vertical Motions Upon Coastal Zone Air Pollution Dispersion, *29*(2), 283–301.

Makar, P. a., Zhang, J., Gong, W., Stroud, C., Sills, D., Hayden, K. L., Brook, J., et al. (2010). Mass tracking for chemical analysis: the causes of ozone formation in southern Ontario during BAQS-Met 2007. *Atmospheric Chemistry and Physics*, *10*(22), 11151–11173. doi:10.5194/acp-10-11151-2010

Mao, H., M. Chen, J. D. Hegarty, R. W. Talbot, J. P. Koermer, A. M. Thompson, and M. A. Avery (2010), A comprehensive evaluation of seasonal simulations of ozone in the northeastern US during summers of 2001 – 2005, *Atmos. Chem. Phys.*, (2004), 9–27.

Martin, R. V., B. Sauvage, I. Folkins, C. E. Sioris, C. Boone, P. Bernath, and J. Ziemke (2007), Space-based constraints on the production of nitric oxide by lightning, *J. Geophys. Res.*, *112*(D9), D09309, doi:10.1029/2006JD007831.

Martin, R. V., C. E. Sioris, K. Chance, T. B. Ryerson, T. H. Bertram, P. J. Wooldridge, R. C. Cohen, J. A. Neuman, A. Swanson, and F. M. Flocke (2006), Evaluation of space-based constraints on global nitrogen oxide emissions with regional aircraft measurements over and downwind of eastern North America, *J. Geophys. Res.*, *111*(D15308), doi:10.1029/2005JD006680.

Martini, M., D. J. Allen, K. E. Pickering, G. L. Stenchikov, A. Richter, E. J. Hyer, and C. P. Loughner (2011), The impact of North American anthropogenic emissions and lightning on long-range transport of trace gases and their export from the continent during summers 2002 and 2004, *J. Geophys. Res.*, *116*(D7), D07305, doi:10.1029/2010JD014305.

Mauzerall, D., B. Sultan, N. Kim, and D. Bradford (2005), NO emissions from large point sources: variability in ozone production, resulting health damages and economic costs, Atmospheric Environment, 39(16), 2851–2866, doi:10.1016/j.atmosenv.2004.12.041

Mitovski, T., I. Folkins, R. V. Martin, and M. Cooper (2012), Testing convective transport on short time scales: Comparisons with mass divergence and ozone anomaly patterns about high rain events, *J. Geophys. Res.*, *117*(D2), 1–13, doi:10.1029/2011JD016321.

Morris, G. a., a. M. Thompson, K. E. Pickering, S. Chen, E. J. Bucsela, and P. a. Kucera (2010), Observations of ozone production in a dissipating tropical convective cell during TC4, *Atmos. Chem. Phys.*, *10*(22), 11189–11208, doi:10.5194/acp-10-11189-2010.

Mueller, S. F., Q. Mao, and J. W. Mallard (2011), Modeling natural emissions in the Community Multiscale Air Quality ( CMAQ ) model – Part 2 : Modifications for simulating natural emissions, *Atmos. Chem. Phys.*, 293–320, doi:10.5194/acp-11-293-2011.

Murray, L. T., D. J. Jacob, J. a. Logan, R. C. Hudman, and W. J. Koshak (2012), Optimized regional and interannual variability of lightning in a global chemical transport model constrained by LIS/OTD satellite data, *J. Geophys. Res. Atmos.*, *117*(D20307), doi:10.1029/2012JD017934.

Nesbitt, S. W., R. Zhang, and R. E. Orville (2000), Seasonal and global NOx production by lightning estimated from the Optical Transient Detector (OTD), *Tellus*, *52B*, 1206–1215, doi:10.1034/j.1600-0889.2000.01121.x.

OrVille, R., G. Huffines, W. Burrows, R. Holle, and K. Cummins (2002), The North American Lightning Detection Network ( NALDN )— First Results : 1998 – 2000, *Mon. Weather Rev.*, *130*, 2098–2109.

Ott, L. E.,K.E. Pickering, G.L.Stenchikov, R.-F. Lin,B.Ridley, M. Loewenstein, and E. Richard (2003), Trace gas transport and lightning NOx production during a CRYSTAL-FACE thunderstorm simulated using a 3-D cloud-scale chemical transport model, Eos Trans. AGU, 84(46), Fall Meet. Suppl., Abstract AE32A-0156.

Ott, L. E., K. E. Pickering, G. L. Stenchikov, H. Huntrieser, and U. Schumann (2007), Effects of lightning NO x production during the 21 July European Lightning Nitrogen Oxides Project storm studied with a three-dimensional cloud-scale chemical transport model, *J. Geophys. Res.*, *112*(D5), D05307, doi:10.1029/2006JD007365.

Ott, L. E., K. E. Pickering, G. L. Stenchikov, D. J. Allen, A. J. DeCaria, B. Ridley, R.-F. Lin, S. Lang, and W.-K. Tao (2010), Production of lightning NO x and its vertical distribution calculated from three-dimensional cloud-scale chemical transport model simulations, *J. Geophys. Res.*, *115*(D4), D04301, doi:10.1029/2009JD011880.

Pickering, K. E., Y. Wang, W. Tao, C. Price, and J. Mtiller (1998), Vertical distributions of lightning NO / for use in regional and global chemical transport models, *103*.

Pierce, R. B. et al. (2007), Chemical data assimilation estimates of continental U.S. ozone and nitrogen budgets during the Intercontinental Chemical Transport Experiment–North America, *J. Geophys. Res.*, *112*(D12), D12S21, doi:10.1029/2006JD007722.

Price, C., J. Penner, and M. Prather (1997), NOx from lightning 1 . Global distribution based on lightning physics, *J. Geophys. Res.*, *102*(D5), 5929–5941.

Price, C., and D. Rind (1993), Modeling Global Lightning Distributions in a General Circulation Model, *Mon. Weather Rev.*, *122*, 1930–1939.

Schumann, U., and H. Huntrieser (2007), The global lightning-induced nitrogen oxides source, *Atmos. Chem. Phys. Discuss.*, *7*, 3823–3907, doi:10.5194/acpd-7-3823-2007.

Smith, S. N., and S. F. Mueller (2010), Modeling natural emissions in the Community Multiscale Air Quality (CMAQ) Model–I: building an emissions data base, *Atmos. Chem. Phys.*, *10*(10), 4931–4952, doi:10.5194/acp-10-4931-2010.

Spak, S. N., and T. Holloway (2009), Seasonality of speciated aerosol transport over the Great Lakes region, *J. Geophys. Res.*, *114*(D8), 1–18, doi:10.1029/2008JD010598.

Sunyer, J., X. Basagaña, J. Belmonte, and J. M. Antó (2002), Effect of nitrogen dioxide and ozone on the risk of dying in patients with severe asthma., *Thorax*, *57*(8), 687–93.

Thompson, A. M., W. Tao, K. E. Pickering, J. R. Scala, and J. Simpson (1994), Tropical Deep Convection and Ozone Formation, *Bull. Am. Meteorol. Soc.*, 1043–1054.

Tong, D. Q., and D. L. Mauzerall (2008), Summertime state-level source-receptor relationships between nitrogen oxides emissions and surface ozone concentrations over the continental United States. Environmental science & technology, 42(21), 7976–84.

Tong, D. Q., N. Z. Muller, H. Kan, and R. O. Mendelsohn (2009), Using air quality modeling to study source-receptor relationships between nitrogen oxides emissions and ozone exposures over the United States. Environment international, 35(8), 1109–17, doi:10.1016/j.envint.2009.06.008.

Tost, H., P. Jöckel, and J. Lelieveld (2007), Lightning and convection parameterisations – uncertainties in global modelling, *Atmos. Chem. Phys. Discuss.*, *7*(3), 6767–6801, doi:10.5194/acpd-7-6767-2007.

Tost, H., M. G. Lawrence, C. Brühl, and P. Jöckel (2010), Uncertainties in atmospheric chemistry modelling due to convection parameterisations and subsequent scavenging, *Atmos. Chem. Phys.*, *10*(4), 1931–1951, doi:10.5194/acp-10-1931-2010.

U.S. EPA. (1993), Air Quality Criteria for Oxides of Nitrogen Volume I of III.

U.S. EPA Office of Air and Radiation, Office of Air Quality Planning and Standards, Air Quality Strategies and Standards Division, Innovative Strategies and Economics Group (2004), Benefits of the Proposed Inter-State Air Quality Rule.

U.S. EPA. 2008. Risk and Exposure Assessment to Support the Review of the NO2 Primary National Ambient Air Quality Standard. Research Triangle Park, NC:Office of Air Quality Planning and Standards, U.S. Environmental Protection Agency.

U.S. EPA (2011), Combined National and State-level Health Benefits for the Cross-State Air Pollution Rule and Mercury and Air Toxics Standards, , *EPA-452/R-11-014*.

U.S. EPA Office of Air and Radiation and Office of Air Quality Planning and Standards (2011), Combined National and State-level Health Benefits for the Cross-State Air Pollution Rule and Mercury and Air Toxics Standards.

U.S. EPA (2013a), Integrated Science Assessment for Ozone and Related Photochemical Oxidants.

US EPA (2013b). *8-Hour Ozone Nonattainment Areas (2008) Standard*. 5 December 2013. Web. 12 June 2014

US EPA (2013c). *PM-2.5 Nonattainment Areas (2006) Standard*. 5 December 2013. Web. 12 June 2014

U.S. EPA. "Progress Cleaning the Air and Improving People's Health." 22 April 2014. Web. 30 May 2014.

U.S. EPA, "Clean Air Interstate Rule Basic Information.", 31 July 2012. Web. 20 May 2014.

Wang, L., M. J. Newchurch, A. Pour-Biazar, S. Kuang, M. Khan, X. Liu, W. Koshak, and K. Chance (2013), Estimating the influence of lightning on upper tropospheric ozone using NLDN lightning data and CMAQ model, *Atmos. Environ.*, *67*, 219–228, doi:10.1016/j.atmosenv.2012.11.001.

Weinmayr, G., E. Romeo, M. De Sario, S. K. Weiland, and F. Forastiere (2010), Short-term effects of PM10 and NO2 on respiratory health among children with asthma or asthma-like symptoms: a systematic review and meta-analysis., *Environ. Health Perspect.*, *118*(4), 449–57, doi:10.1289/ehp.0900844.

Wellman, D. L., Gunter, R. L., Watkins, B. A., & Oceanic, N. (1992). Lake Michigan Ozone Study (LMOS): Measurements From an Instrumented Aircraft. *Atmospheric Environment*, *26*(18).

WHO. “7 million premature deaths annually linked to air pollution.” 25 March 2014. Web. 30 May 2014.

Yuan, T., L. a. Remer, H. Bian, J. R. Ziemke, R. Albrecht, K. E. Pickering, L. Oreopoulos, S. J. Goodman, H. Yu, and D. J. Allen (2012), Aerosol indirect effect on tropospheric ozone via lightning, *J. Geophys. Res.*, *117*(D18), D18213, doi:10.1029/2012JD017723.

Zhang, R., X. Tie, and D. W. Bond (2003), Impacts of anthropogenic and natural NO(x) sources over the U.S. on tropospheric chemistry., *Proc. Natl. Acad. Sci. U. S. A.*, *100*(4), 1505–9, doi:10.1073/pnas.252763799.

Zhao, C., Y. Wang, Y. Choi, and T. Zeng (2009), Summertime impact of convective transport and lightning $NO_x$ production over North America: modeling dependence on meteorological simulations, *Atmos. Chem. Phys.*, *9*(13), 4315–4327, doi:10.5194/acp-9-4315-2009.

# Chapter 2: Data and Methods

## Air quality modeling

This study utilizes an air quality model to gain a comprehensive analysis of pollutant levels across the U.S. and the Great Lakes Region. Models help to supplement sparse ground based observational networks and satellite data, while providing a tool to examine atmospheric processes and sensitivities. The EPA monitoring network has about 1,000 monitors for ozone and about 400 for $NO_2$ (Figure 2.1 and 2.2), most concentrated in urban areas. Observations from satellites offer a valuable new resource, but there are limited pollutants measured, limited temporal coverage, and known errors and biases [*Lee et al.,* 2011]. Air quality models help to fill in the gaps in measurements, and allow analysis of a multitude of atmospheric constituents, with continuous spatial and temporal coverage.

Air quality models utilize mathematical and numerical techniques to simulate the dispersion and chemical reactions of pollutants in the atmosphere. Air quality modeling involves a complex system of inputs in order to generate accurate levels of atmospheric pollution. The modeling system utilizes several datasets for these inputs, including meteorology along with anthropogenic and biogenic emissions. Because the air quality model simulates pollution levels over an entire domain, continuous meteorology and emissions must be generated and input into the air quality model. This study examines air quality in the U.S., both on a continental scale and with higher resolution over the Upper Midwest.

For this study, the EPA Community Multi-scale Air Quality (CMAQ) Model version 4.7.1 [*Byun and Schere,* 2006] was employed. CMAQ is a state-of-the-art chemical transport model that is widely used for policy analysis, state implementation plans (SIP), and quantifying air pollution health risk. CMAQ has the capability to model at both continental and regional scales, at a multitude of resolutions.

CMAQ requires meteorology and emissions data as inputs. Emissions data was obtained through the Lake Michigan Air Directors Consortium (LADCO) Base C version 7 2007 inventory. This inventory includes: biogenic, point source, area source, motor vehicle on-road and non-road, and low point source emissions. This inventory is appropriate to use for most applications focused on ground-level air quality and regulation. However, the inventory introduces errors when comparing with satellite data because it omits emissions from lightning, fires, or Mexico. Mexico emissions are uncertain in all inventories. Because LADCO focuses on the northern U.S., it has not been developed to the same level as other components of the inventory. Lightning emissions, however, can be significant when comparing to satellite measurements because the satellite makes column measurements and lightning contributes to the upper troposphere. To best compare model and satellite data, lightning must be added to the standard LADCO inventory, which was the motivation for this work. Forest fires are also an important addition to the inventory, but are not discussed in this work because of the lack of time in developing the inventory to its final form. For anthropogenic emissions LADCOs estimates are considered stat-of-the-art. Biogenic emissions are estimated by the widely used MEGAN model.

The next input into CMAQ is meteorology, which was generated by a fellow group member Dr. Monica Harkey, who utilized the Weather Research and Forecasting (WRF) Model version 3.2.1 [*Skamarock and Klemp,* 2008]. WRF is a necessary component to air quality modeling in order to generate continuous meteorology data at the correct resolution, and over the same domain as the emissions data. WRF simulations for this study were constrained using the North American Regional Reanalysis (NARR) [*Harkey and Holloway*, 2012]. WRF data was generated with 27 vertical layers and at a 36 km by 36 km resolution over the continental U.S. and at 12 km by 12 km over the Great Lakes Region. The WRF data is output in a form that is not directly compatible with CMAQ, and therefore needed to be processed through the EPA Meteorology-Chemistry Interface Processor (MCIP) version 3.2. CMAQ can output concentrations of over 130 constituents, at ground level and vertically throughout the 27 layers, along with dry and wet deposition rates. CMAQ outputs concentration values once every hour throughout every day the simulation is ran for.

Here we use gas and aqueous phase chemistry from the Carbon-Bond Five (CB05) mechanism [*Yarwood et al.,* 2005] and the aerosol chemistry by Aero5 [*Carlton et al.,* 2010] in the CMAQ simulations. The CB-05 mechanism contains 51 species and 156 chemical reactions [*Yarwood et al.,* 2005], and is utilized, along with AERO5, for its improved performance over previous versions of aqueous phase and aerosol chemistry.

For boundary conditions, we utilized time varying, dynamic, boundary conditions that were calculated by the Model for Ozone and Related Chemical Tracers version 4 (MOZART-4) [*Emmons et al.,* 2010]. Boundary conditions define the flux of pollutants entering the domain around the boundary, and reflect global chemical inflow to the U.S.

CMAQ, in particular, estimates ozone concentrations fairly well, with a slight high bias overall, but particularly near coastal areas [*Eder and Yu*, 2006]. Eder and Yu [2006] also find that CMAQ performs well for $PM_{2.5}$, with a slight positive bias that is reduced in summer time. The U.S. EPA [2005] found that CMAQ over predicts $PM_{2.5}$ by 9% and over predicts ozone, resulting in a $R^2$ value of 0.49 in the summer. A comprehensive seven-year evaluation was conducted by Zhang et al. [2014] who conclude that $PM_{2.5}$ is biased slightly high, but is within performance standards. Zhang et al. [2014] also conclude that ozone performance meets EPA criteria, with biases within +/- 0.15. Use of observational data sets, as a point of comparison, helps us to validate the use of CMAQ as a tool to further understand tropospheric pollution.

## Mexico emissions inventory

Because the LADCO 2007 inventory did not include emissions from Mexico, we supplemented the inventory with data from the Mexico National Emissions Inventory (NEI) 1999 version (Eastern Research Group and TransEngineering, 2006). 1999 is the newest year of which existing Mexico emissions are available. Pollutants reported by the Mexico NEI for motor vehicle, non-road mobile sources, and area source emissions are $NO_x$, $SO_x$, VOC, CO, $PM_{10}$, $PM_{2.5}$, and $NH_3$ and point source emissions excluding $NH_3$. Biogenic emissions were already calculated for the entire domain, including Mexico, using MEGAN version 2.10.

Each pollutant for every sector was reported in the Mexico NEI as a yearly value in Mg/yr by state. We then allocated each pollutant uniformly across each state in Mexico and separated evenly across the year. Unit conversions were calculated to either g/s or mole/s using molecular weights specified within the chemical mechanism of CMAQ. Emissions for motor vehicle, non-road mobile sources, and area sources were allocated in the lowest model layer, whereas point source emissions were distributed within the lowest seven layers, which were calculated to be at or below the average planetary boundary layer height for July 2007.

CMAQ does not accept $NO_x$, $SO_x$, VOC, $PM_{10}$, and $PM_{2.5}$ as direct inputs; they need to be separated into components. Each pollutant was separated according CMAQ 4.7.1

documentation (spec_def.conc). Separations are as follows:

$NO_x = 0.1 * NO + 0.9 * NO_2$

$SO_x = SO_2$

VOC = PAR * 0.04 + ETH * 0.05 + ETOH * 0.05 + OLE * 0.05 + TOL * 0.17 + XYL * 0.19 + FORM * 0.04 + ALD2 * 0.05 + ISOP * 0.12 + TERPB * 0.24

$PM_{10}$ = CCRS * 0.5 + PMC * 0.5

$PM_{2.5}$ = FCRS * 0.1666 + PEC * 0.1666 + PMFINE * 0.1666 + PNO3 * 0.1666 + POC * 0.1666 + PSO4 * 0.1666

Despite that these emissions were developed in 1999, we used them as inputs along with the 2007 inventory for simplicity and lack of available information to expand the inventory to the same year as the rest of the inventory.

## Observational data

To compare model data with observations, ground measurement data from the EPA's Air Quality System (AQS) Data Mart, and Clean Air Status and Trends Network (CASTNet) were obtained. To complement ground measurements, and provide broader spatial coverage, model data were also compared to satellite measurements of $NO_2$ from the Ozone Monitoring Instrument (OMI) onboard the Aura satellite.

OMI $NO_2$ data was obtained from the Tropospheric Emission Monitoring Internet Service (TEMIS) that was processed by the Royal Netherlands Meteorological Institute (KNMI) [*Boersma et al.,* 2007]. These data are output as column totals, and not readily comparable with the grid used. In order to conduct quantitative comparisons, satellite data need to be on the same grid as the model across the domain. In the standard Level-2 format, the data is provided as a 2600 km swath at a resolution of 13-26 km along the track, and 26-135 km across track, depending on the viewing angle [*Boersma et al.,* 2008]. To process the satellite data to the model grid, a tool called the Wisconsin Horizontal Interpolation Program for Satellites (WHIPS) is utilized. Using this tool, the Level-2 OMI $NO_2$ data was interpolated to a custom Level-3 product to match the grid layout of the CMAQ simulations. Because OMI $NO_2$ is output as column totals, an averaging kernel is applied to the CMAQ data to calculate a comparable metric, and CMAQ data are extracted to match the satellite overpass time. Although this satellite can give information over a larger area in comparison to the ground-based measurements, it only provides one early afternoon measurement per day, corresponding with the overpass time and frequency.

The statistics that will be utilized to analyze the model data against these observational datasets include: the correlation coefficient (mean-r), normalized mean bias (NMB), and normalized mean error (NME). The correlation coefficient ranges from -1 to 1, 1 showing the highest positive correlation, 0 showing no correlation, and -1 indicating negative correlation. The normalized mean bias was calculated by averaging the sum of daily model minus the satellite observations, then dividing by the average satellite observations, and the normalized mean error was calculated by averaging the absolute value of the model daily value minus the observation, then divided by the average of observations. Using these statistics, both satellite and ground-based measurements can be used to validate model data.

# Figures

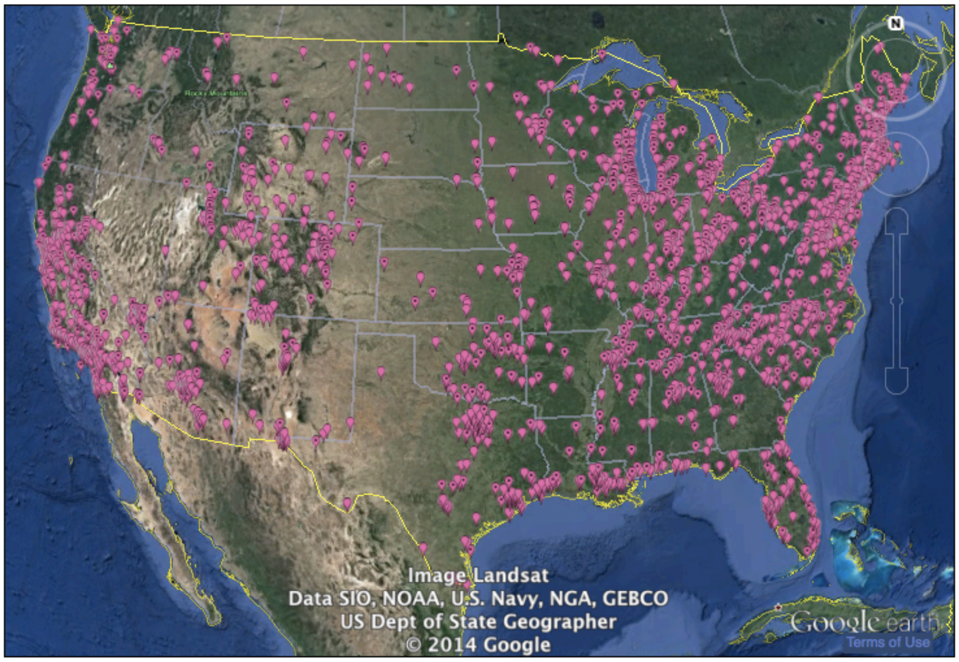


**Figure 2.1: EPA ozone monitor locations, both active and inactive.**

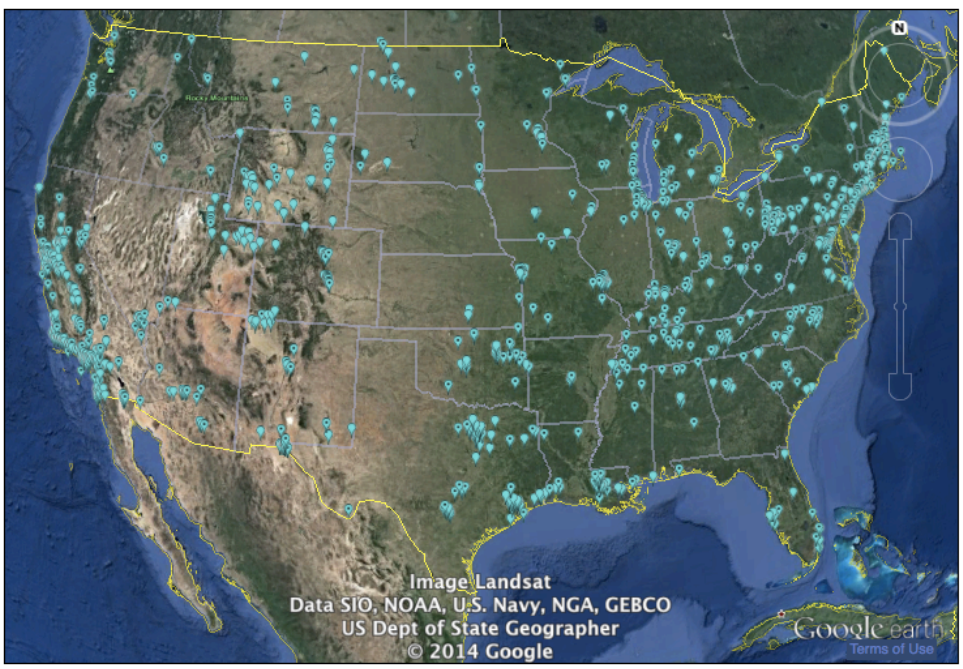


**Figure 2.2: EPA $NO_2$ monitor locations, both active and inactive.**

## References

Boersma, K.F., H.J. Eskes, J.P. Veefkind, E.J. Brinksma, R.J. van der A, M. Sneep, G.H.J. van den Oord, P.F. Levelt, P. Stammes, J.F. Gleason and E.J. Bucsela, Near-real time retrieval of tropospheric NO2 from OMI, *Atm. Chem. Phys.*, 2013-2128, sref:1680-7324/acp/2007-7-2103, 2007

Boersma, K. F., D. J. Jacob, E. J. Bucsela, a. E. Perring, R. Dirksen, R. J. van der A, R. M. Yantosca, R. J. Park, M. O. Wenig, and T. H. Bertram (2008), Validation of OMI tropospheric NO2 observations during INTEX-B and application to constrain NOxNOx emissions over the eastern United States and Mexico, *Atmos. Environ.*, *42*(19), 4480–4497, doi:10.1016/j.atmosenv.2008.02.004.

Byun, D., and K. L. Schere (2006), Review of the Governing Equations, Computational Algorithms, and Other Components of the Models-3 Community Multiscale Air Quality (CMAQ) Modeling System, *Appl. Mech. Rev.*, *59*(2), 51, doi:10.1115/1.2128636.

Carlton, A. G., P. V Bhave, S. L. Napelenok, E. O. Edney, G. Sarwar, R. W. Pinder, G. a Pouliot, and M. Houyoux (2010), Model representation of secondary organic aerosol in CMAQv4.7, *Environ. Sci. Technol.*, *44*(22), 8553–60, doi:10.1021/es100636q.

Eastern Research Group and TransEngineering (2006), MEXICO NATIONAL EMISSIONS INVENTORY, 1999

Eder, B., and S. Yu (2006), A performance evaluation of the 2004 release of Models-3 CMAQ, *Atmos. Environ.*, *40*(26), 4811–4824, doi:10.1016/j.atmosenv.2005.08.045.

Emmons, L. K. et al. (2010), Description and evaluation of the Model for Ozone and Related chemical Tracers, version 4 (MOZART-4), *Geosci. Model Dev.*, *3*(1), 43–67, doi:10.5194/gmd-3-43-2010.

Lee, C. J., J. R. Brook, G. J. Evans, R. V. Martin, and C. Mihele (2011), Novel application of satellite and in-situ measurements to map surface-level $NO_2$ in the Great Lakes region, *Atmos. Chem. Phys.*, *11*(22), 11761–11775, doi:10.5194/acp-11-11761-2011.

Skamarock, W. C., and J. B. Klemp (2008), A time-split nonhydrostatic atmospheric model for weather research and forecasting applications, *J. Comput. Phys.*, *227*(7), 3465–3485, doi:10.1016/j.jcp.2007.01.037.

US EPA (2005), CMAQ Model Performance Evaluation for 2001 : Updated March 2005, *Environ. Prot. Agency*.

US Environmental Protection Agency. Air Quality System Data Mart [internet database] available at http://www.epa.gov/ttn/airs/aqsdatamart. Accessed *May 29, 2013*.

Yarwood, G., S. Rao, M. Yocke, and G. Whitten (2005), Updates to the Carbon Bond Chemical Mechanism: CB05, *Yocke Co*.

# Chapter 3: Lightning Emissions Inventory

## Inventory development

The lightning inventory implemented in this research was developed based on the methodologies utilized in Koo et al. [2010]. Koo et al. [2010] estimated emissions by setting an amount of total nitrogen emissions by lightning per year, and allocating it spatially and temporally through cloud-top height and convective precipitation through the following equation:

$$E(\bar{x},t) = R_{NO}P_c(\bar{x},t)D(\bar{x},t)p'(\bar{x},t)$$

where $E(\bar{x},t)$ is the emissions rate of NO in mol/hr at the grid location $\bar{x}$ and time t, $R_{NO}$ is the NO emissions factor, $P_c(\bar{x},t)$ is the convection precipitation in m/hr, $D(\bar{x},t)$ is the convective cloud depth in meters, and $p'(\bar{x},t)$ is the pressure in Pascals. Koo et al. (2010) defined the emissions factor $R_{NO}$ as 3.9 x $10^{-12}$ by setting the summation of $E(\bar{x},t)$ to 1.06 Tg N per year. This value was a bit low in comparison to other studies, here I set $E(\bar{x},t)$ equal an average of those studies, to a value of 1.6 Tg N per year. As another difference from Koo et al. [2010], we employed a bimodal vertical distribution of NO emissions following Allen et al. [2012] (Figure 3.1a). Koo et al. [2010] applied a unimodal distribution shown in Figure 3.1b. The vertical profile from Allen et al. (2012) was also used because it is a newer model generated profile that was developed to capture IC and CG stokes in different vertical levels of the atmosphere, because of IC strokes only occurring higher in the atmosphere, and CG strokes extending down towards the surface. Whereas Allen et al. [2012] calculated the distribution over 16 layers, and here we include 27 layers.

Total lightning NO emissions for July 2007 show maximum values greater than 500 moles/hour, and are seen in the southeast area of the domain (Figure 3.2a). The highest emission total inland is in Florida, southeastern Texas and southern Louisiana. In these areas strong convective activity produces more frequent lightning [*Koo et al*., 2010]. Total emissions over the domain, are similar in spatial distribution and magnitude to Koo et al. [2010] (Figure 3.2b). Differences in magnitude could be due to differences in frequency and severity of convection from Koo et al. [2010] study year of 2002 and this study for 2007 (see Table 3.1 for a summary) as well as differences in the assumed NO per lightning strike. The emissions calculated here were similar to many other studies in distribution [*Cooper et al.,* 2006; *Bond et al.,* 2001; *Allen et al.,* 2012; *Fang et al*., 2010; *Smith and Mueller*, 2010], but different in magnitude. The magnitude is hard to compare with other studies due to the use of different and unreported metrics. Rough calculations put the values calculated here at about average between Cooper et al. [2006], Bond et al. [2001], Allen et al. [2012], Fang et al. [2010], Koo et al. [2010], and Smith and Mueller [2010].

## Discussion

### *$NO_2$ Discussion*

To fully examine the effects of lightning NO changes in $O_3$, VOC, $PM_{2.5}$, and $NO_x$ between the two CMAQ runs and AQS observations have been investigated. First I will look at changes in $NO_2$ concentrations between both CMAQ runs and the AQS observations. The AQS database generally provides information for $NO_2$ because $NO_2$ is a criteria pollutant regulated under the NAAQS. The AQS observations of $NO_2$ show the highest values (15 ppb to > 25 ppb) in California, Illinois, and along the upper east coast (Figures 3.3a). The highest concentrations are seen in highly populated areas, namely Los Angeles, San Diego, Chicago, and New York City (> 25 ppb). $NO_2$ monitors are typically located in populated areas, with anywhere from 1 monitor to greater than 10 per state.

$NO_2$ concentrations from both CMAQ runs show highest levels (>25 ppb) in the most populated areas, including the same list of cities as with the AQS data (Figures 3.3b and c). The most frequent values range from 0 to 3 ppb, and mostly occur in rural areas. As expected, lightning does not affect modeled $NO_2$ in these surface sites, and no difference between the CMAQ simulations is readily apparent in Figure 3.3.

To characterize the impact of lightning on surface $NO_x$, Figure 3.4 compares the base case (BC) run and the run including lightning. The largest percent difference (>80%) is located in the Gulf of Mexico, the North Atlantic Ocean, and off the west coast of Mexico (Figure 3.4). The largest changes are located in areas where $NO_x$ concentrations are the lowest. There are sporadic patchy areas of negative percent change, no greater than -2%, for which the cause is not known at this time. Because lightning contributes the most in remote areas with low total $NO_x$, absolute difference maps show close to zero change across the entire domain, between -0.25 ppb and 0.25 ppb (not shown). So, even though the percent change is large in areas for $NO_x$, the absolute change does not show more than a 0.5 ppb deviation from the base case.

CMAQ $NO_2$ can also be compared with the satellite retrieval of $NO_2$ from the Ozone Monitoring Instrument (OMI). Figure 3.5 shows a comparison of $NO_2$ between the CMAQ BC simulation (Figure 3.5a), the CMAQ lightning case (Figure 3.5b), and OMI (Figure 3.5c).

Higher concentrations of $NO_2$ are seen in the OMI data across the domain in comparison to both simulation, with the exception of large cities, like Chicago, New York City and Los Angeles, where CMAQ is higher by a range of 1-4 molecules/cm$^2$ x $10^{15}$ in each city (Figure 3.5a and b). Adding lightning emissions to CMAQ increased the $NO_2$ across the domain, most predominantly in the eastern U.S., showing a better correlation with the satellite data (Figure 3.5b and c). There is still the same difference between large cities, but the difference in the eastern U.S. decreased by about 1 molecules/cm$^2$ x $10^{15}$. These differences are also shown with statistics in Table 3.2.

Table 3.2 shows the temporal correlation coefficient (mean-r), normalized mean bias (NMB), and normalized mean error (NME) based on daily one-hour values. These calculations were conducted by comparing the daily average value of AQS and CMAQ against the single overpass time in the OMI data. Comparing CMAQ BC and lightning against OMI, mean-r increases from 0.08 to 0.12 when including lightning. This is indicative of a greater positive correlation between OMI and the lightning run, showing a 50% improvement in agreement. Still, day-to-day variation in OMI is not well captured by CMAQ, due perhaps to the model's ability to correctly estimate diurnal $NO_2$ change needed to capture the early afternoon values seen by OMI. The NMB increases in the lightning case, while NME decreases. This means that the CMAQ run with lightning has less error and bias as compared to the satellite observations.

A comparison with AQS was also conducted. The statistics are all the same between AQS and the two CMAQ runs because lightning has little affect on surface, urban $NO_2$. The error and bias are much less between these two data sets than with the model against the satellite. The mean r is much larger between CMAQ and AQS, at 0.64 versus about 0.1 for the satellite against the model. This indicates a higher correlation of CMAQ with AQS data vs. CMAQ and the satellite data. It should be noted that the agreement between observational datasets (OMI $NO_2$ and AQS data) shows a much higher correlation (0.7) than when either observation dataset shows against either model simulation.

### *Ozone Discussion*

Observational data of 8-hour maximum average ozone has been obtained from the AQS database, and is compared with the two CMAQ runs in this section. Maximum values of ozone from the AQS database for July 2007 are seen in southern California and Colorado, with values greater than 75 ppb (Figure 3.6a). Minimum values of about 25-35 ppb are located in southern Texas and Louisiana. The most frequent values range from 50-65 ppb across most of the U.S. There are more ozone than $NO_2$ monitors, allowing for a widespread area to be covered, and evaluated with direct measurements.

The locations of highest values in the observational data have similar spatial distributions to the CMAQ runs, but ozone concentrations in the model runs are too high (Figures 3.6b and c). Elevated values are seen across the upper east coast, over the lower Great Lakes, the Ohio River Valley, Southeast U.S., and California, ranging from 55 to greater than 75 ppb for both runs. Locations of higher concentrations appear to be correlated with areas of higher population centers. Minimum values are located in the far northern and southern areas of the domain. The lightning shows similar spatial distribution as compared to the BC and lightning runs, with slightly elevated values (about 5ppb) located in the southeastern portion of the U.S. This increase is spatially correlated with the areas of increase $NO_2$ seen in Figure 3.2a. It is hard to visibly see the differences between both runs, so percent difference and absolute change are present in Figures 3.7a and b.

The percent difference in ozone with the addition of lightning $NO_x$ shows a mostly positive difference with maxima around 15%. These differences are seen in the southern and southeastern section of the domain, with about a 3 to 4 ppb maximum change in ozone in that area. The region of largest change, seen in this research, is similar to Koo et al. [2010], who stated that this area typically sees the largest changes due to strong convective activity and increases in biogenic VOC emissions. This also coincides with the area of the largest increase in NO lightning emissions seen in Figure 3.2a. This research then shows that on average, adding lightning $NO_x$ in the model can impact ground concentrations of ozone, by 0 - 3 ppb. This is similar, but less than, the results seen in Koo et al. [2010], who concluded that implementing their lightning emissions inventory in CMAQ resulted in a 0 - 6 ppb increase.

Further comparing CMAQ output with observations, time series data from three CASTNet sites were obtained. Two of the sites are located in rural areas, and one site in an urban area. The first rural site is located in Macon County, NC (latitude 35.06, longitude -83.43), and the second rural site is in Liberty County, FL (latitude 30.11, longitude -84.99). Overall, both CMAQ runs followed the same trend as at the CASTNet sites, but the magnitude in both runs were almost always larger, more so in NC than in FL (Figures 3.8a and b). In both counties, the largest deviations between observational and model output is seen in the daily minima. The model does not perform well in predicting the overnight decrease in ozone each day, but more so in NC than FL. The model seems to capture the daily fluctuations in ozone better in Liberty County, FL, matching much better with the daily minima. The lightning run is always larger or equal in magnitude to the BC run, and both runs are larger in magnitude than the observations. Because the lightning run is even larger than the BC, the lightning deviates further from the observations. This deviation is on the order of 0 to 3 pbb in NC and 0 to 5 ppb in FL. The lightning inventory developed here generated higher levels of NO in Florida as opposed to North Carolina, which allowed for the larger 0-5 ppb deviation in FL.

The final CASTNet site analyzed here is an urban site, located in Blount County, TN (latitude 35.63, longitude -83.94; Figure 3.8c. Here, both CMAQ runs and the observational data match fairly well for this location in both magnitude and trends. The ozone from the lightning run at this location is higher than the BC run, which seems to match the observations equally as well due to the observations frequently exceeding the model runs on multiple occasions. This may indicate the model performs better for urban sites as opposed to rural sites.

### *Additional Species*

In efforts to fully analyze each scenario, $SO_2$, $PM_{2.5}$, and VOC concentrations have also been examined. Changes in $SO_2$ are minimal, with a maximum percent decrease of about 7%, located off the southwest coast of Florida (Figure 3.9). The majority of the changes in $SO_2$ are seen over the Gulf of Mexico, and off the southeast coast of the U.S. The largest decrease in $SO_2$ over land is located in the south-central portions of the U.S. and north-central Mexico, with a maximum of a 2% decrease. The absolute difference of $SO_2$ between the lightning and BC runs are minuscule, with ranges between -0.25 and 0 ppb.

Changes in $PM_{2.5}$ are also very minimal, but unlike $SO_2$, show an overall increase in concentrations. This maximum increase is about 1-3%, and is located over the central and southeast portions of the U.S. (Figure 3.10). The largest values are located in select few places in Florida, and south of Cuba. The absolute differences between these two runs are minimal, at a maximum 0.25 $ug/m^3$, and show no distinct pattern across the domain.

Changes in VOC concentrations occur across most of the U.S., northern Mexico, the Gulf of Mexico, and off the east coast of the U.S. (Figure 3.11a). The percent difference is an overall decrease with maxima of about 10%, located in the Gulf of Mexico, and the Atlantic Ocean. The average percent difference across the rest of the U.S. is about a 2% decrease. The areas of largest decreases over land are in Florida, south-central U.S., and northern Mexico, with values around -4%. The largest absolute differences are located in western Mexico, Mississippi, Alabama, Georgia, and Florida, with values at about 1 ppb decrease (Figure 3.11b). The absolute differences across the northern half of the U.S. is about zero, with the southern half averaging around a 0.75 ppb decrease.

# Figures

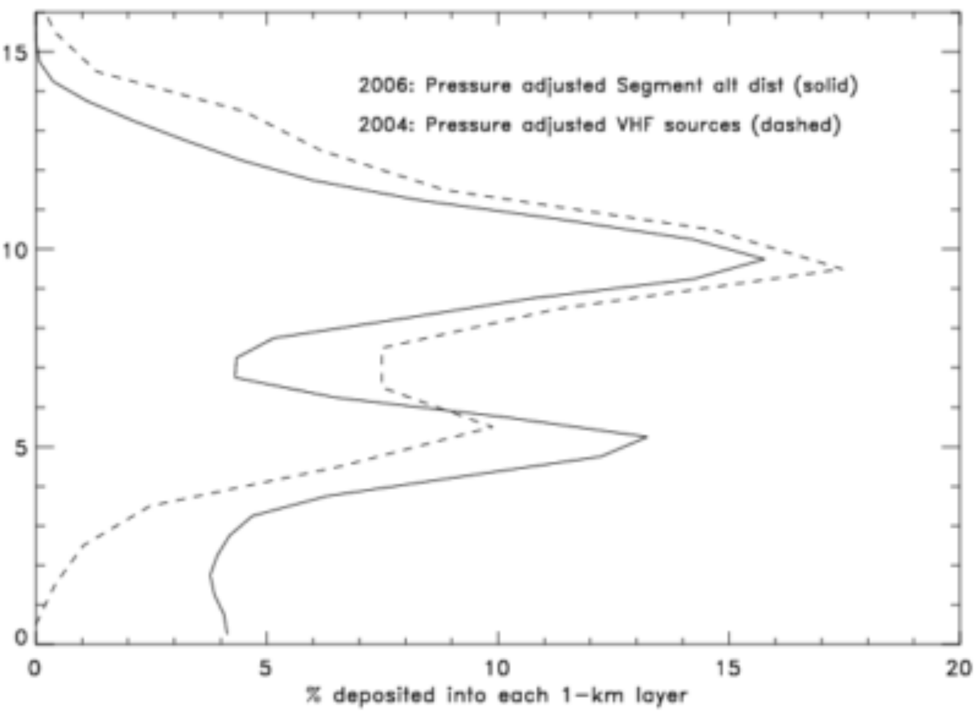


**Figure 3.1a: Vertical profile of lightning NO production for 2004 (dashed) and 2006 (solid) from Allen et al. (2012).**

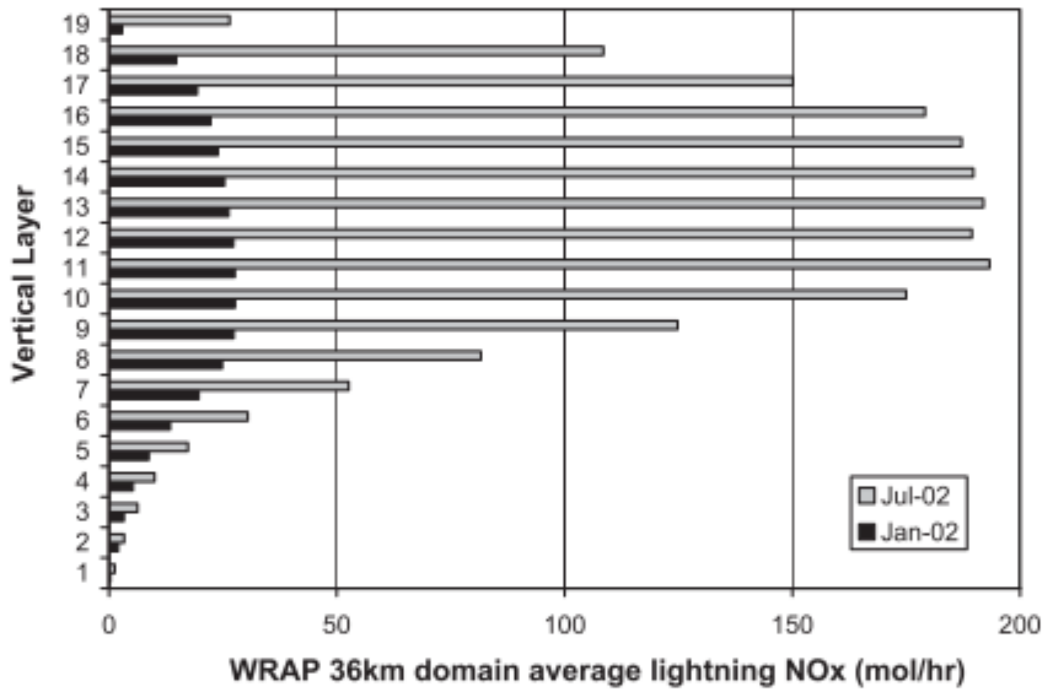


**Figure 3.1b: Vertical profile of domain averaged lightning $NO_x$ emissions, averaged over January and July 2002 in Koo et al. (2010).**

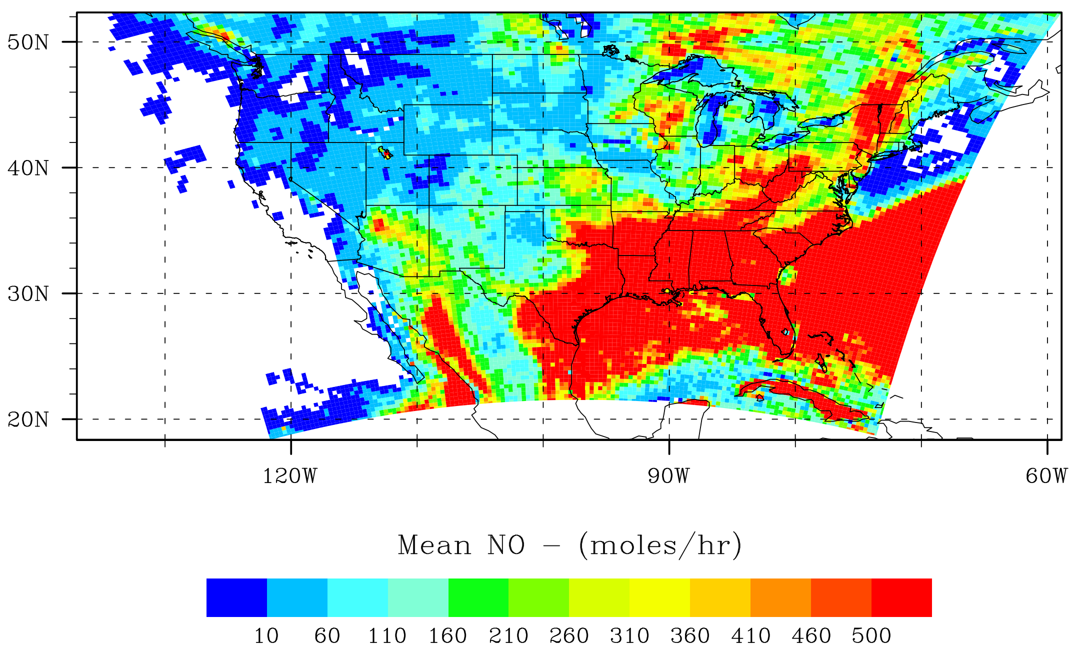


**Figure 3.2a: Averaged column total lightning $NO_x$ emissions in moles/hr.**

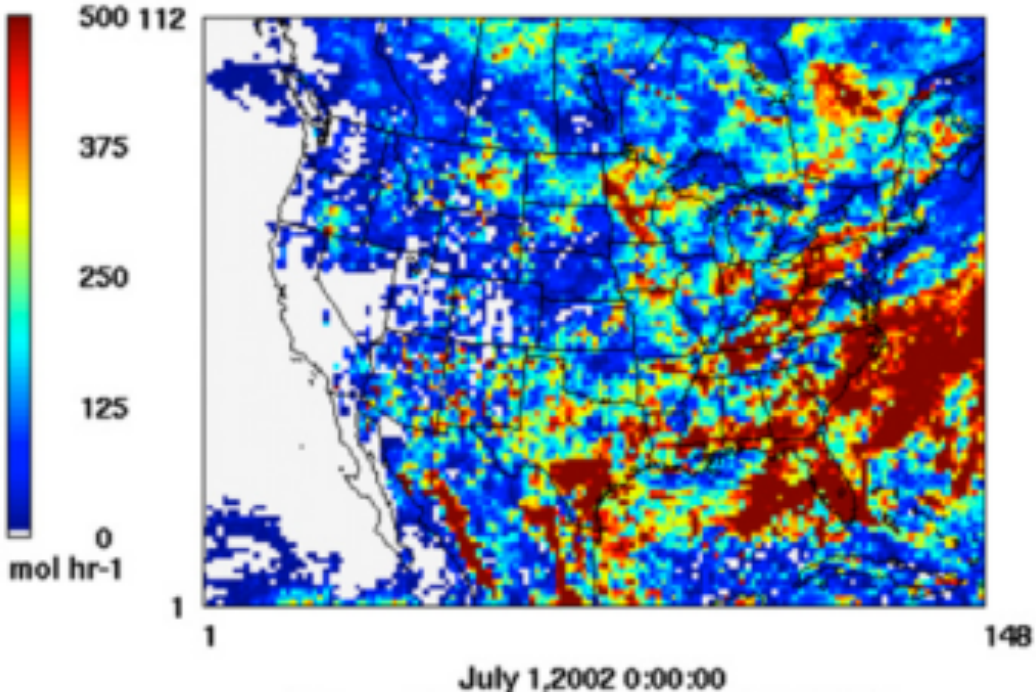


**Figure 3.2b: Lightning emissions of $NO_x$ for Koo et al., (2010) for July 2002. Values were determined by averaging column totals.**

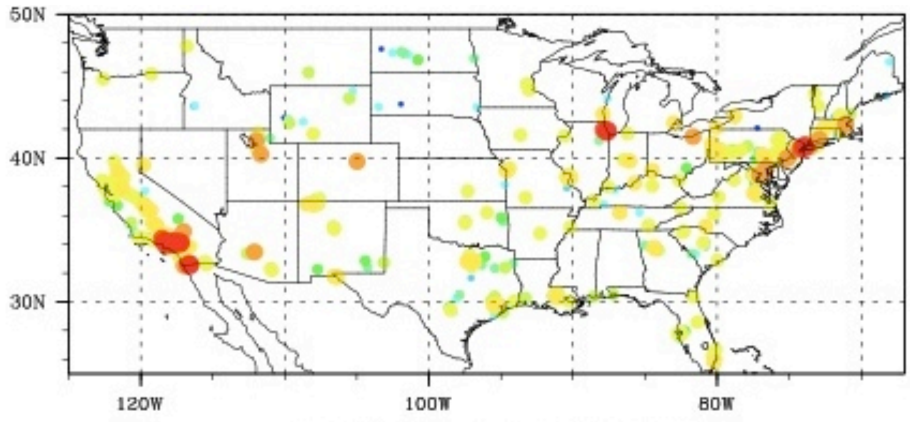


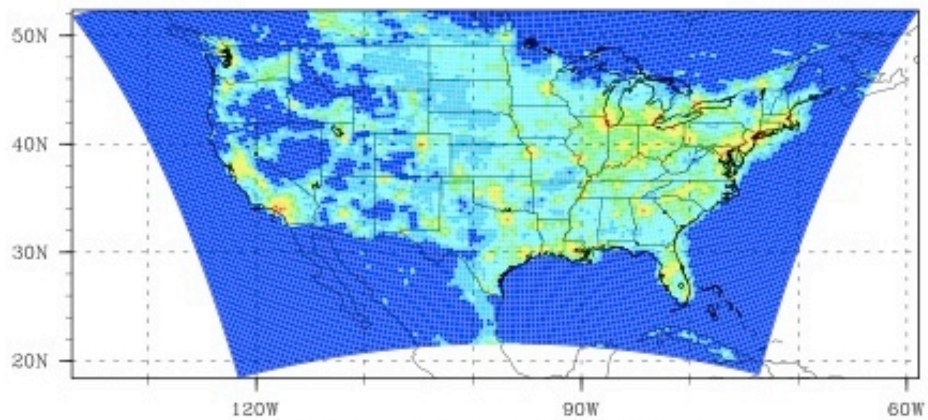


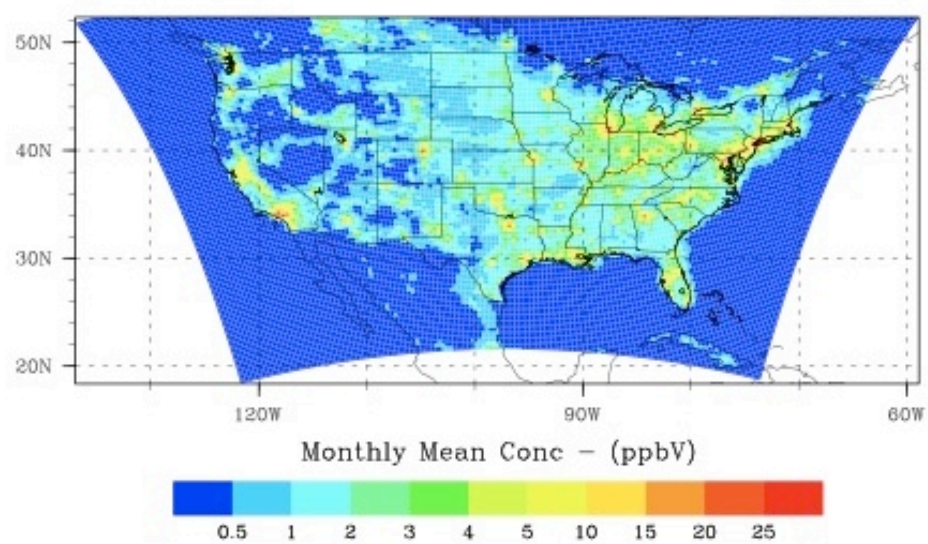


**Figure 3.3: Mean NO2 concentrations for July 2007 in ppb for a) (top) AQS data, b) (middle) CMAQ base case, and c) (bottom) CMAQ with lightning.**

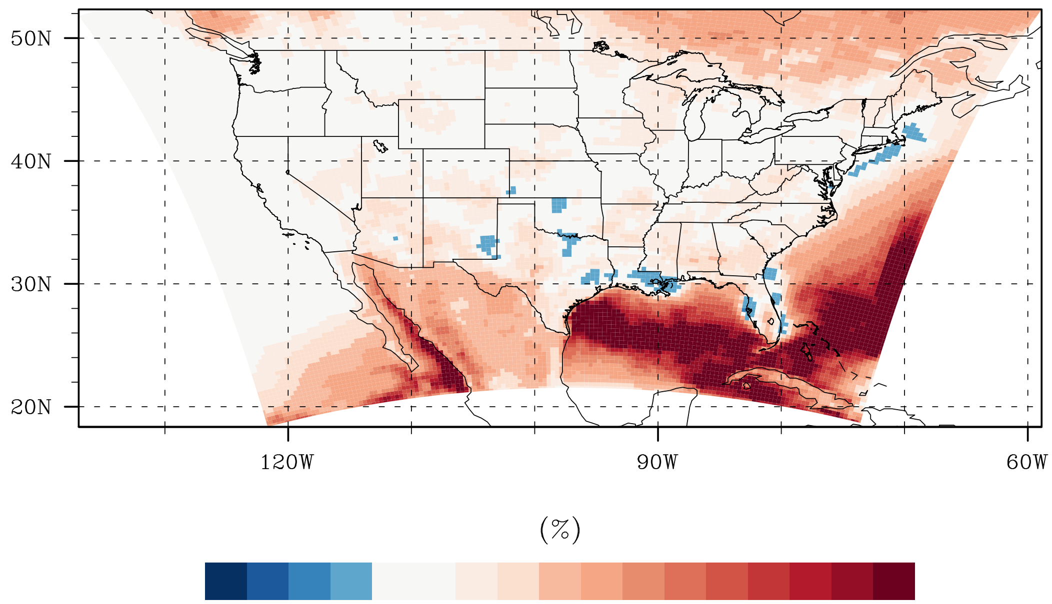


**Figure 3.4: Percent difference of $NO_x$ between lightning and BC simulations.**

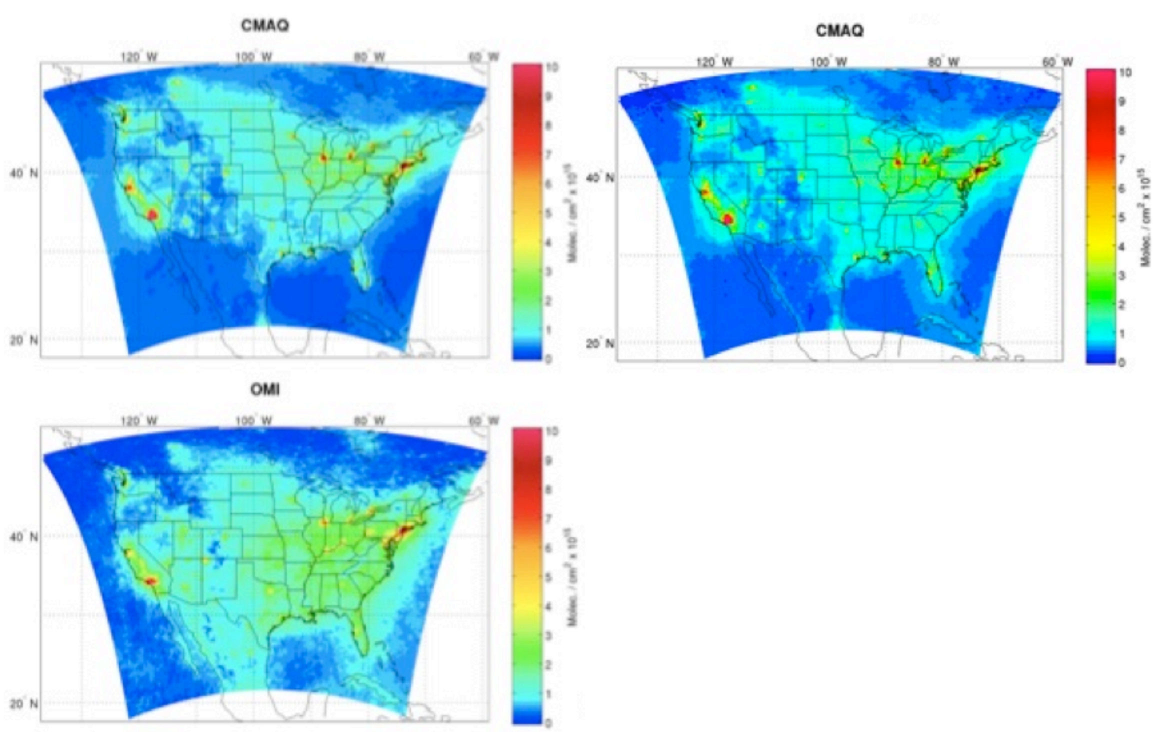


**Figure 3.5: a) (top left) BC CMAQ $NO_2$ calculated using the OMI $NO_2$ averaging kernel then averaged over the month. b) (bottom left) OMI $NO_2$ converted from level 2 to level 3 using WHIPS, c) (top right) Lightning CMAQ $NO_2$ calculated using the OMI $NO_2$ averaging kernel then averaged over the month.**

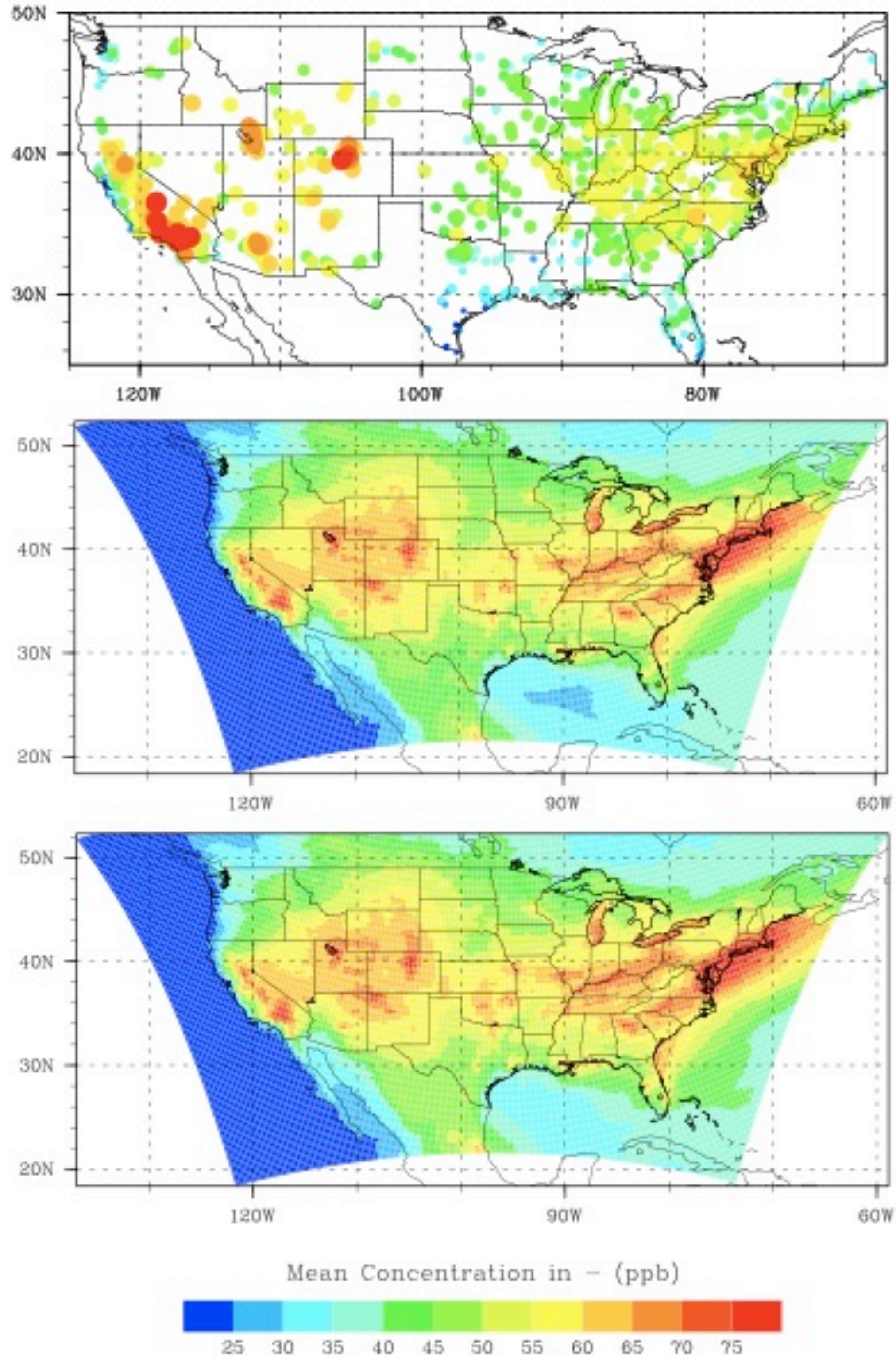


**Figure 3.6: a) (top) AQS observational maximum 8-hour average ozone concentration for July 2007, b) (middle) CMAQ base case maximum 8-hour average ozone concentration for July 2007, and c) (bottom) CMAQ lightning case maximum 8-hour average ozone concentration for July 2007.**

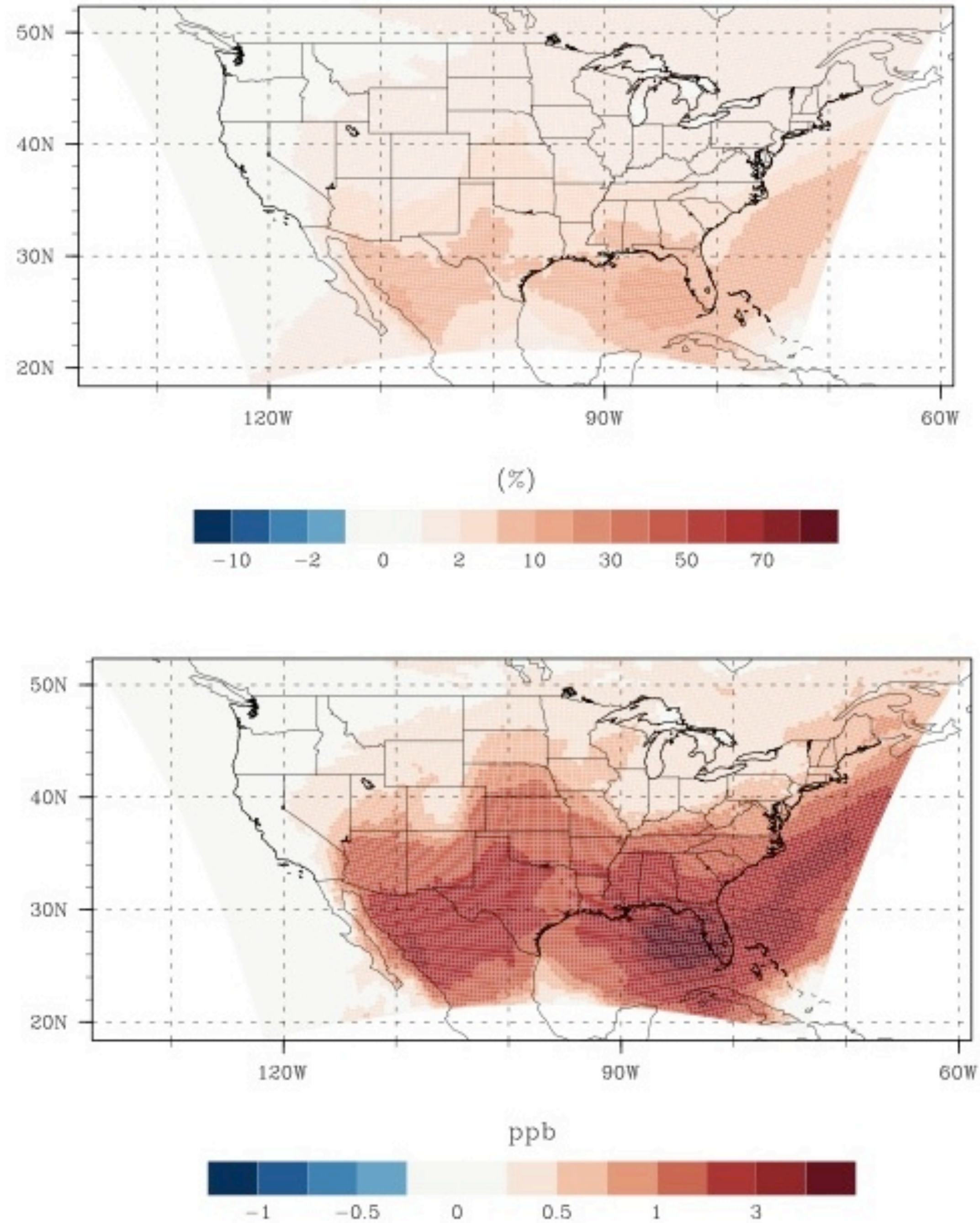


**Figure 3.7: a) (top) CMAQ 8-hour ozone percent difference between the lightning and base case and b) (bottom) CMAQ 8-hour ozone percent difference between the lightning and base case.**

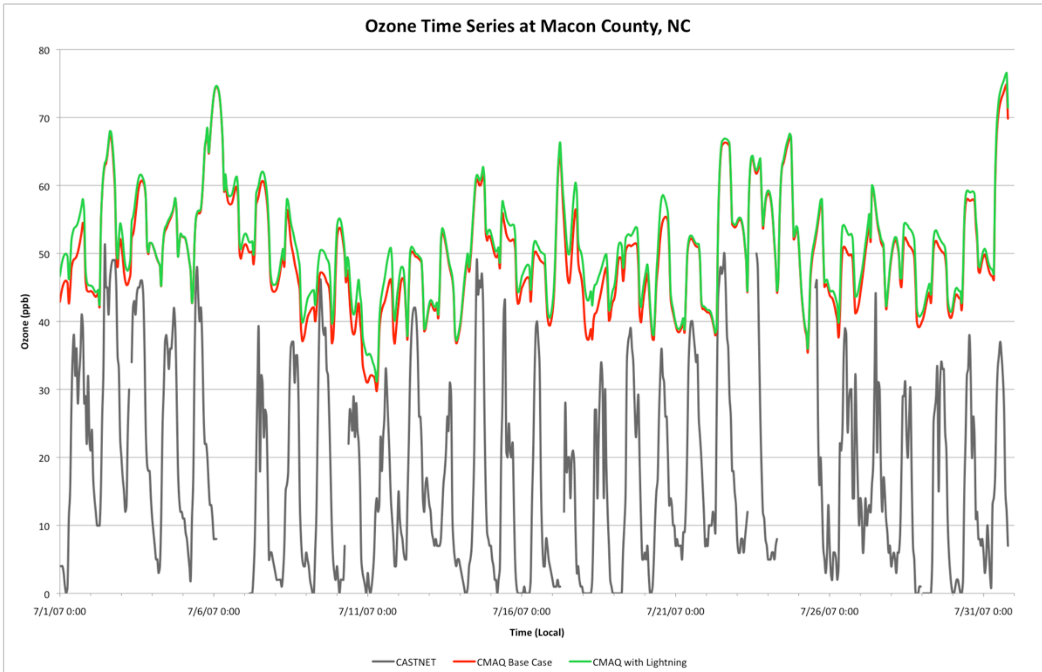


**Figure 3.8a: Ozone time series a rural location in Macon County, NC. Gray line is CASTNet observations, the green line in CMAQ with lightning, and the red line is the BC. The time series is taken from July 2007.**

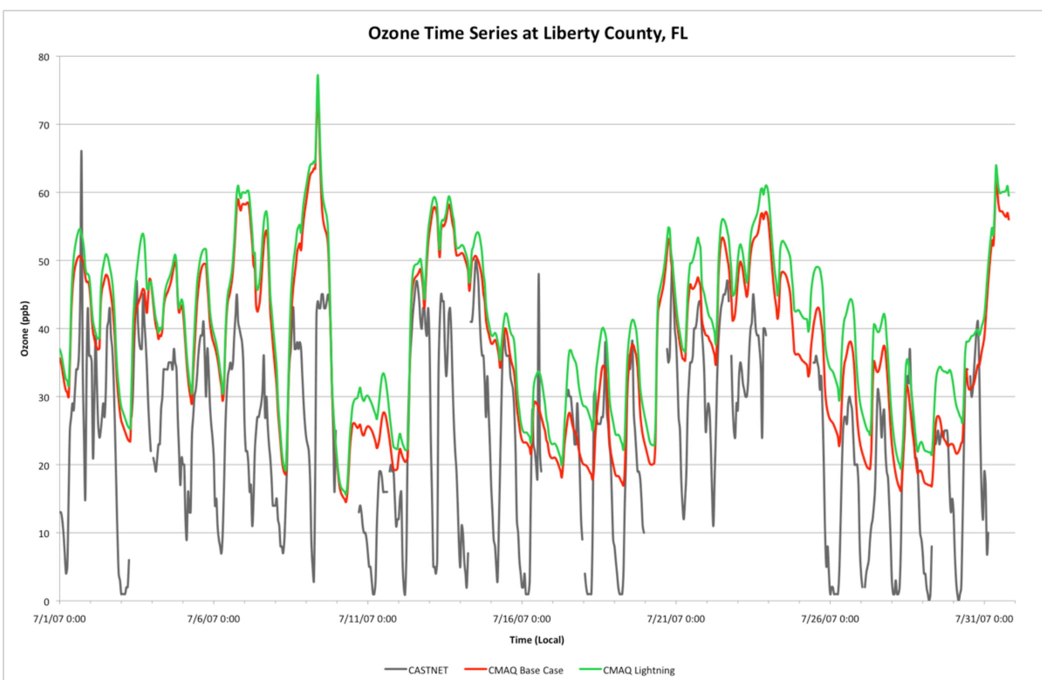


**Figure 3.8b: Ozone time series a rural location in Liberty County, FL. Gray line is CASTNet observations, the green line in CMAQ with lightning, and the red line is the BC. The time series is taken from July 2007.**

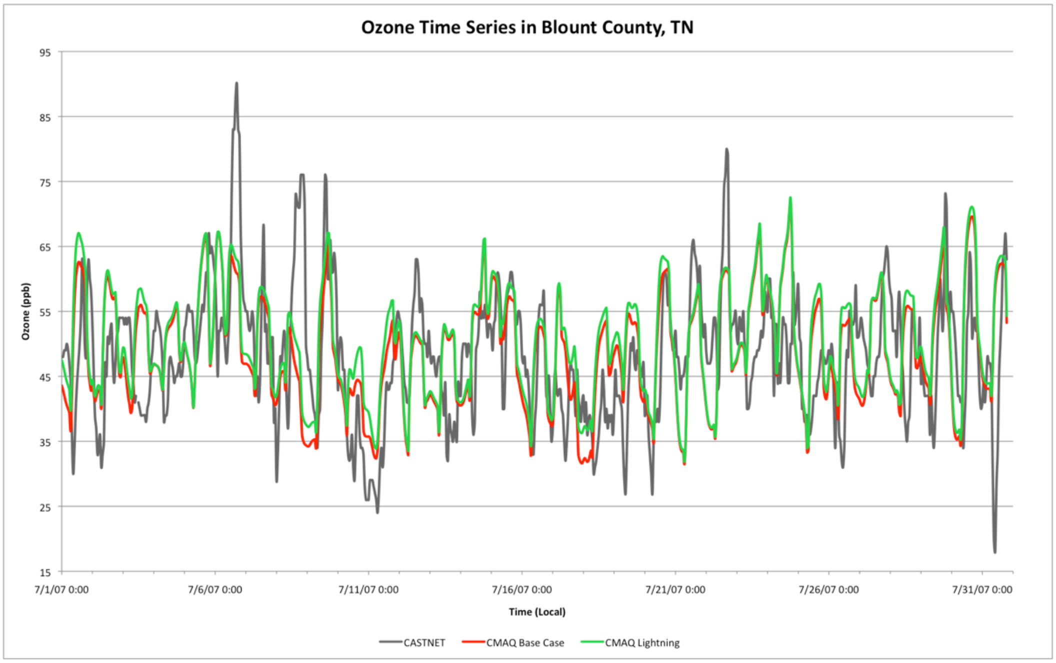


**Figure 3.8c: Ozone time series at an urban location in Blount County, TN. Gray line is CASTNet observations, the green line in CMAQ with lightning, and the red line is the BC. The time series is taken from July 2007.**

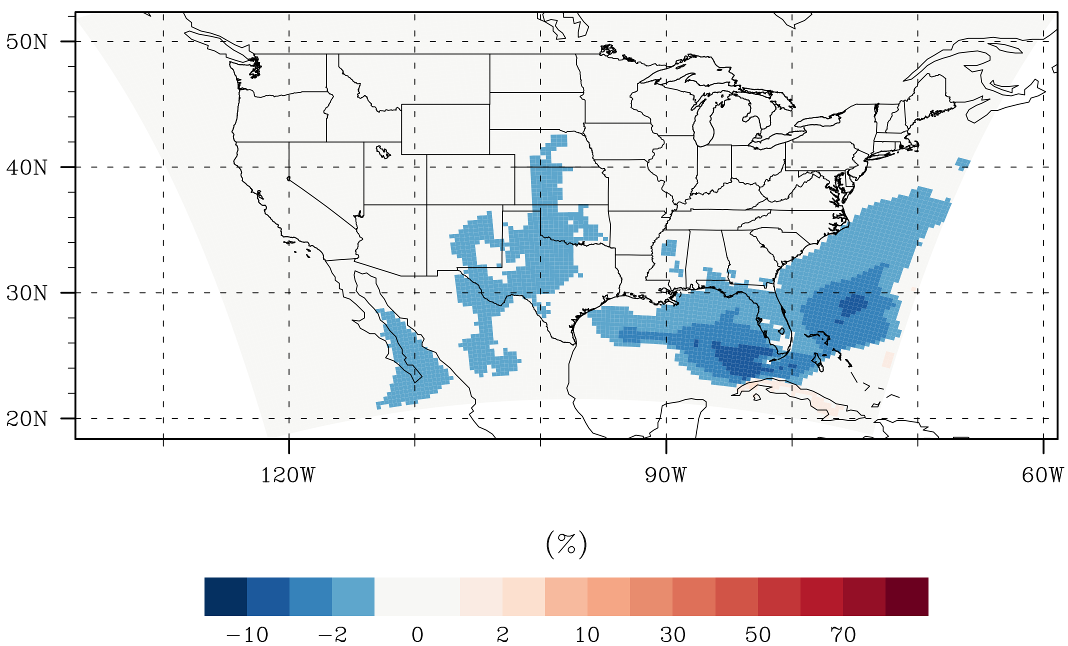


**Figure 3.9: Percent difference in $SO_2$ between the lightning and BC simulations.**

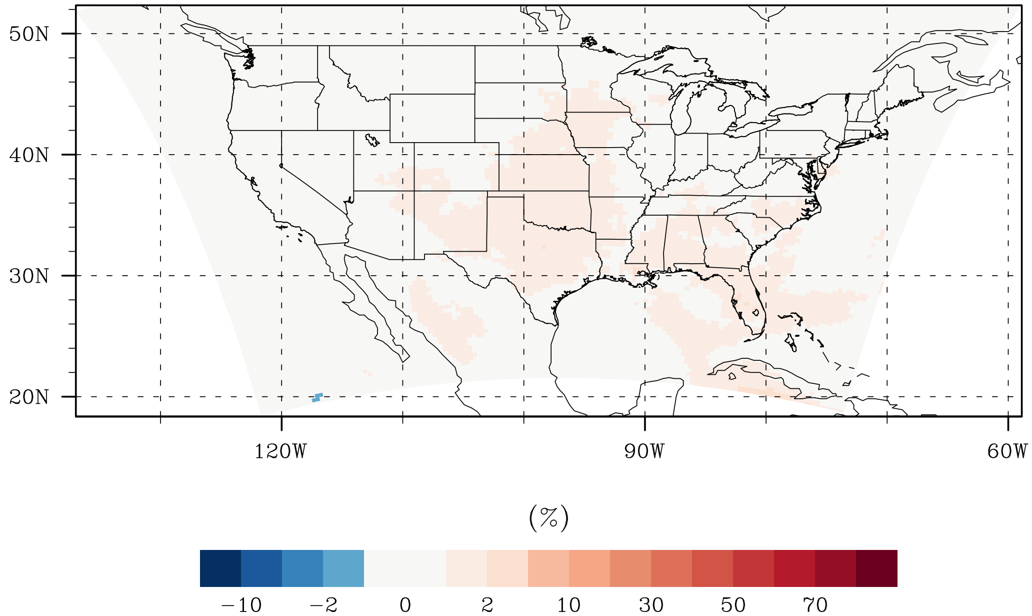


**Figure 3.10: Percent difference in $PM_{2.5}$ between the lightning and BC simulations.**

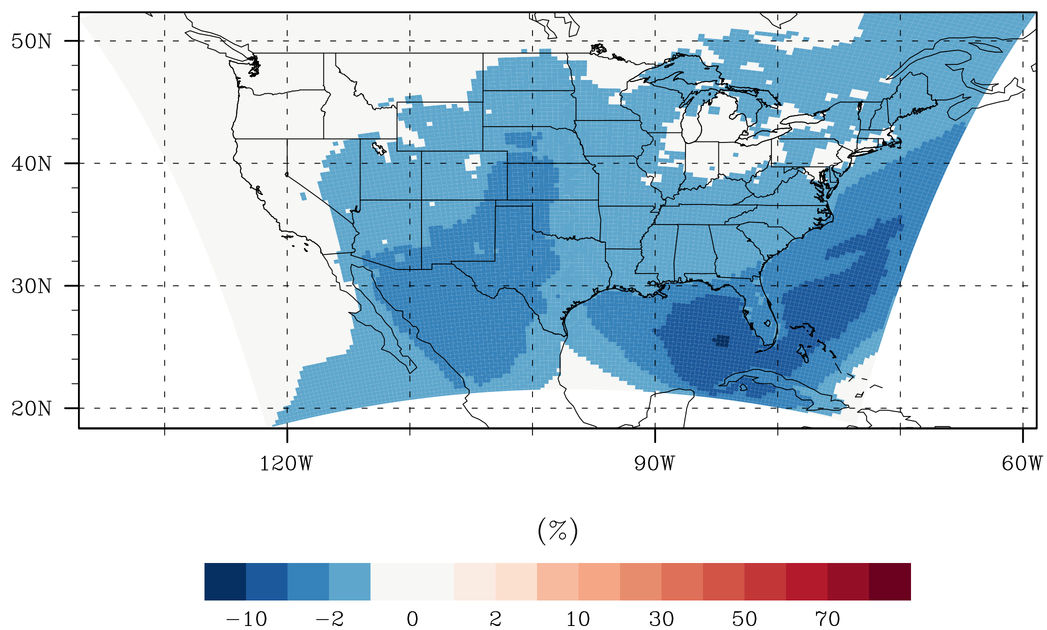


**Figure 3.11a: Percent difference in VOC concentrations between lightning and BC simulations.**

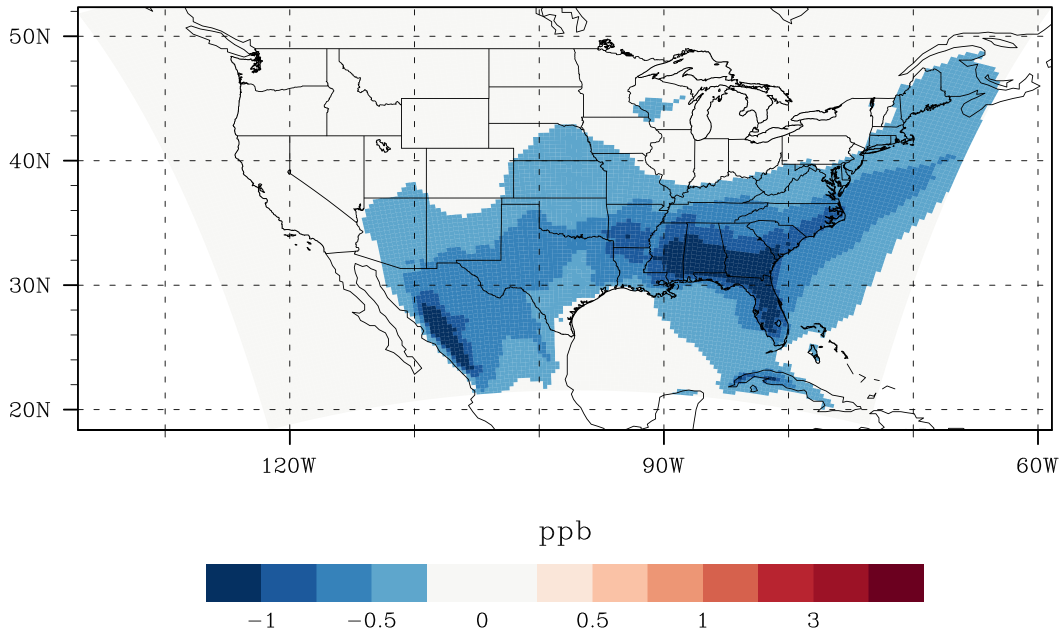


Figure 3.11b: Absolute difference in VOC concentrations between the lightning and BC simulations.

# Tables

| | Year Modeled | Sum of Emissions per year (Tg N/yr) | Vertical Distribution | Model Used |
|---|---|---|---|---|
| Koo et al. (2010) | 2002 | 1.06 | unimodal | CMAQ |
| This study | 2007 | 1.6 | bimodal | CMAQ |

Table 3.1: Comparison between this study and Koo et al. (2010)

| | Modeled vs. Satellite | | Modeled vs. AQS Observations | | OMI vs. AQS |
|---|---|---|---|---|---|
| | BC | BC +Lightning | BC | BC +Lightning | Observations |
| r | 0.08 | 0.12 | 0.64 | 0.64 | 0.70 |
| NMB | -21.88 | -15.26 | -0.02 | -0.02 | |
| NME | 60.52 | 56.86 | 0.44 | 0.44 | |

Table 3.2: Mean r, normalized mean bias (NMB), and normalized mean error (NME) between model and satellite (left), AQS and model (middle), and OMI vs. AQS (right) at the AQS locations across the CONUS domain.

## References

Allen, D. J., K. E. Pickering, R. W. Pinder, B. H. Henderson, K. W. Appel, and a. Prados (2012), Impact of lightning-NO on eastern United States photochemistry during the summer of 2006 as determined using the CMAQ model, *Atmos. Chem. Phys.*, *12*, 1737–1758, doi:10.5194/acp-12-1737-2012.

Bond, W., R. Xhang, X. Tie, G. Brasseur, G. Huffines, E. Orville, and J. Boccippio (2001), NOx production by lightning over the continental United States, *J. Geophys. Res.*, *106*(D21), 27,701–27,710.

Cooper, O. R. et al. (2006), Large upper tropospheric ozone enhancements above midlatitude North America during summer: In situ evidence from the IONS and MOZAIC ozone measurement network, *J. Geophys. Res.*, *111*(D24), D24S05, doi:10.1029/2006JD007306.

Fang, Y., a. M. Fiore, L. W. Horowitz, H. Levy, Y. Hu, and a. G. Russell (2010), Sensitivity of the NO y budget over the United States to anthropogenic and lightning NO x in summer, *J. Geophys. Res.*, *115*(D18), D18312, doi:10.1029/2010JD014079.

Koo, B., C.-J. Chien, G. Tonnesen, R. Morris, J. Johnson, T. Sakulyanontvittaya, P. Piyachaturawat, and G. Yarwood (2010), Natural emissions for regional modeling of background ozone and particulate matter and impacts on emissions control strategies, *Atmos. Environ.*, *44*, 2372–2382, doi:10.1016/j.atmosenv.2010.02.041.

Smith, S. N., and S. F. Mueller (2010), Modeling natural emissions in the Community Multiscale Air Quality (CMAQ) Model–I: building an emissions data base, *Atmos. Chem. Phys.*, *10*(10), 4931–4952, doi:10.5194/acp-10-4931-2010.

# Chapter 4: Sensitivity of Lake-County and Sectoral Reductions in Anthropogenic Emissions

## Differences in model data

The setup of CMAQ for this section is similar to that described in Chapter 3, with several exceptions as follows. For this chapter, the meteorology and air quality were simulated at a 12 km x 12 km resolution over the Great Lakes Region. The WRF meteorology was generated using the Grell Convection Scheme instead of Kain-Fritsch Cumulus Parametarization. The emissions inventory was the same version, LADCO base C July 2007, just at a 12 km x 12 km resolution. This work was conducted prior to the developments of the lightning and Mexico inventories, so none of those are included here. Other than those exceptions, the model runs were set up and executed the same as in Chapter 3.

## Description of scenarios

The motivating factor for these scenarios was to quantify the sources of NAAQS exceedances in the counties around Lake Michigan. Our hypothesis was that pollution sources directly bordering the lake have the largest impact on the amount of ozone pollution that builds up over the lake. To test this hypothesis, three scenarios involve altering emissions in the counties that directly surround Lake Michigan. One of these scenarios eliminates all emissions from the lake bordering counties, which will now be called Zero-LC. The next scenario reduces all emissions in the lake bordering counties by 50%, which will be called 50%-LC. The last scenario that alters emissions around the lake involves a reduction in motor vehicle emissions by 50% in the counties bordering Lake Michigan, which will from now on be called MV-LC. Motor vehicle emissions were targeted because it has been concluded that emissions from motor vehicles are the largest contributors to VOC emissions near the shore of Lake Michigan [*Foley et al.,* 2011], and because motor vehicle emissions account for about half of the $NO_x$ emissions in the U.S. [*Logan*, 1983]. Another reason for this reduction in all motor vehicle emissions, both non-road and on-road, is because Foley et al. [2011] concluded that changes between $NO_x$ and VOC limited regimes around Lake Michigan was a result of alterations in motor vehicle traffic near the lake. To further analyze the affects of motor vehicle emissions across the domain, the last scenario is a reduction of all motor vehicle emissions across the domain by 50%, which will now be called MV-All. In total, there are five CMAQ runs performed for this section, including the base case (BC). All of these scenarios were chosen to assess the source contributions, and the affects on pollution around Lake Michigan.

## Discussion

### *Ozone Discussion*

Ozone concentrations from the AQS database show the highest values in Ohio River Valley, with maxima around 60 ppb (Figure 4.1a). The lowest concentrations are between 30-35 ppb, and are located in the upper west portion of the domain. The BC simulation results in much higher concentrations as compared to the observations (Figure 4.1b). The largest concentrations are located in the Ohio River Valley, as with the AQS, but the concentrations range from 65-75 ppb, about 5 to 10 ppb higher than the observations. There are also maxima over the Great Lakes, most notably over Lake Michigan, Lake Erie, and

Lake Ontario, with values ranging from 65-75 ppb. Unfortunately, there are no monitor in/on the lake for comparison. Most of the domain experiences concentrations around 55 ppb. The lowest concentrations are located in the upper quarter of the domain, reaching minima of about 30 ppb. As an extreme test case, we zero out all emission in all counties adjacent to the lake.

The Zero-LC scenario displays lower ozone concentrations, most notably, over Lake Michigan (Figure 4.1c). Concentrations over Lake Michigan, which peak at 75 pbb in the BC, are reduced to a maximum of 55 ppb for the Zero-LC. Concentrations over the Ohio River Valley, and the remaining Great Lakes, also show reductions of around 2-5 ppb. The 50%-LC scenario results in fewer reductions across the domain, and over Lake Michigan (Figure 4.1d). The concentrations over Lake Michigan reduce by about 10 ppb. Concentrations over Lake Erie, Lake Ontario, and in the Ohio River Valley show less of a spatial reduction as compared to the Zero-LC. The MV-LC scenario (Figure 4.1e), produces the largest change over Lake Michigan, with reductions around 5 ppb near the lower east portion of the lake. The remaining differences are difficult to visibly detect. The reduction in motor vehicle emissions across the domain results in a larger reduction over Lake Michigan, and the entire domain than the MV-LC scenario (Figure 4.1f). The MV-All scenario results in the largest spatial decrease, with many locations showing a reduction in ozone concentrations by about 5 ppb. Lake Michigan experiences reductions of about 5 pbb, but over a larger area as compared to the MV-LC. To further quantify these reductions, absolute and percent differences in ozone will be discussed further.

The scenario of zero emissions from lake counties around Lake Michigan (Zero-LC), yield a maximum decrease in concentrations around 20% (Figure 4.2a), or about 16 ppb

(Figure 4.2b). Zero-LC impacts extend over most of Michigan, averaging around a 4% decrease in ozone relative to the base case, and a 1-15 ppb absolute reduction. There is a slight increase in concentrations in Milwaukee and Chicago of about 1 ppb or about a 1% decrease. Reductions in lake county emissions affect many states around the Great Lakes Region, some as far south as Virginia and as far west as western Ohio and Missouri. This scenario generated the largest changes in ozone concentrations of all scenarios examined.

Reducing motor vehicle emissions in the Lake Michigan bordering counties by 50% (50%-LC) reduces above-lake ozone by about 10% or 7ppb (Figure 4.3a and b). These changes extend to the east over Michigan, with maximum decreases up to 8%. There is a slight 1% increase in Milwaukee and Chicago for this run as well, which is only about a maximum of 1 ppb increase. Reductions of over 1 ppb reach across about one quarter of the domain, through Wisconsin, Michigan, Illinois, Ohio, Indiana, and Canada. Overall, the pattern of change is similar to Zero-LC, but of lesser magnitude.

The next run also altered emissions from the Lake Michigan bordering counties, but this time only a reduction in motor vehicle emissions was implemented (MV-LC). The largest reductions in ozone are located in more sporadic areas in this run than the previous two (Figure 4.4a). The largest decrease is between a 1 and 4% reduction, mainly seen over the northern portion of Lake Michigan, and the western half of Michigan. This run produced the greatest areas of increases, again in the Milwaukee and Chicago areas. This increase is still very small, around 1 ppb, but does reach farther north and south of Milwaukee, and west of Chicago than previous scenarios (Figure 4.4b). There is a maximum absolute difference of between 1 and 4 ppb across the eastern side of Lake Michigan and western Michigan. The remainder of the domain does not experience changes of more than 1% or 1 ppb.

The final scenario analyzed here is a domain-wide reduction in motor vehicle emissions by 50% (MV-All). This reduction invokes a 4 to 8% reduction across most of the domain (Figure 4.5a). The far north and western portions of the domain experience the least amount of change (about 1 – 4%), along with areas surrounding Chicago and Milwaukee. There are areas of minimal change in Milwaukee and Chicago, with a slight increase in the Chicago area. The absolute difference calculated for this scenario shows a reduction of between 1 and 4 ppb across most of the domain. Maximum changes are locating around the Ohio River Valley, with values around a 5 ppb decrease. The change in Milwaukee and Chicago are minimal, from 0 to a 1 pbb increase. This run, as expected, produced the largest changes over the largest area, but did not decrease ozone in and around the lake, more than the zero emissions from lake bordering county run.

Each reduction scenario showed some increases in concentrations over Milwaukee and Chicago, as opposed to the decreases that were seen across the remainder of the domain. Because of this, data from both cities were extracted, and analyzed. First, is a time series of 8-hour maximum ozone in Chicago during all of July 2007 (Figure 4.6). The 8-hour ozone for each run (total of five including the BC) was plotted along with the EPA standard for ozone (75 ppb) and the AQS data for each city. Each run shows similar concentrations with the rest for most of the time series, but the AQS ozone date measurement only matches well for the final third of the time series. Most of the ozone concentrations in Chicago stay below the AQS standard, with the exception of July 27$^{th}$. For this date, all runs were above the standard, and the AQS measurement was below. In most instances, the Zero-LC scenario generated lower ozone values throughout the time series, with the exception of the 16$^{th}$ through the 19$^{th}$. During this stretch of time, the Zero-LC and 50%-LC scenarios show an increase in ozone, while the other three scenarios (including the BC) show a decrease. The largest deviation between runs for this period of time is about 15 ppb. Looking through animations of the ozone fluctuation over that time period (not pictured here), there is a significant decrease in ozone during the overnight hours that lingers in the BC run, but not in the Zero-LC scenario. Further comparison of these runs, using percent difference and absolute difference calculations are utilized next.

The absolute difference shows an overall increase in ozone concentration in Chicago for all of July, except for the Zero-LC scenario (Figure 4.7a). On average, ozone decreased by 1.6 ppb for the month in the Zero-LC scenario. The largest average increase, of 2.5 ppb, occurred in the 50%-LC scenario. The largest increases in ozone occurred in the Zero-LC scenario, on the 5$^{th}$ and 26$^{th}$, with increases in concentrations of 26 and 29 ppb consecutively. The largest decreases occurred in the same scenario on the 15$^{th}$ and 31$^{st}$ of 16 and 19 ppb consecutively. The reduction in motor vehicle emissions across the entire domain resulted in the lowest impact on ozone concentrations for Chicago. Overall, the absolute difference does not appear to have a correlation with minimum or maxima on ozone concentrations.

The percent difference of 8-hour maximum ozone between the BC and all four scenarios is mostly positive, with the exception of the domain-wide reduction in motor vehicle emissions (Figure 4.7b). On average, reducing the MV-all scenario results in the largest reduction in ozone for Chicago. Although this scenario resulted in an average decrease in concentrations, it resulted in the least amount of overall change in concentrations for Chicago. The Zero-LC scenario produced the largest change in ozone for Chicago, but on average, increased ozone by about 6.5%. The largest percent difference occurs on July 5$^{th}$, which results in a 97% difference between the BC and Zero-LC scenario. The next largest difference occurs on July 26th, between the same two scenarios, at a maximum of 69%. The largest percent decrease occurs on July 15th, again between the same scenarios, at a maximum of a 25% decrease. To further analyze how the percent changes correlate with ozone concentrations, scatter plots of percent change and 8-hour maximum ozone concentrations have been examined.

In order to assess if the percent difference showed any correlation with extrema in ozone concentrations, scatter plots of these two metrics were generated for each scenario (Figures 4.8a, b, c, and d). The correlation between these metric for all scenarios is close to zero, with the largest correlation between the BC and the Zero-LC scenario, with an $R^2$ value of 0.011. This scenario produced a few outliers of high percent difference (30% - 98%), and the corresponding concentrations were within the mid-range of values. The other scenario that produced outliers of high percent difference (about 20% - 60%) was the reduction of emissions by 50% around the lake. These high percent differences fell within the lowest half of concentration values. The remaining two scenarios had lower percent differences, below 20%, and did not show any particular correlation with ozone extrema.

This same analysis method was also incorporated for ozone in Milwaukee, WI. Overall, each scenario does not deviate much from the BC, with the exception of the Zero-LC scenario (Figure 4.9). That scenario consistently produced values lower than the other runs, by as much as 25 ppb. The AQS observational data generally follows the same pattern as the model runs, but almost always shows lower concentrations. There are seven instances where four of the CMAQ runs exceed the NAAQS standard of 75 ppb. The Zero-LC run only exceeds the standard three out of the seven days. All of these exceedances recorded from the model runs do not occur in the observational data. Further analysis of these peak events was done using animations, which are not pictured here. Each of these exceedances, with the exception of one, can be attributed to lake-breeze interactions. Ozone typically built-up over the southern or northern section of the lake, and was then advected south or north and slightly to the east. This was not seen in the Chicago concentrations because the wind shifted later in the day when the highest levels had already been advected southern portion of the lake towards the north and when higher concentrations were seen in the northern section of the lake, they did not reach as far south before concentrations started to diminish. The one exception to the lake-breeze interaction occur on the 22$^{nd}$ and 23$^{rd}$. This exceedance occurred due to a persistent high-pressure system, stagnant wind patterns over the Great Lakes Region, and higher wind speeds over the lake. Next, I will again analyze the differences between scenarios, but this time in Milwaukee.

Analysis of the percent difference in ozone for Milwaukee shows that each run increases in ozone, except for the Zero-LC scenario (Figure 4.10a). Reducing motor vehicle emissions around the lake produces the larges increase from the BC, about 4.5%. The Zero-LC scenario produced an overall average reduction in concentration, but only by 0.22%. Peaks in percent difference seem to occur, most often, the day after a peak in ozone concentrations. The largest percent difference occurs on the 19$^{th}$, with a value of 65% for the Zero-LC scenario, down to 31% for the MV-All scenario. The largest reduction occurs on the 22$^{nd}$, with a maximum of 42% for the Zero-LC run.

The absolute difference shows an overall increase in concentrations, except for the Zero-LC scenario (Figure 4.10b). This scenario produces average decreases of 2.4 pbb for the month. The maximum average increase in concentrations was 2.5 pbb for the MV-LC scenario. The largest peak in absolute difference for all scenarios occurs on the 19$^{th}$, with a maximum of 28 ppb for the zero lake county emissions scenario. The largest reduction occurs on the 22nd with a decrease of 38 ppb for that same scenario. Overall the Zero-LC scenario shows the largest variations from the BC.

Scatter plots of concentration vs. percent difference for each scenario have also been analyzed for Milwaukee (Figures 4.11a, b, c, and d). Overall, ozone concentrations in Milwaukee show less of a correlation with percent difference than in Chicago. The largest correlation occurs with the Zero-LC run, with an $R^2$ value of 0.04. There are a few outliers of large percent decreases for each scenario, which occur around median values of ozone concentrations. There is no overall correlation between extrema in ozone concentrations and deviations between each scenario and the BC.

### *Particulate Matter Discussion*

Particulate matter concentrations between each scenario and the AQS observations will be discussed first, followed by the percent and absolute differences in $PM_{2.5}$ for the domain, and for Milwaukee and Chicago. Average $PM_{2.5}$ concentrations, in the AQS data, are largest in the Ohio River Valley, with maxima greater than 18 $\mu g/m^3$ (Figure 4.12a). The upper half of the domain experiences the lowest concentrations, with minima around 2 $\mu g/m^3$. Comparing this with model data, the base case simulation shows maxima in similar areas, with elevated concentrations in larger cities like, Milwaukee and Chicago (Figure 4.12b). Maxima are again, larger than 18 $\mu g/m^3$ across the areas already specified. Minima are located in the upper quarter and far western portions of the domain, with values ranging from 0-6 $\mu g/m^3$. To analyze how the base case compares to other scenarios, $PM_{2.5}$ concentrations have also been utilized for all four scenarios.

The first scenario analyzed will be the Zero-LC (Figure 4.12c). This run shows the largest reductions around Lake Michigan than any other scenario. The concentrations decrease from about 18 μg/m$^3$ to about 6 μg/m$^3$ in the Milwaukee and Chicago areas. Reductions are observed over the entire lake, the bordering counties, and into western Michigan. There are also noticeable slight reductions across a large portion of WI, IL, IN, OH, and MI, but changes are only around 2 μg/m$^3$. The scenario that results in the second largest amount of change is the 50%-LC (Figure 4.12d). This scenario results in a 2 μg/m$^3$ reduction over Lake Michigan, and about a 6 μg/m$^3$ reduction around Milwaukee and Chicago. Along with Chicago and Milwaukee, the next largest decrease is located in the western half of Michigan, ranging from 2 to 4 μg/m$^3$. Both scenarios that reduced motor vehicle emissions reduced $PM_{2.5}$ concentrations the least, with the MV-LC resulting in the least impact. The MC-LC results in slight reductions around Milwaukee and Chicago, along with portions of western Michigan, but they are difficult to visibly quantify (Figure 4.12e). The MV-All scenario results in the largest spatial changes (Figure 4.12f). Reductions from this scenario are most notably seen in the Ohio River Valley, with values decreasing by about 4 μg/m$^3$. Milwaukee and Chicago show slight decreases, but aren't as noticeable as in the Zero-LC and 50%-LC. The areas of lowest concentrations do not show much, if any change from the BC. To further analyze and understand these differences, percent and absolute differences in $PM_{2.5}$ concentrations will be discussed next.

I will again analyze the percent and absolute differences between each scenario and the base case, but this time for $PM_{2.5}$. The first focus will be on the Zero-LC scenario. The largest percent difference, of over a 50% decrease, occurs along the entire west side of Lake Michigan, and a smaller area near Grand Rapids, MI (Figure 4.13a). A percent decrease of 40-50% occurs over the lake, and branches out slightly onshore in eastern WI and western

MI. The percent difference decreases farther out from the lake, where there is an average domain-wide decrease of about 1-4%. The maximum percent difference equates to about a 12 $\mu g/m^3$ decrease (Figure 4.13b). This maximum decrease occurs mainly in the Chicago and Milwaukee areas. The next area of largest decrease occurs in the Grand Rapids, MI area, with a maximum about 8 $\mu g/m^3$. A 1-2 $\mu g/m^3$ decrease is mainly located in the states that directly border Lake Michigan.

The 50%-LC scenario vs. the BC produced maximum percent differences of about a 30% decrease in the Milwaukee and Chicago areas (Figure 4.14a). Changes over Lake Michigan, on average are about a 25% decrease. The majority of the upper half of the domain experiences a percent decrease of 1 to 5%. The lower third of the domain does not change more than 1% from the BC. The absolute difference shows a maximum decreases of about 10 $\mu g/m^3$ in Milwaukee and Chicago (Figure 4.14b). There is an average difference of about 3 $\mu g/m^3$ over Lake Michigan, and in portions over land that directly borders the lake. The rest of the domain does not change more than 1 $\mu g/m^3$ for this scenario.

The MV-LC scenario shows even less of a change than the Zero-LC scenario. The percent difference for this scenario shows a maximum of about a 20% decrease in a small area on the northwest side of Chicago (Figure 4.15a). There is a percent difference of a 1-5% decrease in IL, WI, OH, MI, and IN. The $PM_{2.5}$ across the rest of the domain does not change more than 1% from the BC. The maximum absolute differences occur in the Milwaukee and Chicago areas (Figure 4.15b). In Chicago, the maximum decrease is about 8 $\mu g/m^3$ and the Milwaukee maximum is about 3 $\mu g/m^3$. The remainder of the domain does not experience more than a 1 $\mu g/m^3$ change from the BC.

The final scenario is the domain-wide reduction in motor vehicle emissions. This, like expected, produced the largest domain-wide decreases in $PM_{2.5}$ concentrations (Figure 4.16a). The average percent difference across the domain is about 7%, with maxima of about a 20-30% decrease in urban centers like Detroit, Chicago, Milwaukee, St. Louis, and Minneapolis. This equates an absolute difference of about 2 $\mu g/m^3$ in those urban areas (Figure 4.16b). The city that experiences the largest decreases is Chicago, with a maximum absolute difference of 9 $\mu g/m^3$. Other than in and around these urban centers, absolute changes larger that 1 $\mu g/m^3$ are very patchy across the central portion of the domain.

Since the largest changes $PM_{2.5}$ in are mainly seen again in Chicago and Milwaukee, data has been pulled for those two locations. I will first discuss a time series of $PM_{2.5}$, and then go into differences between each scenario for Chicago (Figure 4.17). The time series for $PM_{2.5}$ in Chicago includes data from all five CMAQ runs, the AQS data values, and the NAAQS standard of 12 $\mu g/m^3$. The AQS data is not continuous, so there are only a few measurements throughout the month. For most of the time series, each scenario except for the Zero-LC exceeds the NAAQS standard. The Zero-LC only exceeds the standard on three occasions as compared to the other scenarios that exceed the standard about eighteen days. There are ten days of AQS measurements for Chicago, and four out of the ten days produce exceedances of the standard. For the days of measurements that are available, the observations and model data match fairly well. Two days of particularly high concentrations occur on the 5$^{th}$ and 24$^{th}$. Analyzing animations for these two days, show a build up of PM over the lake, with an accompanying change in wind direction later in the day to be out of the east. There is less of a build up of PM over the lake for the Zero-LC scenario of about an average of 2 $\mu g/m^3$. Further analysis of each scenario will be examined next in percent and absolute difference plots for Chicago.

Both absolute and percent differences for $PM_{2.5}$ are negative throughout the month of July 2007. The Zero-LC produced the largest deviations from the BC, with maximum percent decreases of over 90% occurring on four separate occasions (Figure 4.18a). There is no instance of the percent difference to be any less than 50% for this scenario, and the average change is about a 70% decrease. The second scenario that produces the larges percent change is the 50%-LC scenario. This scenario shows maximum decreases around 40%. The two scenarios that decreased motor vehicle emissions resulted in the least amount of change, with percent differences less than 10% for the month. This indicates that motor vehicle emissions do not have as much of an impact on PM concentration than other emissions sources. The absolute differences in Chicago show more of a variation through the month (Figure 4.18b). Peaks in the Zero-LC scenario reach over 35 $\mu g/m^3$ on about five days out of the month, but the average decrease for this scenario is 17 $\mu g/m^3$. The 50%-LC scenario results in maximum decreases around 20 $\mu g/m^3$, and average changes of 8 $\mu g/m^3$. Peaks in the two motor vehicle reduction scenarios are no greater than 5 $\mu g/m^3$. Overall, the 50%-LC and Zero-LC produce the largest changes in PM2.5 concentrations in Chicago. To further analyze how these changes are related to extrema in $PM_{2.5}$ concentrations, scatter plots are utilized next.

The largest correlations between percent change and $PM_{2.5}$ concentrations occur in both motor vehicle reduction scenarios (Figures 4.19c and d). The MV-LC scenario shows and $R^2$ value of 0.65 between the percent change and concentrations, and the MV-All scenario has and $R^2$ value of 0.56. This indicates that the larger the concentration of PM, the higher the percent difference between each scenario and the BC. The Zero-LC and 50%-LC scenarios do not show as much of a correlation, with $R^2$ values of 0.16 and 0.11 respectively

(Figures 4.19a and b). The Zero-LC scenario results in a slight negative trend between the two datasets, with days of higher concentrations resulting in the lower percent changes. The 50%-LC results in a slightly positive trend, the larger the concentration, the higher the percent difference. The correlations for these two scenarios are small, but indicate opposite trend between decreasing lakeshore emissions by 50 or 100%. Overall, reducing motor vehicle emissions results in the least amount of change in $PM_{2.5}$ concentrations in Chicago, but shows the highest probability of reducing PM concentrations when they are highest. This same analysis is also done for Milwaukee, and will be discussed next.

Concentrations of $PM_{2.5}$ in Milwaukee can be seen in the time series in figure 4.20. Concentrations of $PM_{2.5}$ for all the scenarios, AQS data, and the NAAQS standard are all displayed in this figure. Concentrations in Milwaukee also show many exceedances for $PM_{2.5}$ throughout the time series. There are 22 days of exceedances for the BC, and two motor vehicle scenarios; there are 3 less exceedances for the 50%-LC scenario, and only 3 exceedances in the Zero-LC scenario. Overall, trends in the AQS observations match well with the model data, and show exceedances 6 out of the 11 days of measurements. Results from these scenarios indicate that reductions in emissions all emissions along the lakeshore greatly reduce $PM_{2.5}$ NAAQS exceedances. Further analysis of the differences between scenarios will be discussed next.

Similarly to Chicago, the largest percent differences occur in the Zero-LC and 50%-LC scenarios (Figure 4.21a). The largest differences occur in the Zero-LC, with maximum decreases around 90%, and an average decrease of 74%. The 50%-LC scenario results in an average decrease of about 37%. The two scenarios that reduce motor vehicle emissions do not change more than 10%. The maximum absolute difference occurs in the Zero-LC scenario, with values as high as 37 μg/$m^3$ (Figure 4.21b). The average absolute difference for this scenario is 18 μg/$m^3$, and the scenario with the second largest amount of change, the 50%-LC, averages a 9 μg/$m^3$ decrease. Both the MV-LC and MV-All do not decrease more than 5 μg/$m^3$ in Milwaukee. The relationship between concentrations and percent change are also investigated for Milwaukee, and will be discussed next.

Analysis of the percent decreases vs. $PM_{2.5}$ concentrations, shows that the largest positive correlation between extrema in $PM_{2.5}$ concentration and percent change occur in the MV-LC and MV-All scenarios (Figures 4.22c and d). Both of these two scenarios show that the larger the concentrations in PM, the larger the concentrations decreased. This percent change is small; with values no greater than a 10% decrease. The $R^2$ values are 0.46 for the MV-LC run, and 0.62 for the MV-All run. The Zero-LC scenario shows the next largest correlation, with an $R^2$ value of 0.26 (Figure 4.22a). This is a negative correlation, which indicates that the larger the concentration, the lower the decrease will be. The 50%-LC scenario shows almost no correlation between the two data sets (Figure 4.22b). Altogether, the reductions in motor vehicle scenarios produce the least change, but the largest correlation between percent decrease and concentration extrema.

# Figures

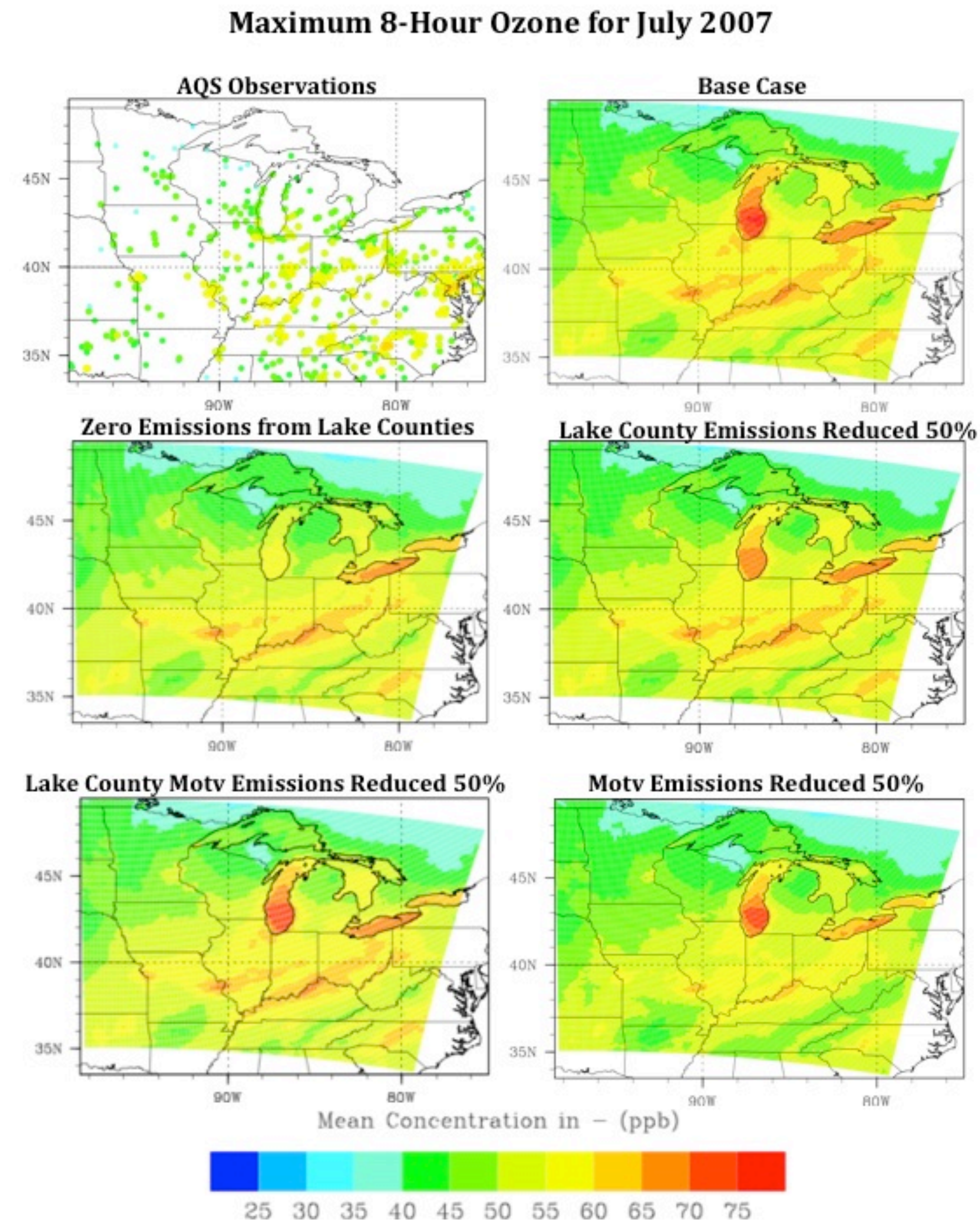


**Figure 4.1: Maximum 8-hr average ozone for a) (top left) AQS observations, b) (top right) base case, c) (middle left) zero emissions from lake county scenario, d) (middle right) lake county emissions reduced**

**50%, e) (bottom left) lake county motor vehicle emissions reduced 50%, and f) (bottom right) domain-wide reduction in motor vehicle emissions.**

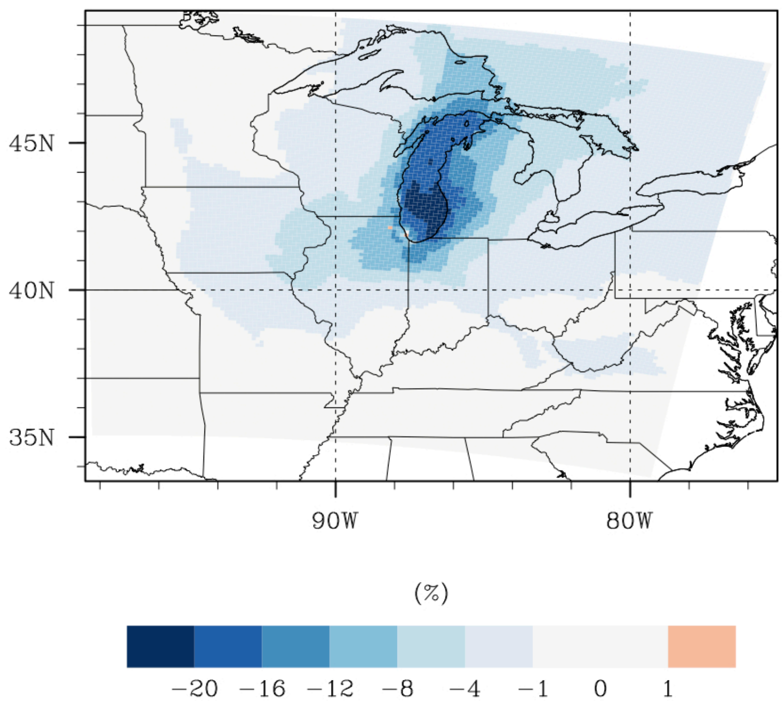


**Figure 4.2a: Percent difference of ozone concentrations between the case of zero emissions from Lake Michigan counties and the base case**

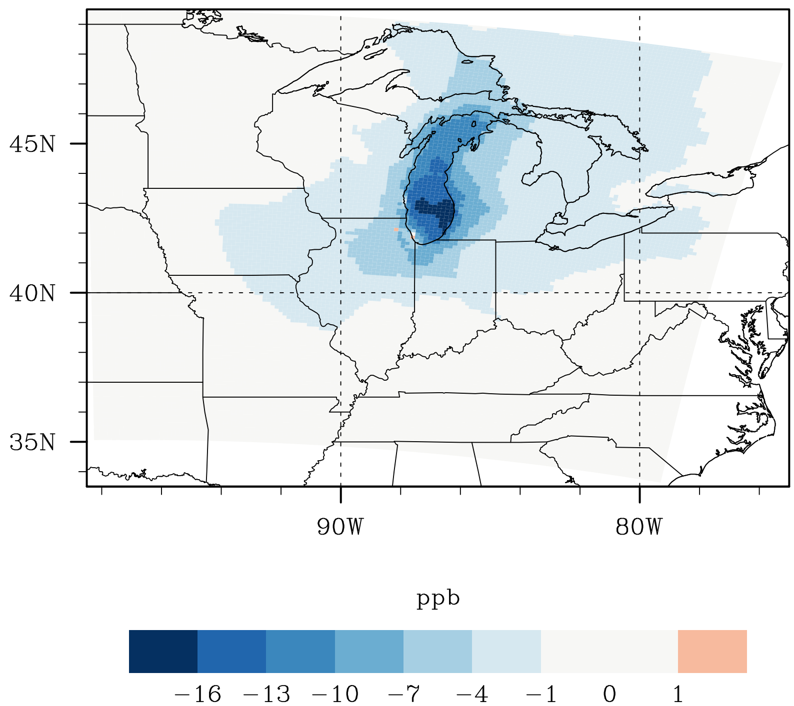


**Figure 4.2b: Absolute difference of ozone concentrations between the case of zero emissions from Lake Michigan counties and the base case.**

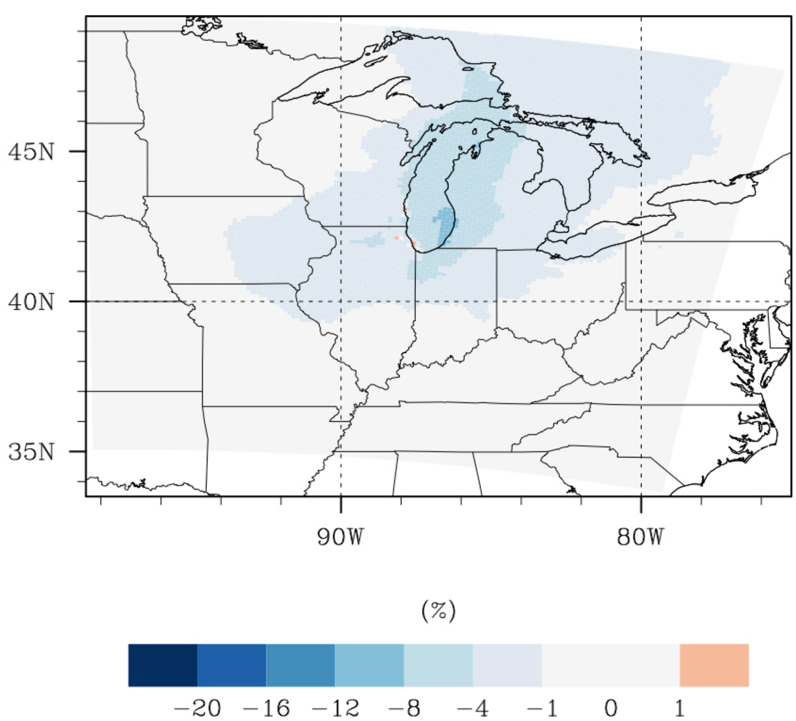


**Figure 4.3a: Percent difference of 8-hr maximum ozone between the lake county emissions reduced 50% and the base case.**

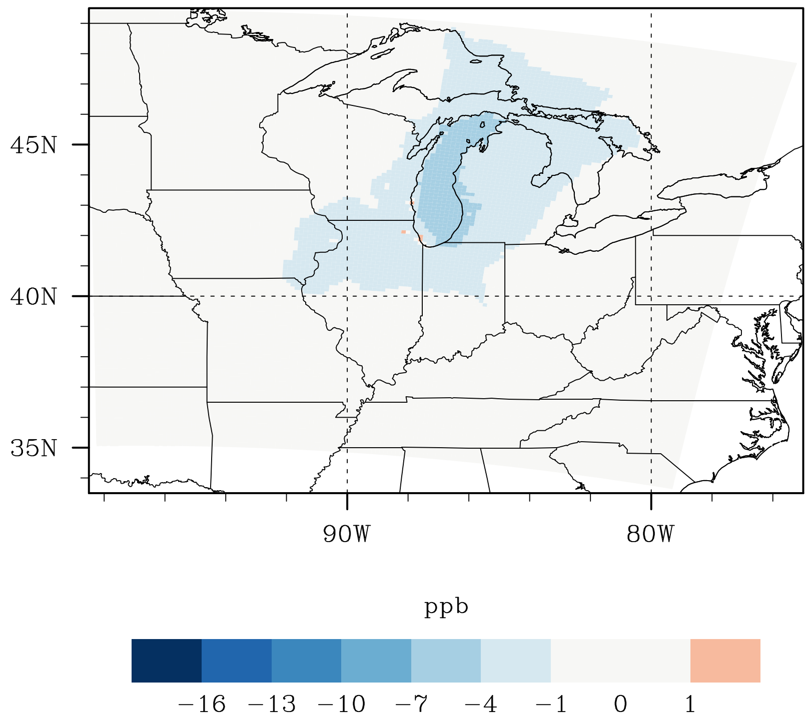


**Figure 4.3b: Absolute difference of 8-hr maximum ozone between the lake county emissions reduced 50% and the base case.**

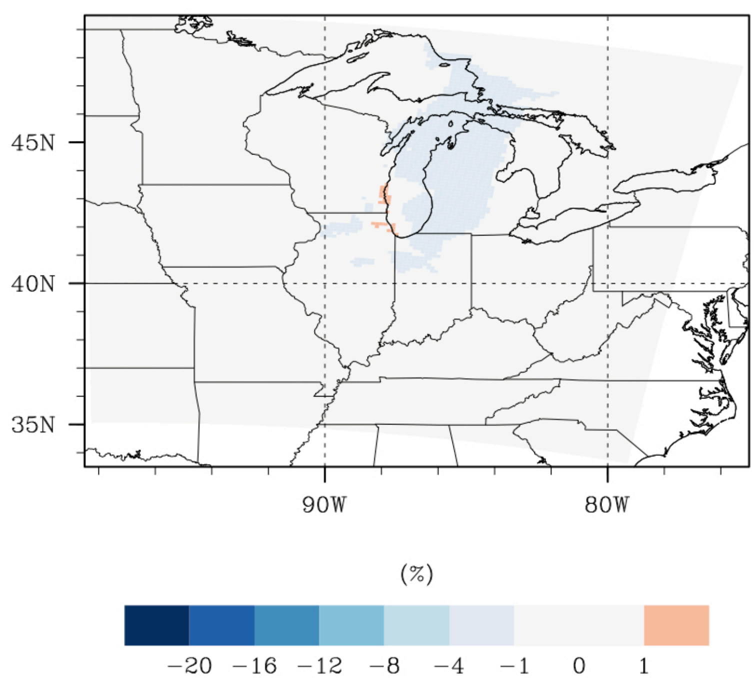


**Figure 4.4a: Percent difference of 8-hr maximum ozone between the lake county motor vehicle emissions reduced 50% and the base case.**

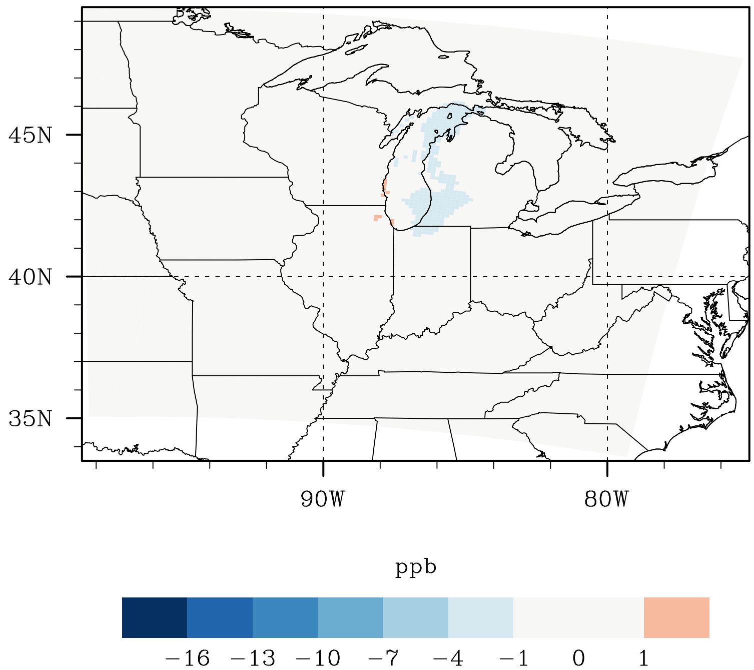


**Figure 4.4b: Absolute difference of 8-hr maximum ozone between the lake county motor vehicle emissions reduced 50% and the base case.**

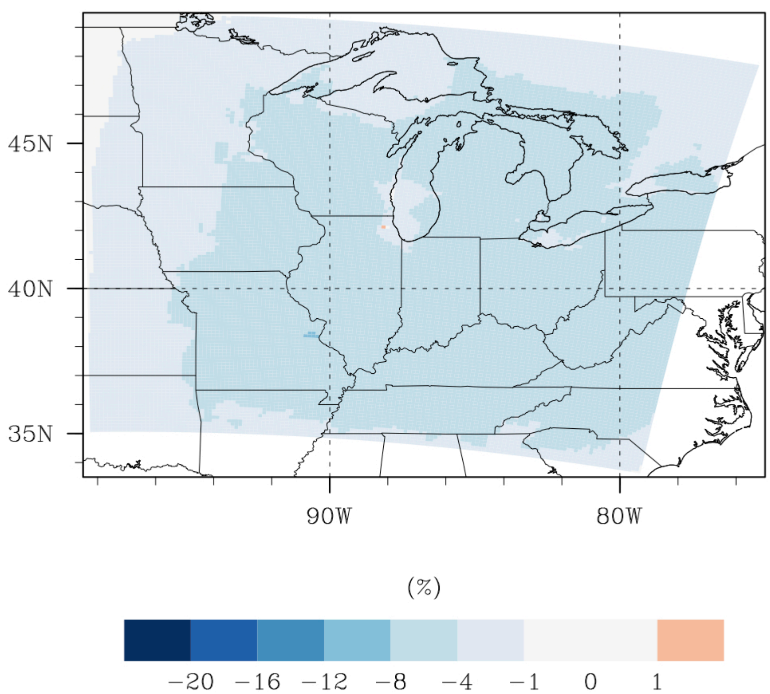


**Figure 4.5a: Percent difference of 8-hr maximum ozone between the domain-wide motor vehicle emissions reduced 50% and the base case.**

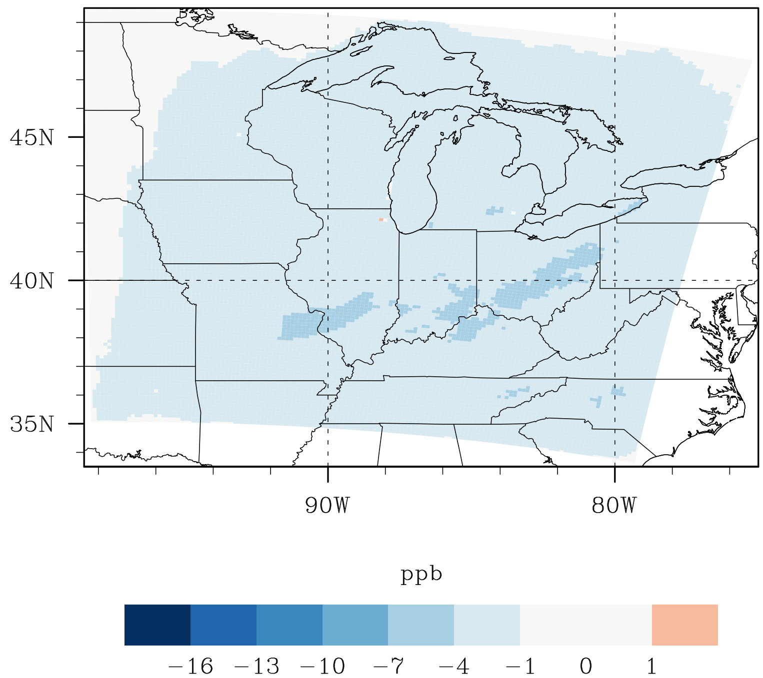


**Figure 4.5b: Absolute difference of 8-hr maximum ozone between the domain-wide motor vehicle emissions reduced 50% and the base case.**

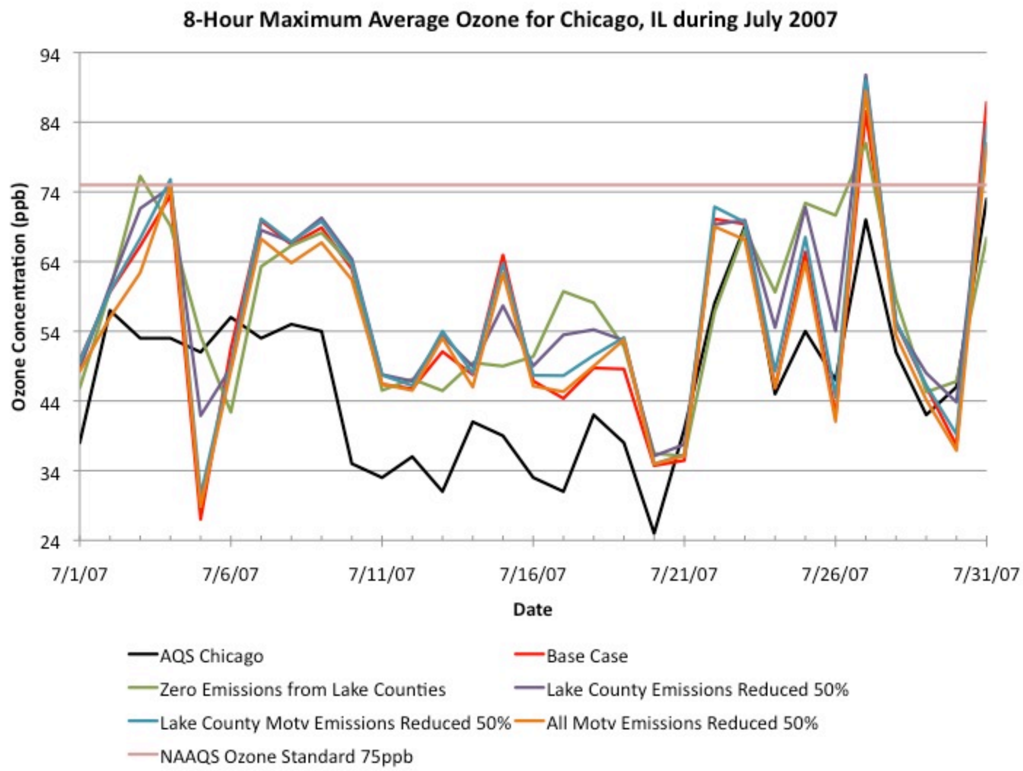


**Figure 4.6: Time series of max 8-hr ozone in Chicago, IL for all scenarios, AQS observations, and the NAAQS standard of 75ppb during July 2007.**

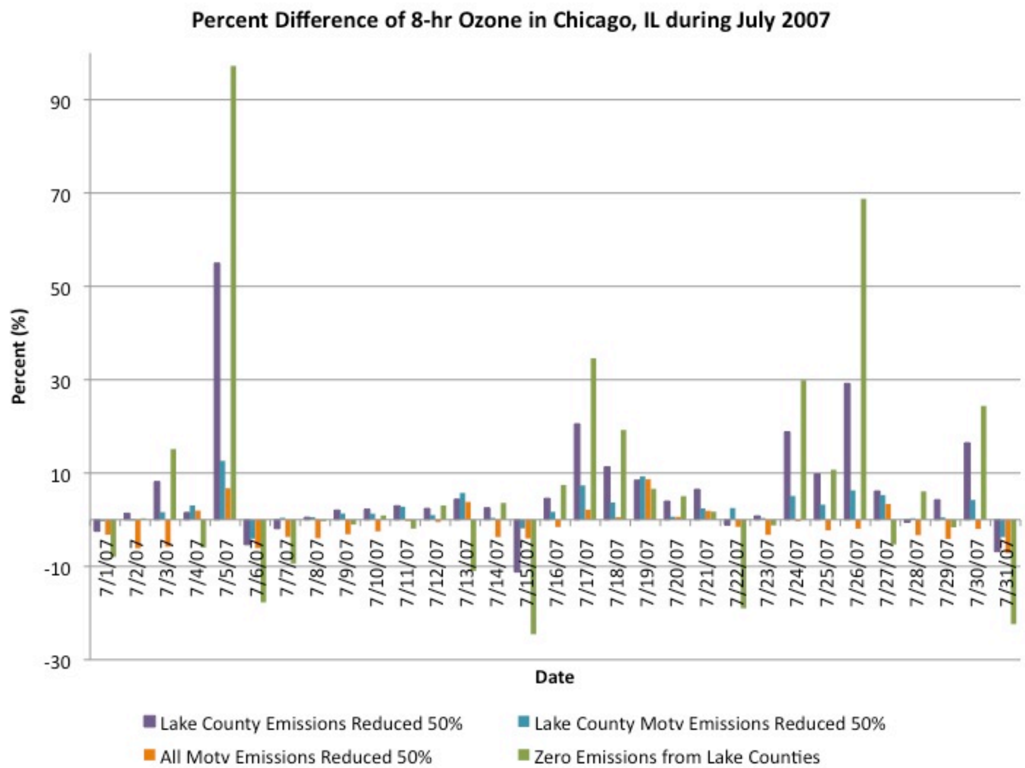


**Figure 4.7a: Percent difference in max 8-hr ozone in Chicago, IL for all scenarios vs. the base case.**

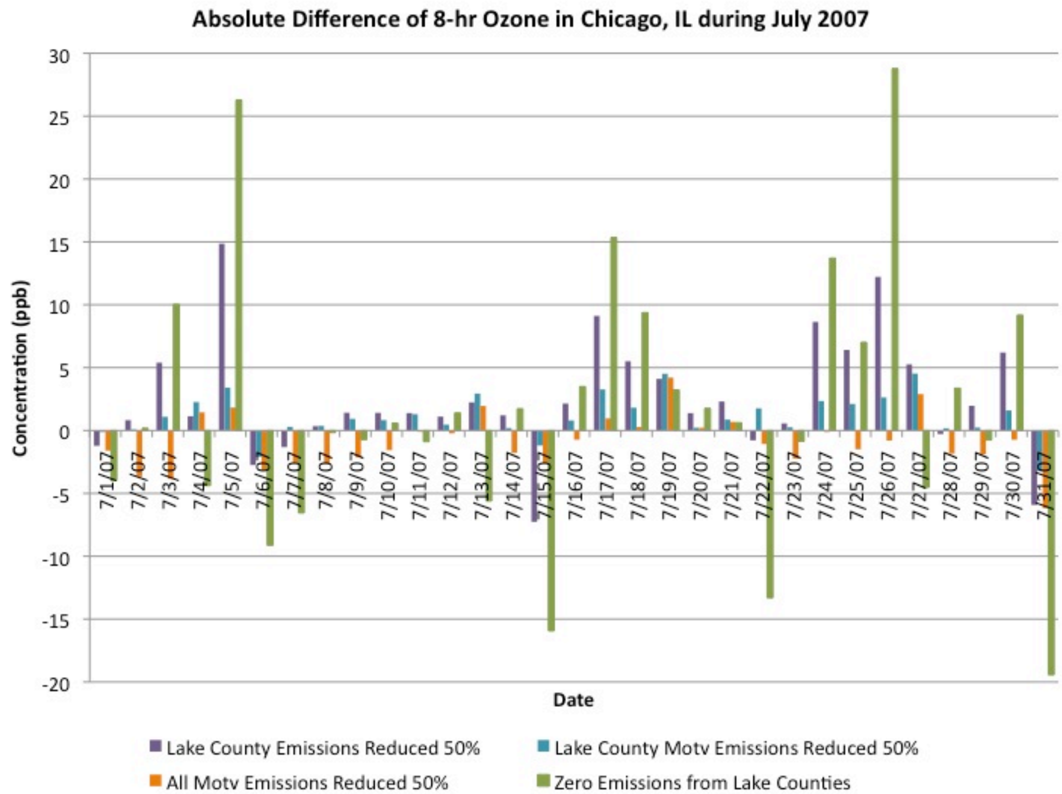


**Figure 4.7b: Absolute difference in max 8-hr ozone in Chicago, IL for all scenarios vs. the base case.**

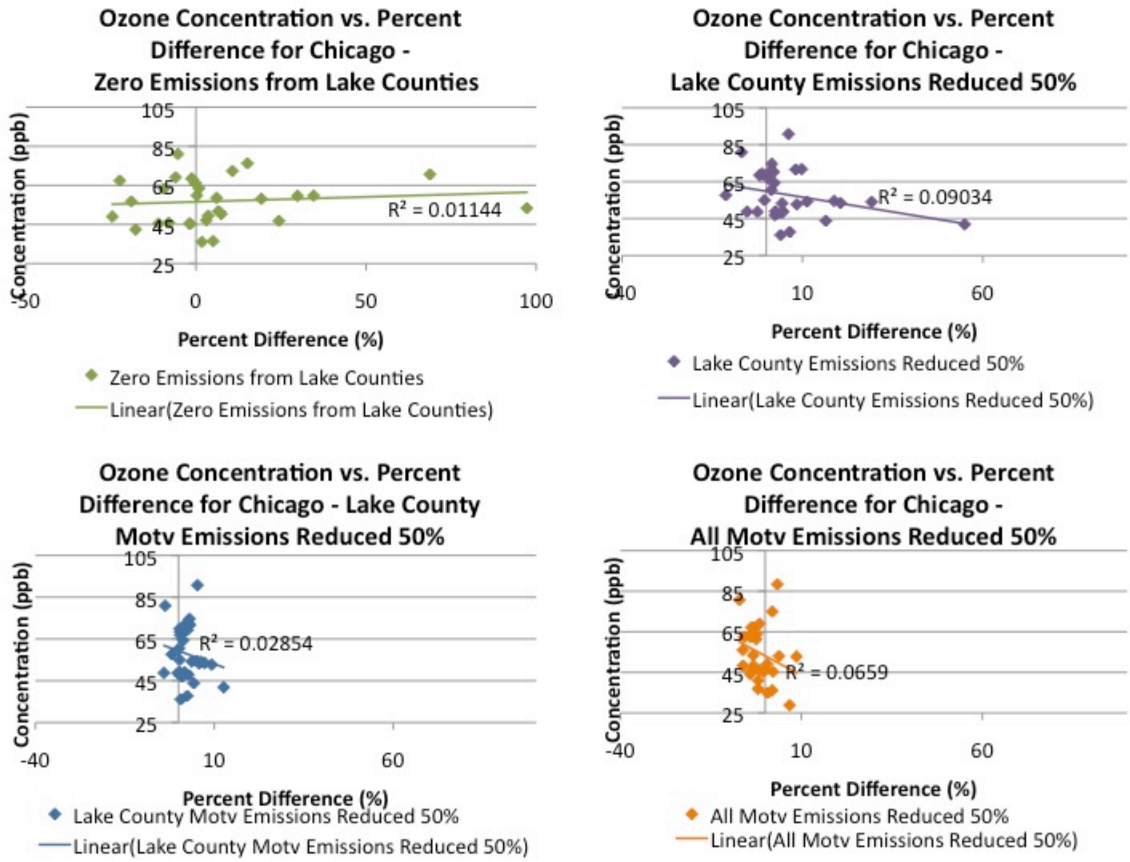


**Figure 4.8: Scatter plots of max 8-hr ozone concentrations vs. the percent difference in Chicago for a) (top left) zero emissions from lake counties, b) (top right) lake county emissions reduced 50%, c) (bottom left) lake county motor vehicle emissions reduced 50%, and d) (bottom right) domain-wide reduction in motor vehicle emissions vs. the base case.**

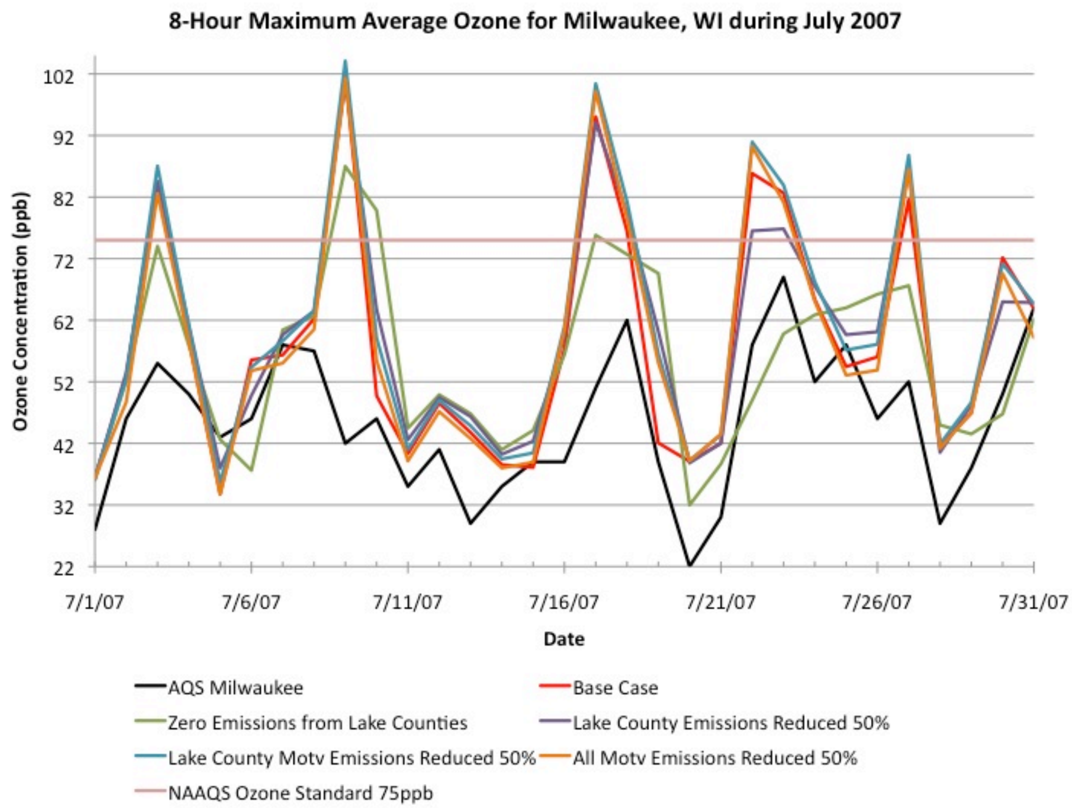


**Figure 4.9: Time serried of max 8-hr ozone in Milwaukee, WI for all scenarios, the AQS observations, and the NAAQS ozone standard of 75ppb.**

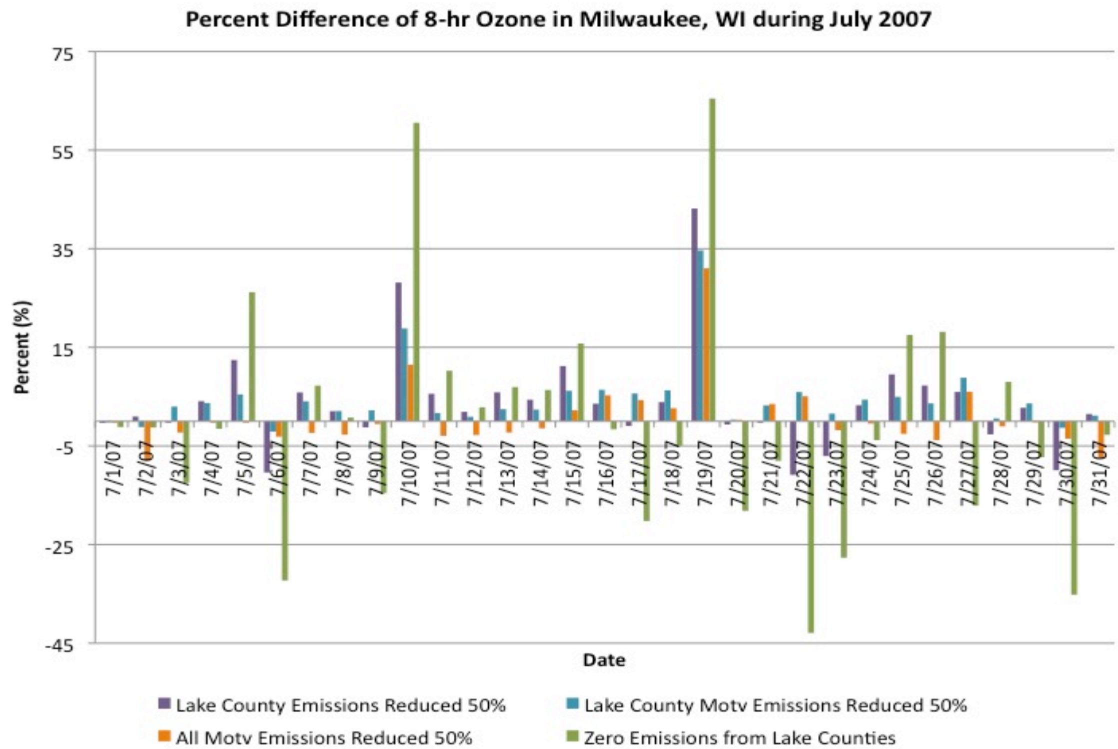


**Figure 4.10a: Percent difference of max 8-hr ozone in Milwaukee, WI for all scenarios vs. the base case.**

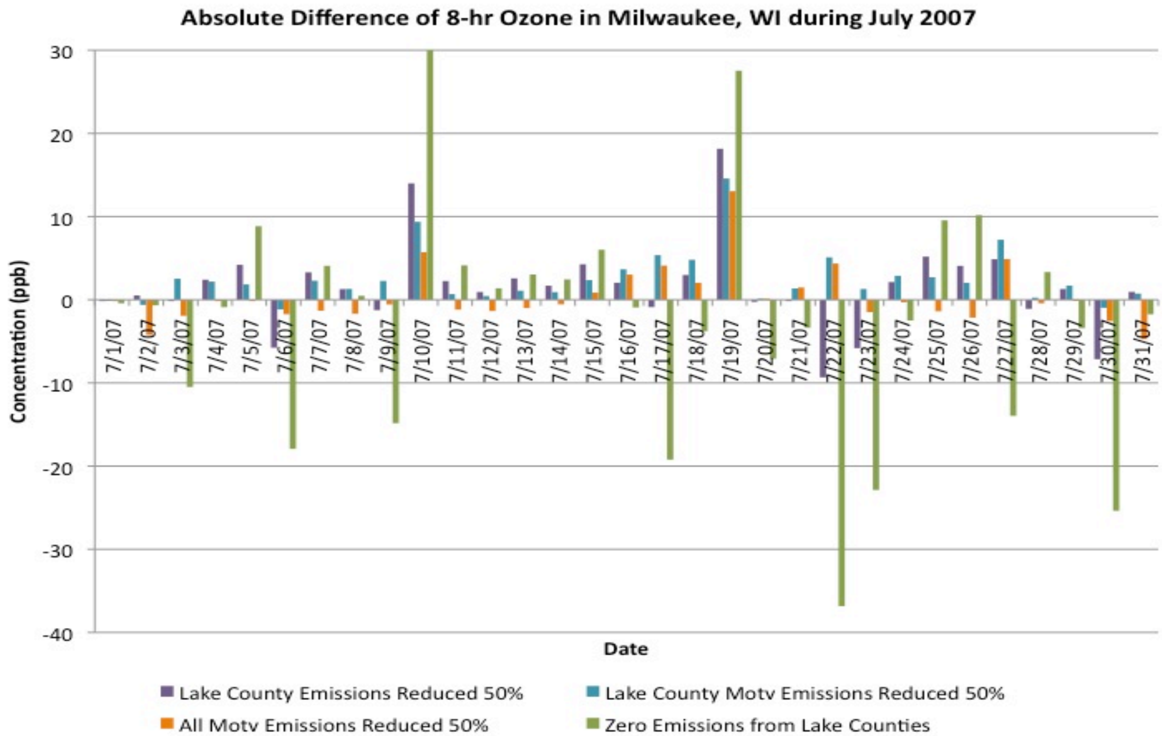


**Figure 4.10b: Absolute difference of max 8-hr ozone in Milwaukee, WI for all scenarios vs. the base case.**

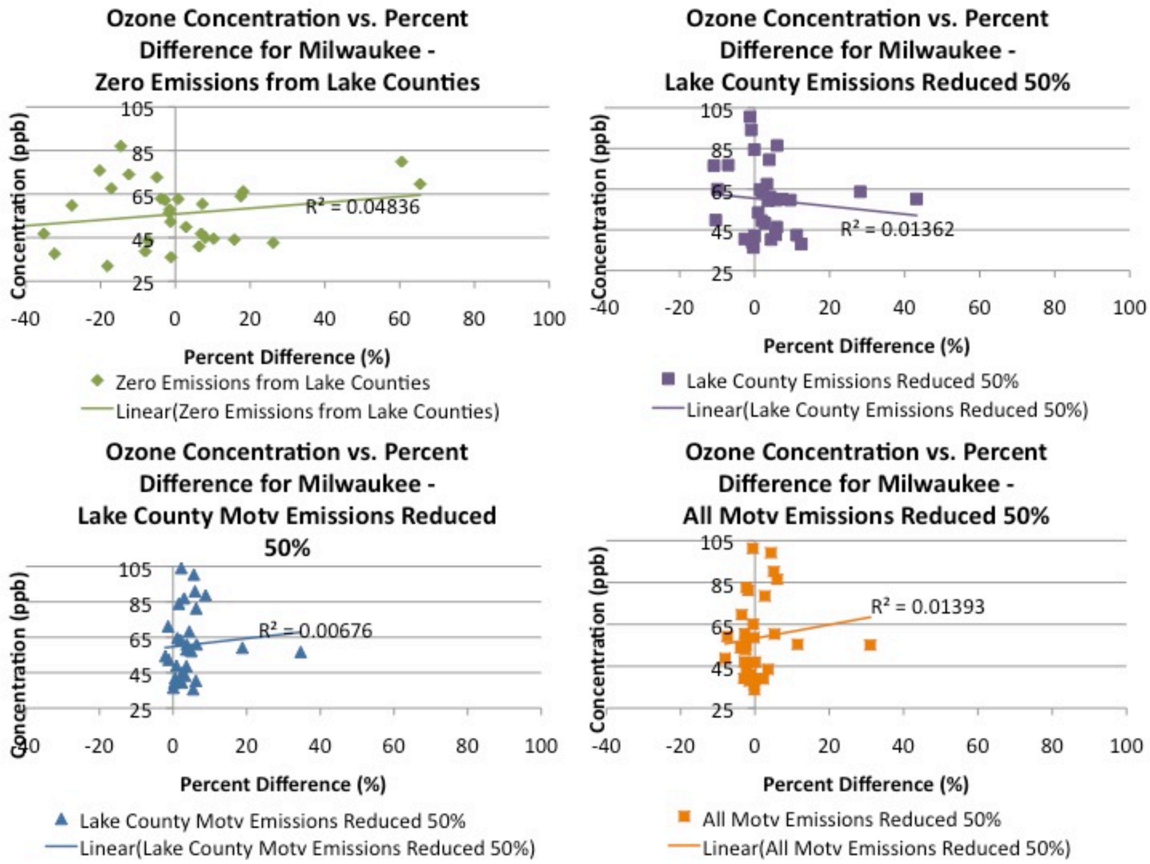


**Figure 4.11: Scatter plots of max 8-hr ozone concentrations vs. percent difference of ozone in Milwaukee for a) (top left) zero emissions from lake counties, b) (top right) lake county emissions reduced 50%, c) (bottom left) lake county motor vehicle emissions reduced 50%, and d) (bottom right) domain-wide reduction in motor vehicle emissions by 50% vs. the base case.**

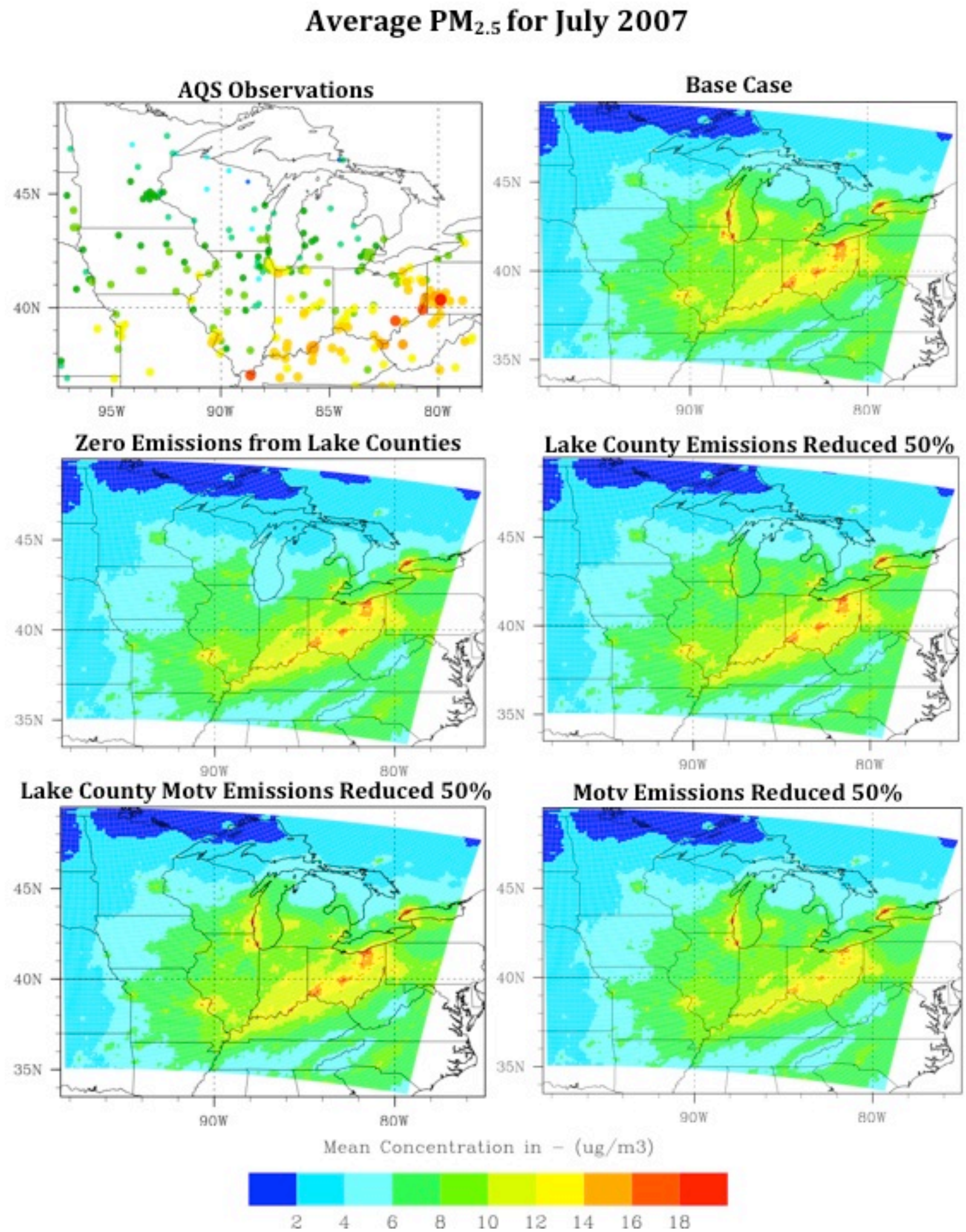


**Figure 4.12: Average $PM_{2.5}$ concentrations for a) (top left) AQS observations, b) (top right) base case, c) (middle left) zero emissions from lake county scenario, d) (middle right) lake county emissions reduced 50%, e) (bottom left) lake county motor vehicle emissions reduced 50%, and f) (bottom right) domain-wide reduction in motor vehicle emissions.**

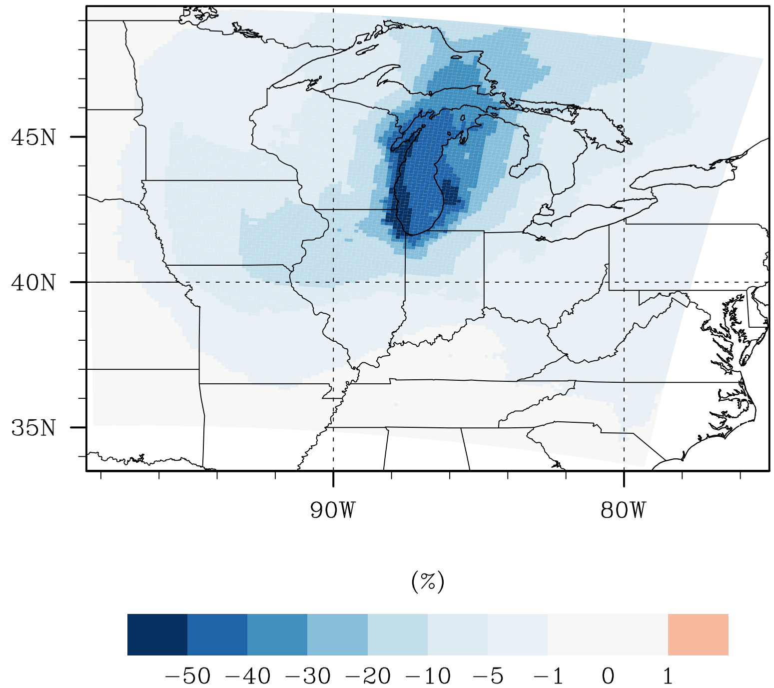


**Figure 4.13a: Percent difference in $PM_{2.5}$ concentrations for the zero emissions from lake counties scenario vs. the base case.**

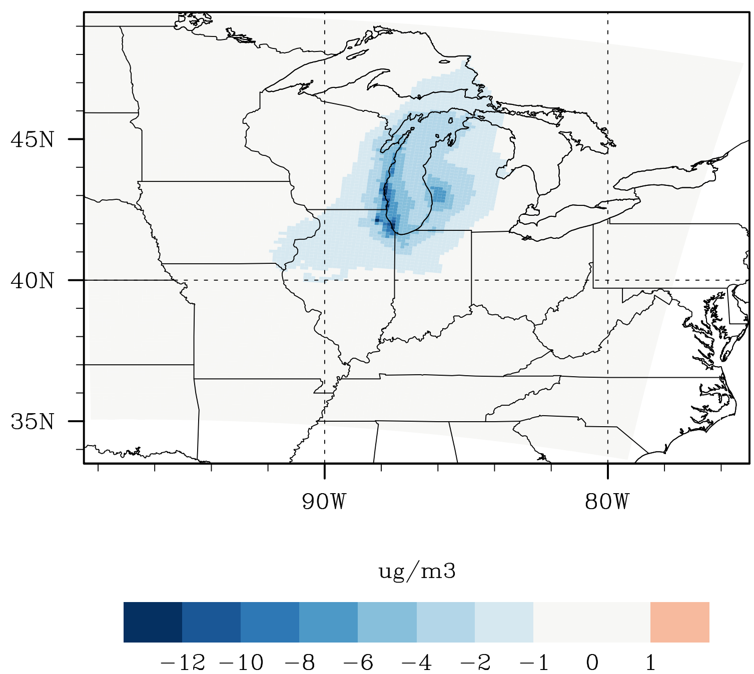


**Figure 4.13b: Absolute difference in $PM_{2.5}$ concentrations for the zero emissions from lake counties scenario vs. the base case.**

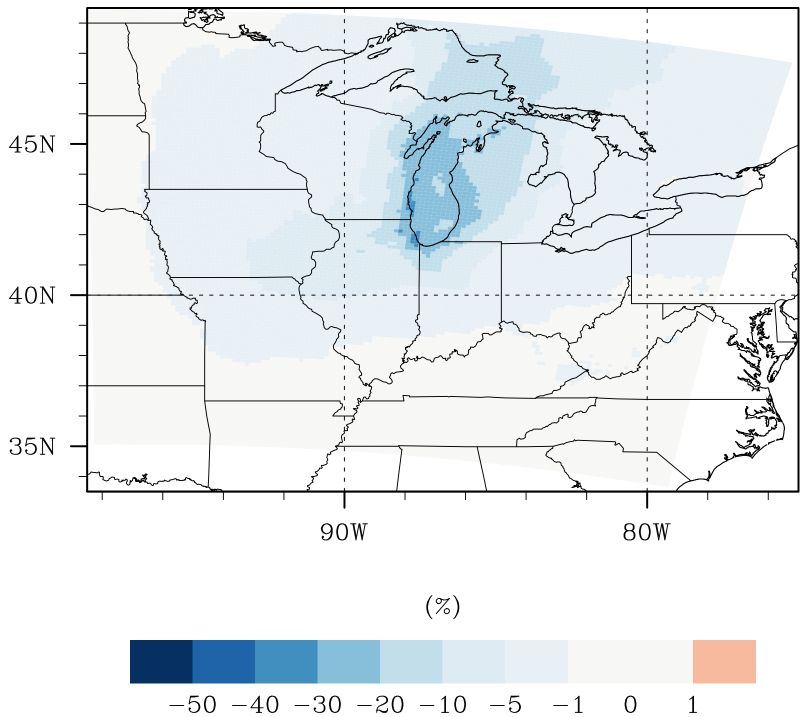


**Figure 4.14a: Percent difference in $PM_{2.5}$ concentrations for the lake county emissions reduced 50% scenario vs. the base case.**

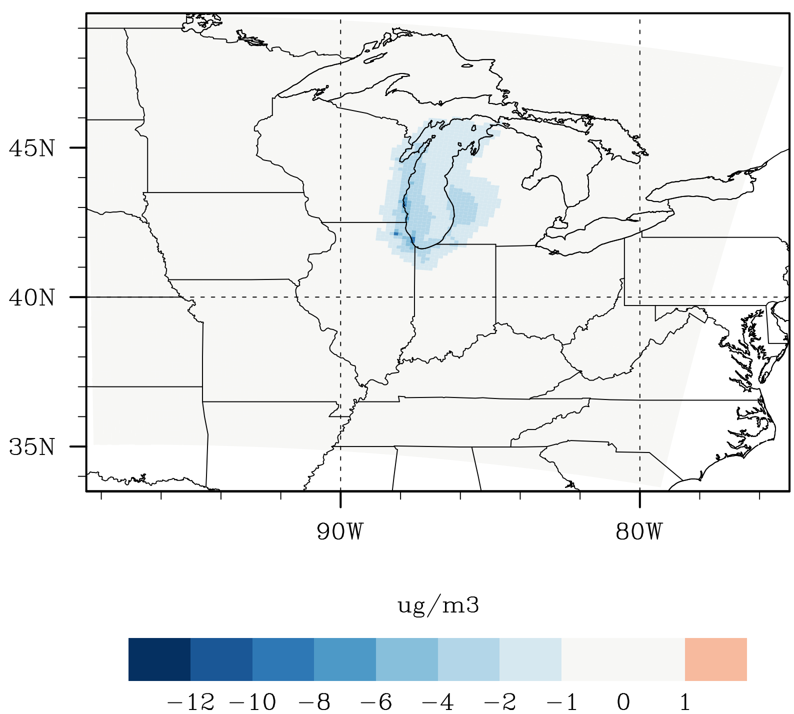


**Figure 4.14b: Absolute difference in $PM_{2.5}$ concentrations for the lake county emissions reduced 50% scenario vs. the base case.**

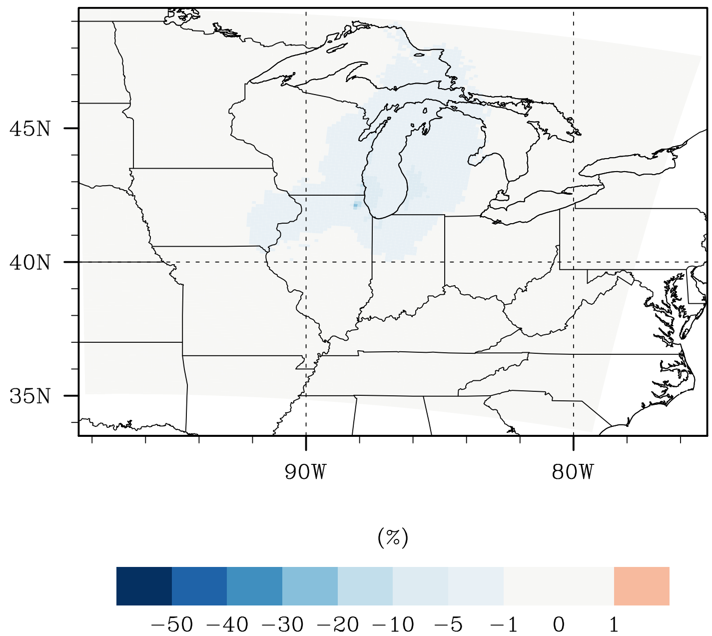


**Figure 4.15a: Percent difference in $PM_{2.5}$ concentrations for the lake county motor vehicle emissions reduced 50% scenario vs. the base case.**

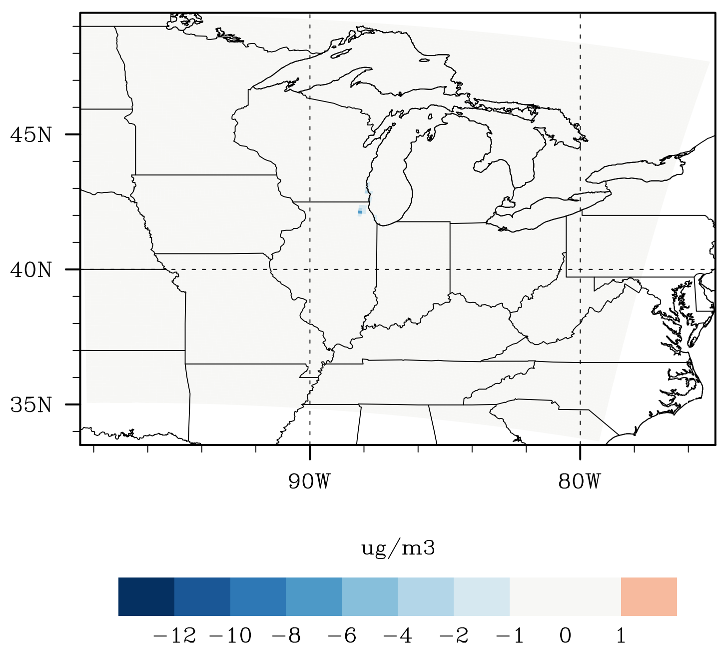


**Figure 4.15b: Absolute difference in $PM_{2.5}$ concentrations for the lake county motor vehicle emissions reduced 50% scenario vs. the base case.**

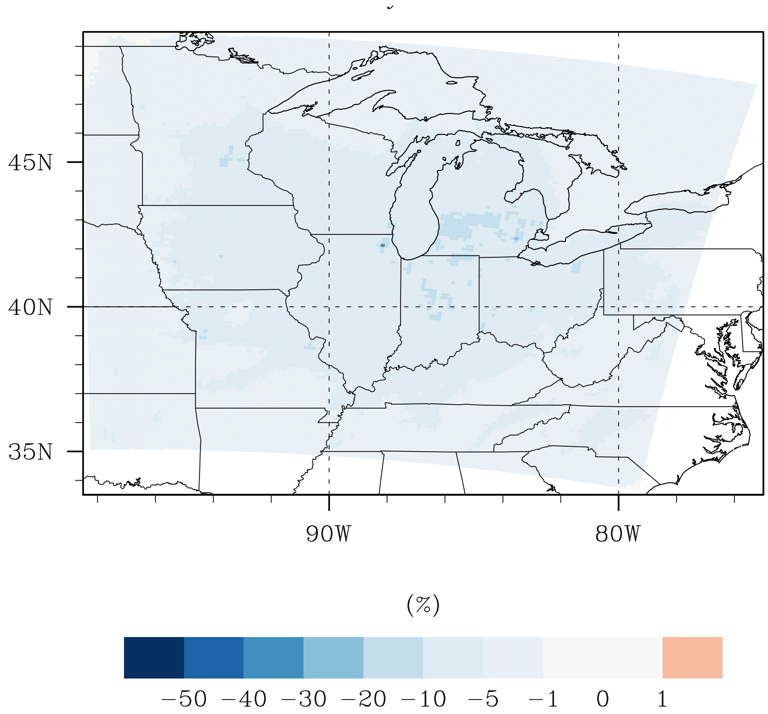


**Figure 4.16a: Percent difference in $PM_{2.5}$ concentrations for the domain-wide reduction in motor vehicle emissions by 50% scenario vs. the base case.**

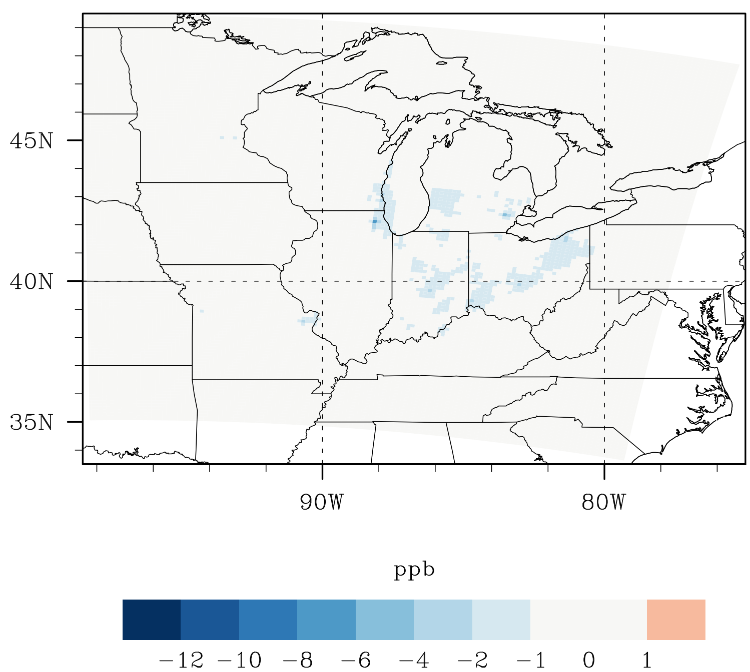


**Figure 4.16b: Absolute difference in $PM_{2.5}$ concentrations for the domain-wide reduction in motor vehicle emissions by 50% scenario vs. the base case.**

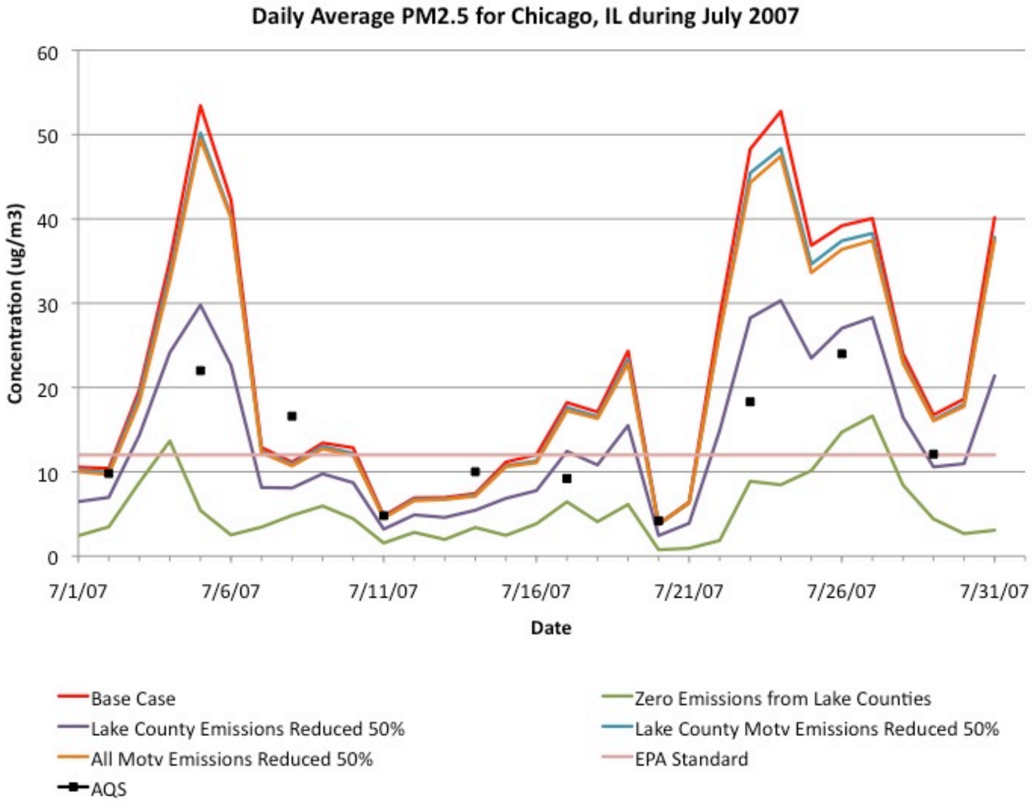


**Figure 4.17: Time series of $PM_{2.5}$ concentrations in Chicago, IL for all scenarios, AQS observations, and the NAAQS standard of 75ppb during July 2007.**

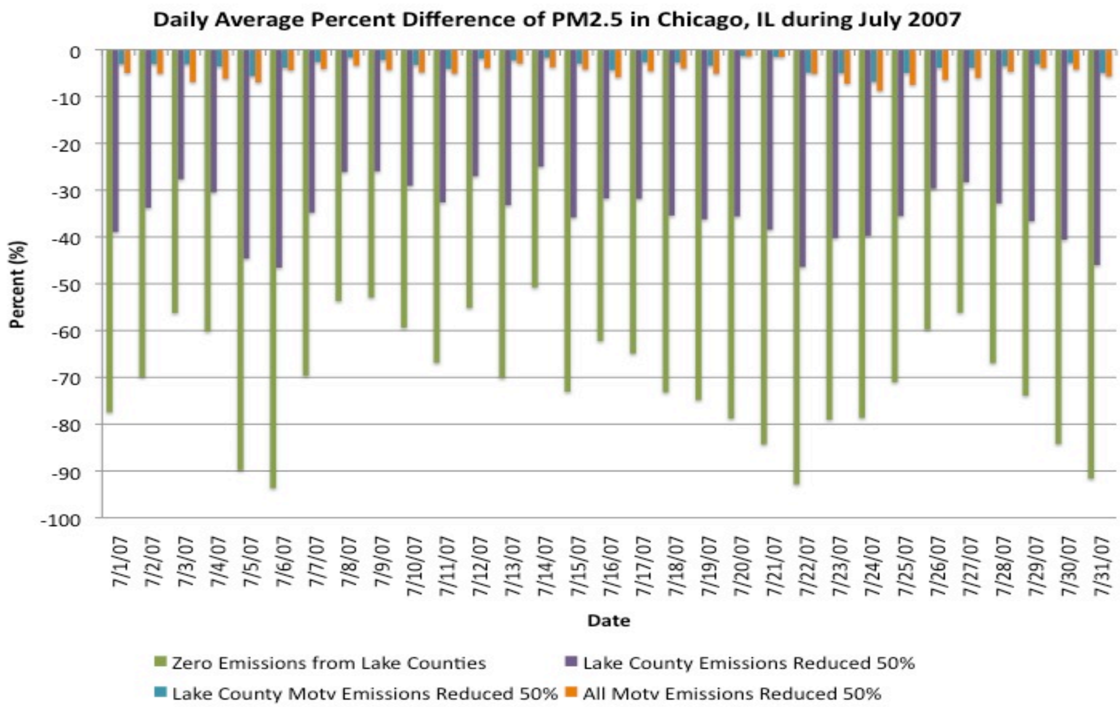


**Figure 4.18a: Percent difference in $PM_{2.5}$ concentrations in Chicago, IL for all scenarios vs. the base case.**

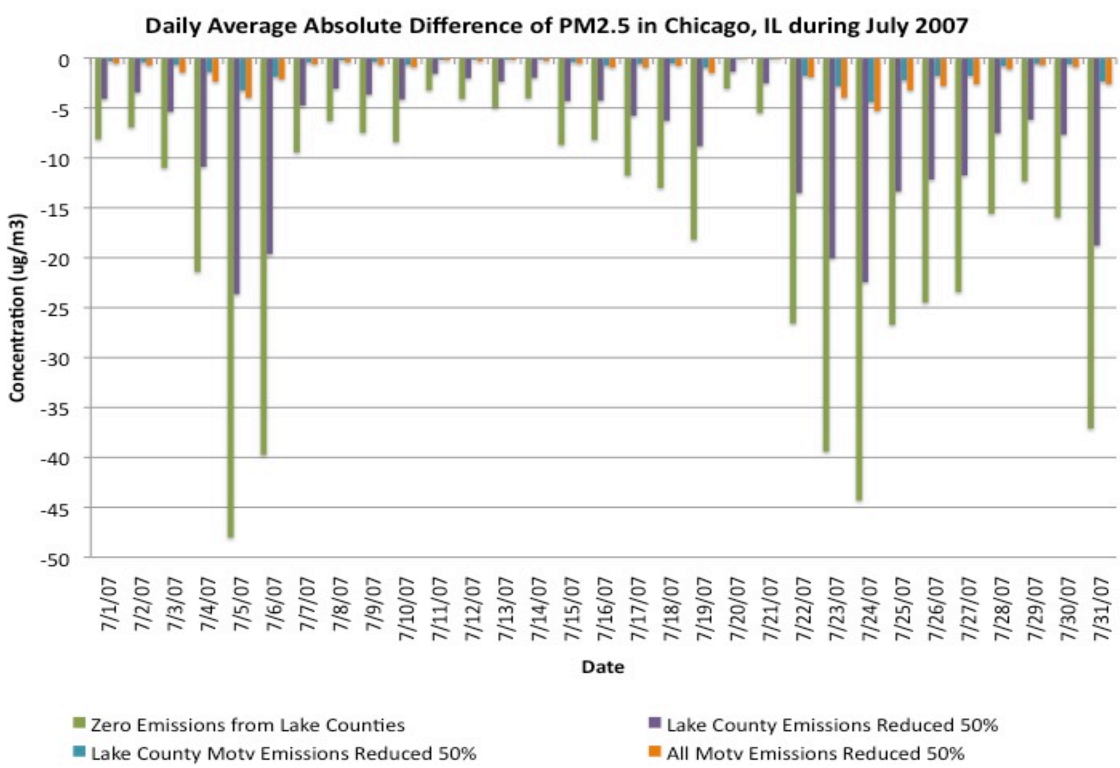


**Figure 4.18b: Absolute difference in $PM_{2.5}$ concentrations in Chicago, IL for all scenarios vs. the base case.**

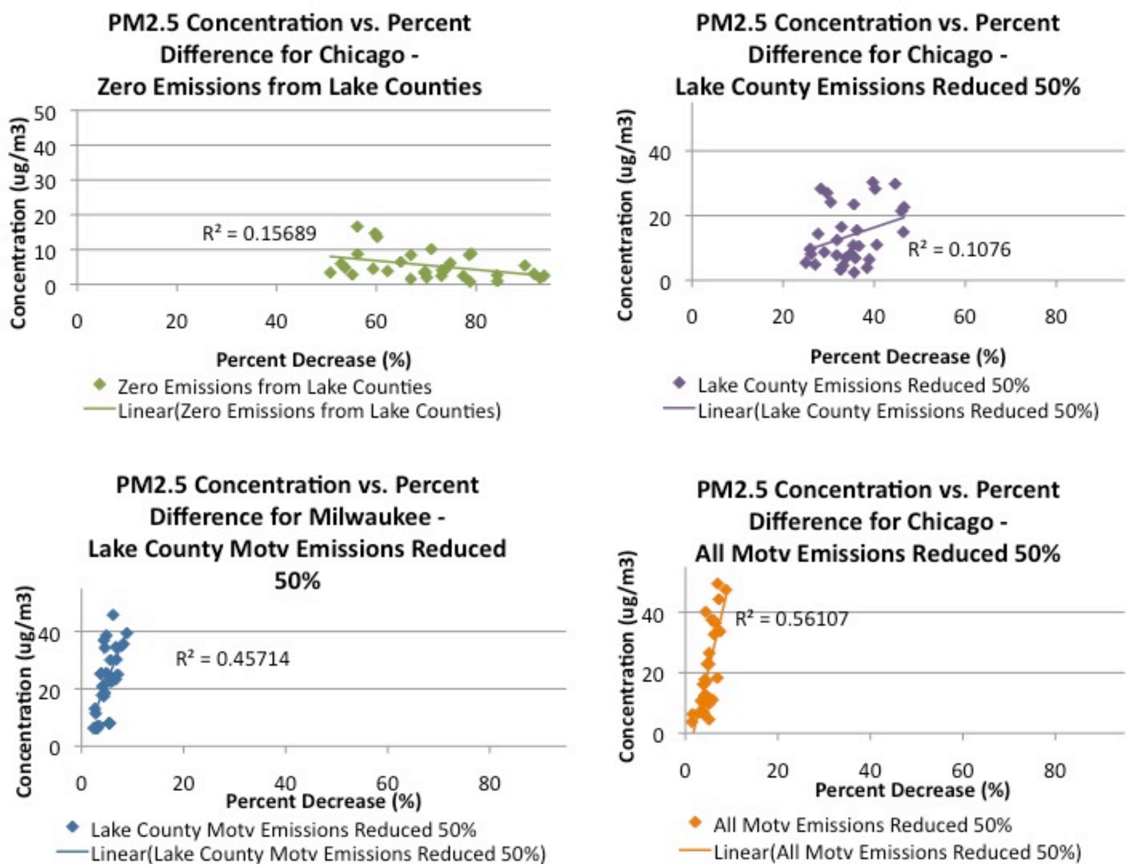


**Figure 4.19: Scatter plots of $PM_{2.5}$ concentrations vs. the percent difference in Chicago for a) (top left) zero emissions from lake counties, b) (top right) lake county emissions reduced 50%, c) (bottom left) lake county motor vehicle emissions reduced 50%, and d) (bottom right) domain-wide reduction in motor vehicle emissions vs. the base case.**

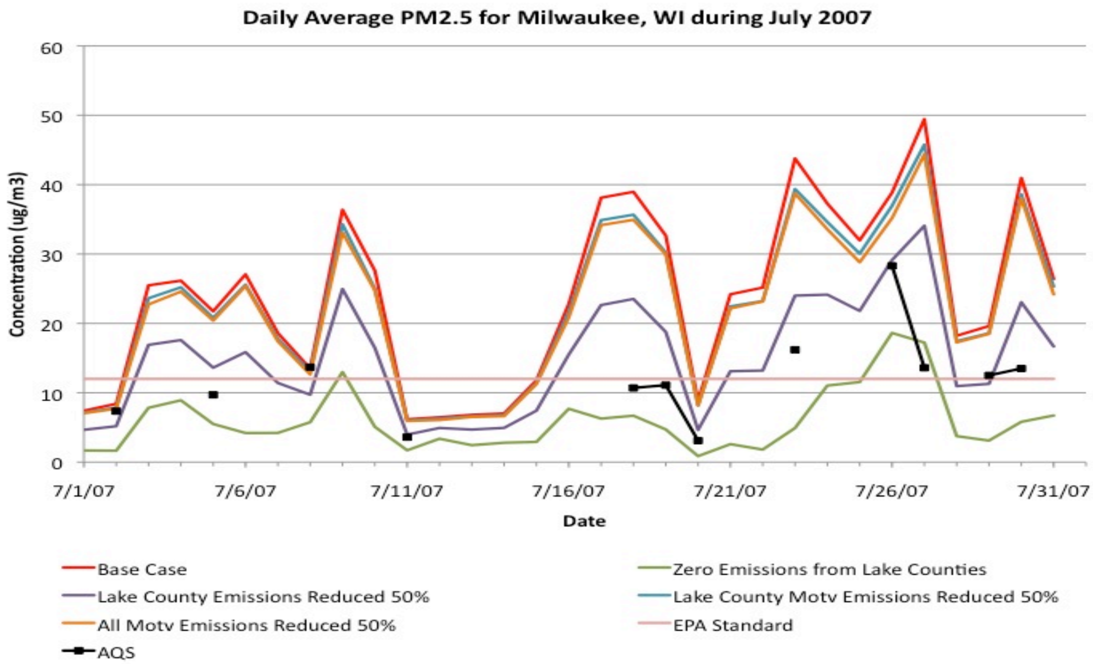


**Figure 4.20: Time serried of $PM_{2.5}$ concentrations in Milwaukee, WI for all scenarios, the AQS observations, and the NAAQS ozone standard of 75ppb.**

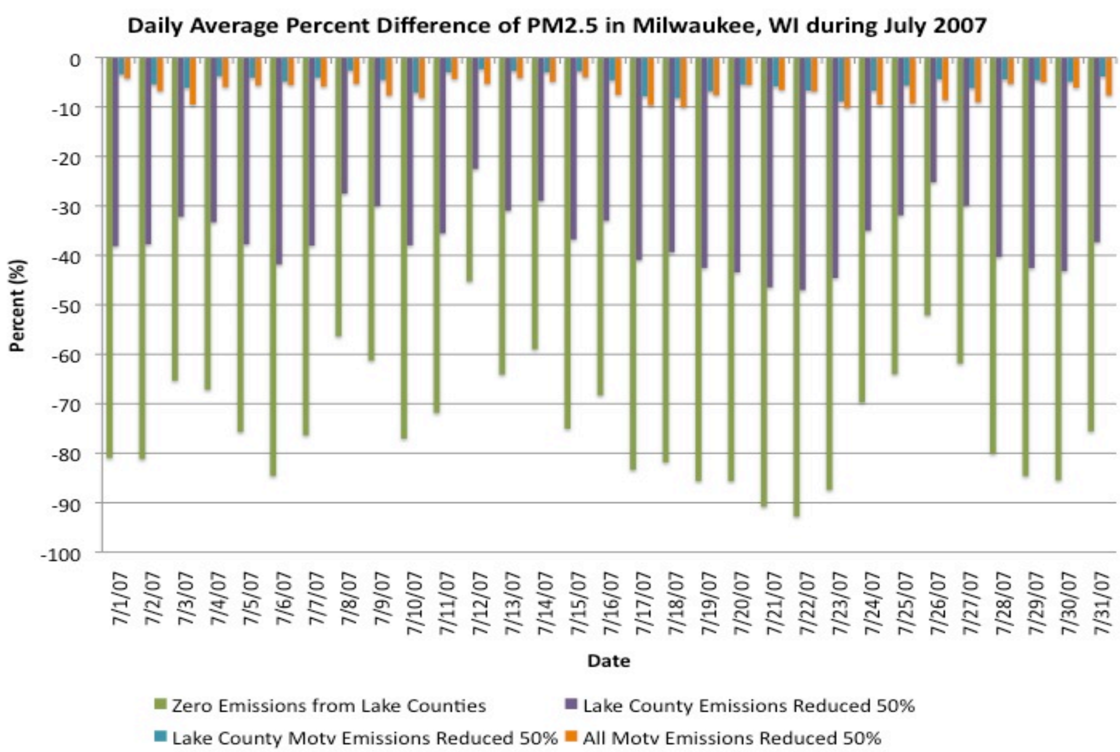


**Figure 4.21a: Percent difference in $PM_{2.5}$ concentrations in Milwaukee for all scenarios vs. the base case.**

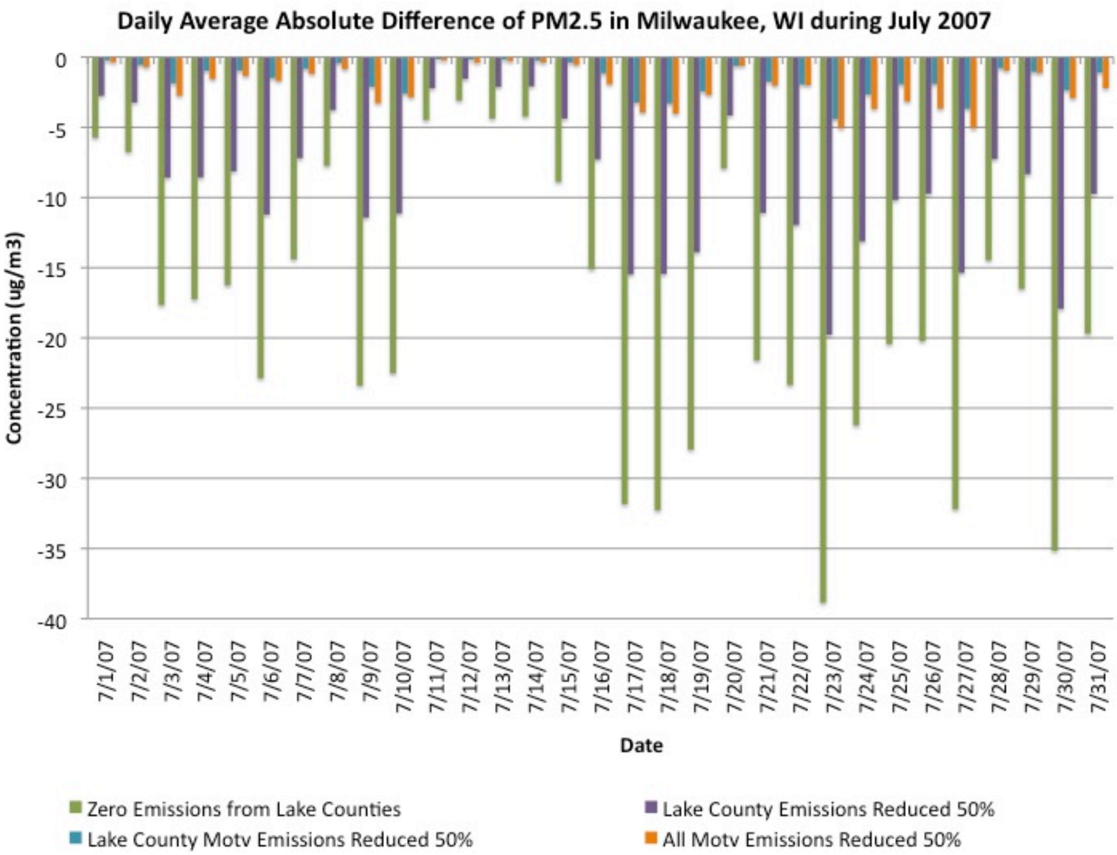


**Figure 4.21b: Absolute difference in $PM_{2.5}$ concentrations in Milwaukee for all scenarios vs. the base case.**

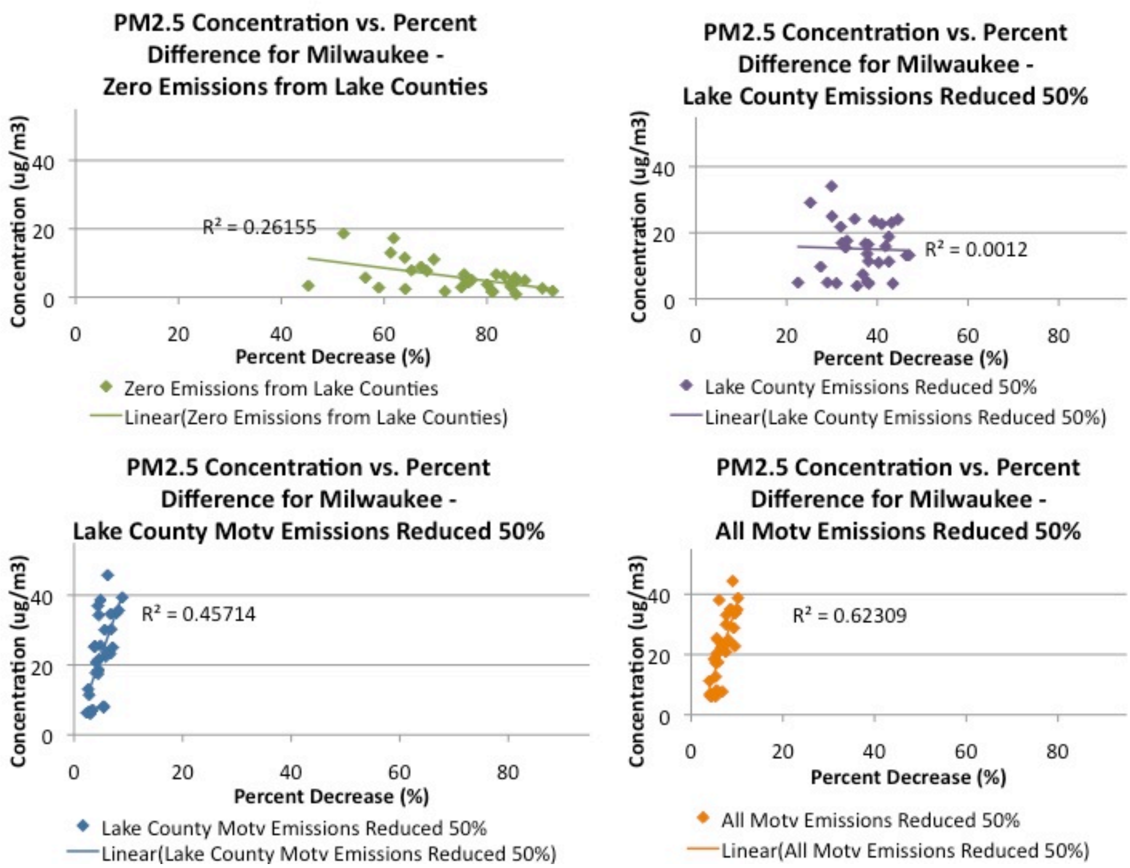


**Figure 4.22: Scatter plots of $PM_{2.5}$ concentrations vs. the percent difference in Milwaukee for a) (top left) zero emissions from lake counties, b) (top right) lake county emissions reduced 50%, c) (bottom left) lake county motor vehicle emissions reduced 50%, and d) (bottom right) domain-wide reduction in motor vehicle emissions vs. the base case.**

## References

Foley, T., Betterton, E. a., Robert Jacko, P. E., & Hillery, J. (2011). Lake Michigan air quality: The 1994–2003 LADCO Aircraft Project (LAP). *Atmospheric Environment*, *45*(18), 3192–3202. doi:10.1016/j.atmosenv.2011.02.033

Logan, J. A. (1983), NItrogen Oxides in the Troposhpere: Global and Regional Budgets, *J. Geophys. Res.*, *88*(C15), 10,758–10,807.

# Chapter 5: Summary and Conclusions

The two sensitivity studies conducted in this work show the connection between altered emissions and air quality through the use of an air quality model. The Community Multi-scale Air Quality (CMAQ) model was used as a tool to understand the effect of 1) the addition of lightning emissions to the existing emissions inventory, and 2) reducing county and domain-wide emissions to understand how each scenario reduces air pollution. Concentrations of ozone and $PM_{2.5}$ were analyzed in both studies, with an additional investigation into $SO_2$, VOC, and $NO_x$ in the lightning study. Model data was compared against data from the Air Quality Systems (AQS) database, the Clean Air Status and Trends Network (CASTNet), and OMI $NO_2$ data in the lightning study. Understanding how air quality changes with alterations in emissions is imperative for advancing our knowledge of these policy and health relevant air pollutants.

## Impacts of lightning emissions inventory

The goal of this work was to develop a lightning emissions inventory in order to build a comprehensive inventory, and to see how much lightning contributed $NO_x$ concentrations. Overall, $NO_x$ emissions increase the most in southeastern U.S. when adding lightning emissions, as this is where convective activity is the most prevalent. When comparing both CMAQ runs against the observational data from OMI, the lightning run shows improved correlation with OMI. Overall agreement is determined by multiple sectors and model processes. The goal of this work was to improve CMAQ performance by adding lightning emission, and that goal was met, with improved correlations with the observations. Because lightning has little impact at the surface in urban areas, the CMAQ/AQS comparison shows no change in correlation. However, the CMAQ/OMI comparison shows a better correlation with the lightning run because OMI reflects total column $NO_2$ in both rural and urban locations.

The relationship between ozone and $NO_x$ is further emphasized in this work, as ozone concentrations increased by as much as 5 ppb in areas of increased $NO_x$ from the added lightning emissions. Ozone varied most in the lower southeast portions of the U.S. where VOC concentrations are the largest. The southeast portion of the U.S. is $NO_x$ limited, so the addition of lightning has the potential to largely increase ozone concentrations, allowing for this portion of the country to be largely sensitive to changes in the amount of $NO_x$ added by lightning emissions [*Biazar and McNider,* 1995]. Further comparison of ozone with CASTNet observation sites shows that CMAQ chemistry in urban areas may be more accurate as opposed to chemical processes in rural areas.

Because NO affects atmospheric chemistry, other species, namely $SO_2$, $PM_{2.5}$, and VOCs are also impacted by changes in lightning $NO_x$ emissions. The largest changes are seen in the VOC concentrations, which is at most, was a 0.75 ppb decrease. This slight decrease in VOCs would cause ozone to decrease. In summary, the addition of lightning emissions caused a 10% increase in $NO_x$ concentrations. These emissions caused a maximum increase of 5ppb for ozone, and a 0.75ppb decrease in VOC's. Lightning emissions minimally impacted $SO_2$ and $PM_{2.5}$ concentrations.

## Effects of altered emissions scenarios on pollution levels

Reductions in emissions around Lake Michigan resulted in significant changes in ozone and $PM_{2.5}$ concentrations above and around the lake. The scenario that resulted in the largest changes in both pollutants was the Zero-LC scenario. This scenario reduced NAAQS exceedances of 8-hour maximum ozone in Milwaukee, and $PM_{2.5}$ exceedances for both Chicago and Milwaukee during the one-month simulation period. About 70% of exceedances in both Milwaukee and Chicago for the $PM_{2.5}$ standard are avoided in the Zero-LC scenario and about 50% of the exceedances for the ozone standard are avoided in Milwaukee. None of these scenarios drastically reduced ozone concentrations in Chicago.

The lake-breeze effect proved to be the governing factor for many of the instances where $PM_{2.5}$ and ozone concentrations were the largest. Animations during these occurrences showed a build up of pollutants over Lake Michigan that was then advected from over the lake to over land later in the day. The alteration of emissions in these scenarios resulted in an overall decrease in pollution levels that build up over the lake. Ozone concentrations did increase on several occasions in both Milwaukee and Chicago, and this was attributed to changes in nighttime destruction of ozone. In the scenarios that altered emissions directly around the lake, ozone did not decrease as much at night as in the BC. This could be due to these scenarios also reducing the pollutants that break down ozone through the nighttime hours.

Reductions in motor vehicle emissions resulted in the least amount of change in both ozone and $PM_{2.5}$ concentrations. $PM_{2.5}$ changed less than 10% for these scenarios in both Milwaukee and Chicago. Ozone changed by a maximum of about 30% in Milwaukee and 10% in Chicago. The 50%-LC scenario resulted in the largest increase in ozone in Milwaukee and Chicago, only reached maximum absolute differences of about 1 ppb. Neither of these runs reduced or increased the number of exceedances of the air quality standards. The 50%-LC resulted in the second largest amount of change in Chicago and Milwaukee, and reduced exceedances in $PM_{2.5}$, but not ozone.

This work shows that reducing emissions near Lake Michigan has the potential to impact pollution levels in the counties most affected by above-lake ozone formation. In analyzing data from Chicago and Milwaukee, multiple violations to the air quality standards occurred. When reducing lake-county emissions, many of these exceedances were avoided, more so for the scenarios that reduced all emissions around the lake. Moving foreword, the combined analysis of ground-based measurements, satellite data, and air quality models hold great potential for the science and regulation of air quality. Future work will expand on lightning estimates presented here, and refine source-receptor analysis relevant to near-lake air quality management.